UNIVERSITÀ DEGLI STUDI DI PARMA
DIPARTIMENTO DI INGEGNERIA E ARCHITETTURA

DOTTORATO DI RICERCA IN
Tecnologie dell'Informazione

XXX CICLO

FIBER LASER APPLICATIONS IN DENTISTRY

Coordinatore:
Chiar.mo Prof. Marco Locatelli

Tutore:
Chiar.mo Prof. Annamaria Cucinotta

Dottorando: Carlo Fornaini

Anni 2014/2017

UNIVERSITÀ DEGLI STUDI DI PARMA
DIPARTIMENTO DI INGEGNERIA E ARCHITETTURA

Dottorato di Ricerca in Tecnologie dell'Informazione
XXX Ciclo

Carlo Fornaini

FIBER LASER APPLICATIONS IN DENTISTRY

DISSERTAZIONE PRESENTATA PER IL CONSEGUIMENTO DEL TITOLO DI DOTTORE DI RICERCA

GENNAIO 2018

To Anna, my wife, who supported me during this job

A person who never made a mistake never tried anything new.
Albert Einstein

Contents

1 Laser-Matter Interactions 9

1.1 Light-matter interactions 9
1.2 Reflection, refraction and scattering 10
1.3 Absorption 12
1.4 Laser-matter processing 13
1.5 Laser manufacturing in the industrial field 17

2 Laser-Tissue Interactions 21

2.1 Experimental models for energy deposition prediction 21
2.2 Role of the chromophores in the energy absorption 24
2.3 Photochemical interactions 26
2.4 Photothermal interactions 30
2.5 Photomechanical interactions 31

3 Laser in Dentistry 35

3.1 History of laser in medicine 35

3.2 Early applications of laser in dentistry 36
3.3 Use of laser in hard dental tissues 37
3.4 Diode lasers in dentistry 39
3.5 Fiber lasers and their possible role in dentistry 40

4 Fiber lasers and soft tissue surgery 42

4.1 Introduction 42
4.2 Materials and Methods 43
4.3 Results 47
4.4 Discussion 50
4.5 Conclusion 50

5 Fiber lasers and di-silicate ceramics 51

5.1 Introduction 51
5.2 Materials and Methods 52
5.3 Results and Discussion 55
5.4 Conclusion 61

6 Fiber lasers and hard dental tissues 62

6.1 Introduction 62
6.2 Results and Discussion 66
6.3 Conclusion 67

7 Project for an “at home” intraoral device based on Random Laser technology . 68

7.1 Introduction 68
7.2 Material and Methods 71
7.3 Conclusion 74

Conclusion and future perspectives 75
Figures Captions 77
Tables Captions 81
List of publications 82
International Conference Papers 84
National Conference Papers 86
References 87
Acknowledgement 109

Introduction

The earliest experimental studies of laser–matter interaction, conducted in the 1960s just after the first laser construction, studied mainly the thermal effects including heating, melting, evaporation of condensed matter, and thermionic electron emission.
When a particle interacts with light, different effects occur together (reflection, absorption, transmission and scattering) leading to decrease or extinction of the incident beam, basically representing the total of absorption and scattering.
Part of the electromagnetic energy of the incident light is absorbed by the particle and changed into a different energy form, mostly thermal energy, through infrared radiance or convection of the surrounding medium.
Once inside the material, absorption causes the light intensity decline with a depth value which is function of the material's absorption coefficient α. While, generally, it is related to wavelength and temperature, for constant α, the intensity I exponentially decays with depth z according to the Beer–Lambert law.
The laser processes may be classified into three major classes: heating (without melting/vaporizing), melting (no vaporizing), vaporising.
While transformations such hardening, bending and magnetic domain control, which rely on surface heating without melting, require low power density laser, surface melting, glazing, cladding, welding and cutting (involving melting) require high power density laser. Similarly, cutting, drilling and similar machining operations which remove material

as vapour hence, need delivery of a substantially high power density within a very short interaction/pulse time.
Laser ablation is the removal of material from a substrate by direct absorption of laser energy and it occurs above a threshold fluence, depending on absorption mechanism, material properties, microstructure, morphology, presence of defects, and on laser parameters, such as wavelength and pulse duration. Typical threshold fluences for metals are between 1 and 10 J/cm^2, for inorganic insulators between 0.5 and 2 J/cm^2, and for organic materials between 0.1 and 1 J/cm^2. With multiple pulses, the ablation thresholds may decrease due to accumulation of defects: above the ablation threshold, thickness or volume of material removed per pulse typically shows a logarithmic increase with fluence, according to the Beer–Lambert law.
The applications of laser-matter interactions have today a great importance in industrial field due to the great number of its advantages. They are laser cutting, laser drilling, laser micro-machining, laser cleaning, laser marking and laser scribing.
The behaviour of the laser beam when interacting with biological tissues is very different. Scattering is very important because it determines the volume distribution of light intensity in the tissue. This is the primary step for tissue interaction, which is followed by absorption and heat generation. Scattering of light in tissue is caused by inhomogeneity such as cell membranes or intracellular structures. The scattering arises due to a relative refractive index mismatch at the boundaries between two such media or structures, e.g. between the extracellular fluid and the cell membrane.
The variety of interaction mechanisms that may occur when applying laser light to biological tissue is multifarious, depending on both the tissue characteristics (reflection, absorption and scattering coefficients, heat conduction and capacity) and the laser parameters (wavelength, exposure time, applied energy, focal spot size, power density and fluence).
Although the number of possible combinations of the experimental parameters is unlimited, most of Authors agree that the three main categories of laser-tissue interactions are:
- photochemical interactions.
- photothermal interactions.
- photomechanical interactions.

The group of photochemical interactions stems from empirical observations that light can induce chemical effects and reactions within macromolecules or tissues and the most popular example, created by the evolution itself, it is represented by the photosynthesis. In the field of medical laser physics, the two main applications of the photochemical interactions are the photodynamic therapy (PDT) and the biostimulation (Low Level

Laser Therapy- LLLT) and both take place at very low power densities, typically 1W/cm^2, and long exposure times ranging from seconds to CW.
The term "photothermal interactions" stands for a large group of laser-tissue interaction types where the increase in local temperature is the significant parameter change, induced by either CW or pulsed laser radiation. Photothermal interaction is a complex process resulting from three distinct phenomena: conversion of light to heat, transfer of heat and tissue reaction, which is related to temperature and heating time.
Mechanical effects can result from either the creation of a plasma, an explosive vaporization, or the phenomenon of cavitation, each of which is associated with the production of a shock wave.
This capacity of the laser to interact with biological tissues has been the basis of the so called "laserology" which is now considered as a medical specialization including all the possible applications of this technology in medical and surgical fields.
Medical lasers have made it possible to treat conditions previously considered untreatable, or difficult to treat. Patients benefit by improved results and less cost. In the last few years, the main focus of the research and development of medical lasers has been on laser hair removal, the treatment of vascular lesions including leg veins, and vision correction. The thrust of current research is directed towards non-ablative laser resurfacing ("laser skin toning"), "no-touch" computerized vision correction, and improved photodynamic therapy for treatment of skin cancer and for hair removal.
The first application of laser technology in dentistry was described by Goldman in 1964, four years after the realization of the first laser device, the "Ruby Laser", by Maiman in 1960.
The main reasons of this delay are, on the one hand the difficulty of the beam delivering in a small cavity such the mouth which was solved only by the finalizing of efficient delivery systems and, on the other hand the necessity to utilize different wavelengths due to the different target tissues present into the oral cavity.
Another problem found by the first researchers who used laser technology in oral applications was the need of limit thermal elevation under values compatible with the biological integrity of the tissues.
Therefore, for many years, the utilization of laser in dentistry was limited only to the soft tissue surgery.
In 1990 laser technology was introduced in conservative dentistry by Hibst and Keller, who described the possibility to use an Er:YAG laser as alternative to conventional instruments, such as the turbine and micromotor.
A great improvement was reached in 2000's with the introduction of the diode lasers: in fact, this family of lasers, based on the semiconductor technology and allowing to reduce

size, costs and the necessity of maintenance, made the utilization of the coherent light in dentistry very popular.
While for many years the diode laser wavelengths used in dentistry have been around 1000 nm, thanks to the great absorption in haemoglobin and so able to give a good haemostasis of the operative field, in the last years a great interest was focused on the lasers emitting in the visible portion, particularly the blue, and in the far infrared, 1500 and 2000 nm, to get all the advantages derived by a great absorption in the water.
Unfortunately, the main limit of the diode laser utilization in dentistry is related to the possibility to treat only the oral soft tissues: in fact, it results very effective when used in oral surgery but it cannot be utilized on the teeth for conservative dentistry.
The employment of laser in dentistry may be summarized in three main targets:
- hard dental tissues (teeth, bone): the clinic utilization includes mainly the conservative dentistry and the bone surgery and it may be performed only by the Erbium family lasers (Er:YAG and Er,Cr:YSGG).
- soft dental tissues (vascularized and keratinized gum): its applications consist of the oral surgery interventions and normally Nd:YAG, CO_2 and diodes are the first choice lasers.
- ceramics surfaces (etchable and non etchable porcelain): its employing is related to the characterization of the internal surfaces of ceramic prosthetics to enhance the adhesion to the teeth and the CO_2, Nd:YAP and Nd:YAG laser are utilized.
By these considerations, it arises that the possibility to have wavelengths able to be effective in all the three targets described might be a great success and the aim of this study is to evaluate the effectiveness of the use of fiber lasers for dental applications, particularly on soft tissues, hard tissues and ceramic surfaces.
The device used for the tests is a 1070 nm pulsed fiber laser (AREX 20, Datalogic, Italy) available in the Photonic Devices Lab at the Engineering and Architecture Department.
This source has a maximum average output power of 20 W and a fixed pulse time duration of 100 ns, while the repetition rate ranges from 20 kHz to 100 kHz.
Fiber lasers are sources where the active medium is an optical fiber where the core is doped by rare earth ions such as Nd (neodymium), Yb (ytterbium), Er (erbium), Tm (thulium). The fundamental difference between traditional solid-state lasers and fiber lasers lies in the form of the gain medium. In fact, while bulk crystal lasers are typically based on conventional rod or slab geometries, in fiber lasers active ions are added into the core of an optical fiber, often with a length of many metres.
The most common applications of fiber lasers regard the industrial field, where they are used mainly for material processing (i.e., for cutting and marking) while the utilizations of fiber lasers in medicine are related to the lithotripsy, the surgical treatment of vascular lesions, the non-surgical skin aesthetic procedures, the urinary surgery, and the eye surgery.

The first step of this work is to analyse the behaviour of fiber laser on oral soft tissues beyond *ex vivo* tests performed on samples obtained by bovine tongues.
Thermal elevation during irradiation was recorded by a Fiber Bragg Grating (FBG) temperature sensor connected to an interrogator while tissue modifications evaluation with a qualitative microscopic observation and a score assigned by a blind pathologist to the incisions made by different parameters.
The second series of tests is focused on di-silicate ceramic samples and, beyond thermal recording performed by FBG interrogator, the morphological analysis of the surface is observed by SEM as well as elemental composition by EDS to investigate the possible structure modifications induced by laser irradiation.
A third session of experiments is conducted on dentinal sections of extracted human teeth to verify the possibility of fiber laser ablation on hard dental tissues; even if the results are not encouraging, it is appreciated the capability to perform a "dentinal welding", also using Hydroxyapatite as filler.
One more topic treated in this thesis is the prototyping of a new laser device to intraorally use for the so-called "at home therapy" based on "random laser" technology and, in the last chapter, a description of all the steps for arriving to project this appliance are described.

The thesis is organized with the following outline:

Chapter I: Laser-matter interactions are described, particularly enhancing the advantages of the use of this technology in the industrial field and making the list of the main laser processing applications.

Chapter II: Laser-tissue interactions are discussed, in function of wavelength, power, time of irradiation and tissue characteristics (presence of chromophores); clinical applications of different types of interactions are also described.

Chapter III: An overview of the use of the laser in medicine, in surgery and finally in dentistry with the description of the fields of application and the wavelengths used.

Chapter IV: Tests on bovine tongue samples with different parameters: discussion about the use of fiber laser in the oral soft tissues surgery.

Chapter V: Tests on di-silicate dental ceramics including SEM and EDS observations to evaluate the roughness surface modification with minimal thermal damage.

Chapter VI: Dentine samples irradiation and SEM observation. Preliminary study on the possibility to weld dentine by Hydroxyapatite apposition.

Chapter VII: Description of a prototype of "At home" intraoral laser device based on "Random laser" technology.

Chapter 1

Laser-Matter Interactions

1.1 Light-matter interactions

The earliest experimental studies of laser–matter interaction, conducted in the early 1960s just after the first high-power lasers construction, studied mainly the thermal effects including heating, melting, evaporation of condensed matter, and thermionic electron emission. Successfully, when higher laser intensities were reached, it became possible to study also the optical breakdown of gas and solid dielectrics. In the 1960s, were also proposed the first theoretical models of laser– matter interaction: the simplest models were related to moderate laser intensity ranges ($I \simeq 105–109$ W/cm^2) and investigated the energy transfer in condensed matter, the kinetics of phase transitions, and the dynamics of evaporated material expansion [1-6].

Despite many simplifications, the theoretical models may provide a basic outline of the actual interaction of laser radiation with solids at moderate laser intensities.

When a particle interacts with light, different effects occur together, as shown in Fig. 1.1, leading to decreasing or extinction of the incident beam, basically representing the sum of absorption and scattering.

Part of the electromagnetic energy of the incidence light is absorbed by the particle and changed into a different energy form, mostly thermal energy, through infrared radiance (thermal radiation) or convection of the surrounding medium, this one without any importance for laser scattering. While for non-transparent particles with a diameter clearly above the wavelength of the used light the quantity of the absorption is simply calculated from their geometric transverse section, for marginal dimension particles and opaque

particles, the absorption coefficient of the material must be known for relating the absorption to particle size. About the scattering, a distinction must be initially drawn between two different basic forms: the inelastic scattering, where the energy and thus the wavelength of the light changes, and the elastic scattering where the wavelength remains the same.

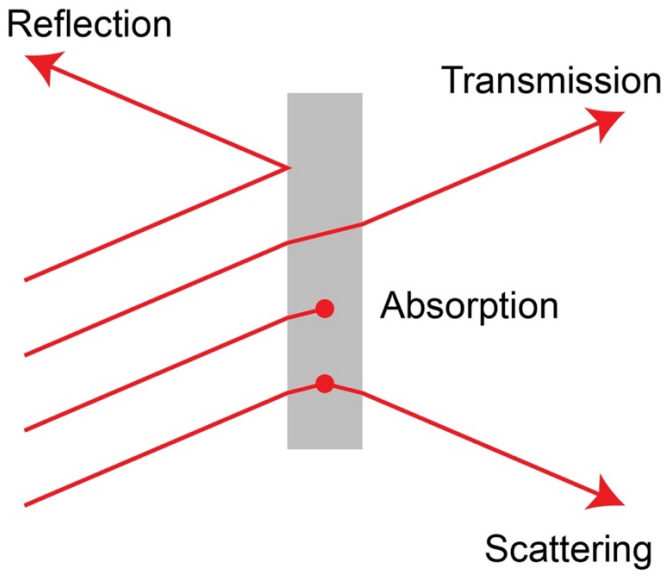

Fig. 1.1 - The four major types of interactions of light with matter: transmission, reflection, scattering and absorption (ref. 106).

1.2 Reflection, refraction and scattering

Scattering is always present when the incident light deflects from its original direction and it can be divided in three parts: reflection, refraction and diffraction.
The reflection, mostly on the surface of the particles, is described, according to the geometric optic, with the law: “angle of incidence equals angle of reflection”. During the refraction, the direction of a light beam changes during the transition between two materials with different indexes of refraction, according to the “Snell refraction law”; the behaviour of an incident light beam when reflected and refracted is shown in Fig. 1.2.
For instance, when a light beam hits a drop of rain, it is refracted towards the middle of the droplet and in the further course, on the outer edge of the rain drop, it is continuously back reflected inside the drop again and again.

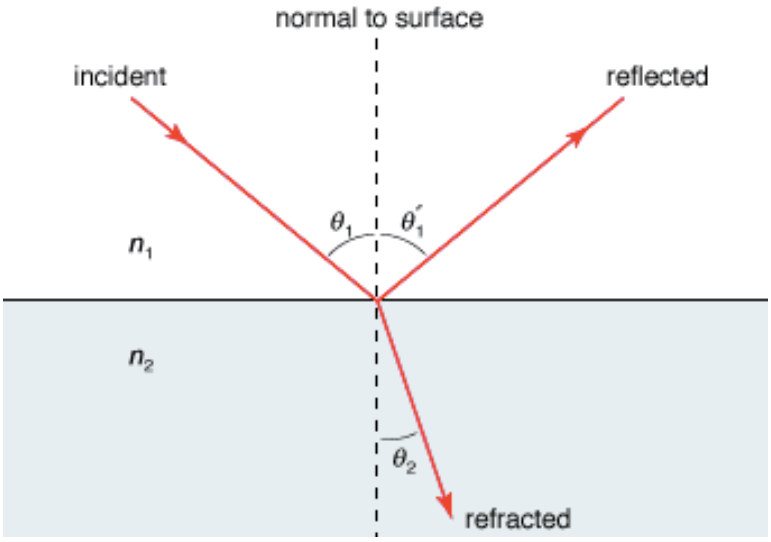

Fig. 1.2 - The behaviour of an incident light beam when reflected and refracted (ref. 106).

The fraction of the incident power reflected from the surface R depends on the polarization and angle of incidence θ_1 of the light as well as the index of refraction of the atmosphere n_1 and the material n_2. The reflection coefficients for the s-polarized and p-polarized components of the light can be calculated from the well-known Fresnel equations:

$$R_s = \left[\frac{E_r}{E_i}\right]^2 = \left[\frac{n_1 cos(\theta_i) - n_2 cos(\theta_t)}{n_1 cos(\theta_i) + n_2 cos(\theta_t)}\right]^2$$

$$R_p = \left[\frac{E_r}{E_i}\right]^2 = \left[\frac{n_1 cos(\theta_i) - n_2 cos(\theta_t)}{n_1 cos(\theta_i) + n_2 cos(\theta_t)}\right]^2$$

and are related to the transmission coefficients through $T_s = 1\text{-}R_s$ and $T_p = 1\text{-}R_p$.
For the case of normally incident light on a flat surface, the above equations reduce to the more familiar form:

$$R = R_s = R_p = \left(\frac{n_1 - n_2}{n_1 + n_2}\right)$$

The reflectivity of a certain material depends on the frequency of the light source through the dispersion relation of its index of refraction: in the case of normal incidence, values for reflectivity of metals in the near UV and visible spectral range are typically between 0.4 and 0.95, and between 0.9 and 0.99 for the IR [7]. In addition, the reflectivity of a

surface depends on the temperature of the material through changes in the permittivity, band structure, plasma oscillations, or material phase [8]. For instance, upon melting, the reflectivity of silicon increases by a factor of about 2 [9] while for a metal such as Ni changes by only a few percent [10]. In the case of small scale or structured materials, additional optical resonances are possible such as surface and bulk plasmons and polaritons and these may enhance absorption or reflection due to the photon–electron interactions [11].

1.3 Absorption

Once inside the material, absorption causes the light intensity decline with a depth value which is in function of the material's absorption coefficient α; while, generally, it is related with wavelength and temperature, for constant α, intensity I exponentially decays with depth z according to the Beer–Lambert law:

$$I(z) = I_0 e^{-\propto z}$$

where I_0 is the intensity just inside the surface after considering reflection loss.
The optical penetration or absorption depth $\delta = 1/\alpha$ is defined as the depth at which the intensity of the transmitted light drops to $1/e$ of its initial value at the interface and, although the interpretation of absorption depth has been developed for a plane wave, the observation that energy absorption is approximately confined within the absorption depth still holds for more general beam profiles. Therefore, a wavelength with short absorption depths can permit local modification of surface properties without causing an alteration of the material bulk.
Even if the above considerations regard only linear optical phenomena, however they are not necessarily valid for all materials, and/or for all incident laser conditions: in fact, some materials such as glasses exhibit strong non-linearity in their index of refraction [12] which can lead to some interesting effects such as self-focusing, defocusing, or soliton propagation [13]. Even if when dealing with CW or nanosecond duration laser pulses, it is typically assumed that most of the absorption is due to single photon interactions, however, for picosecond (ps) and femtosecond (fs) lasers, the extremely high instantaneous intensity enables phenomena such as optical breakdown and multiphoton absorption which can significantly decrease absorption depths [14].
The process of energy deposition from a pulsed/continuous wave (CW) laser beam into the near surface region of a solid involves electronic excitation and de-excitation within an extremely short period of time [15].

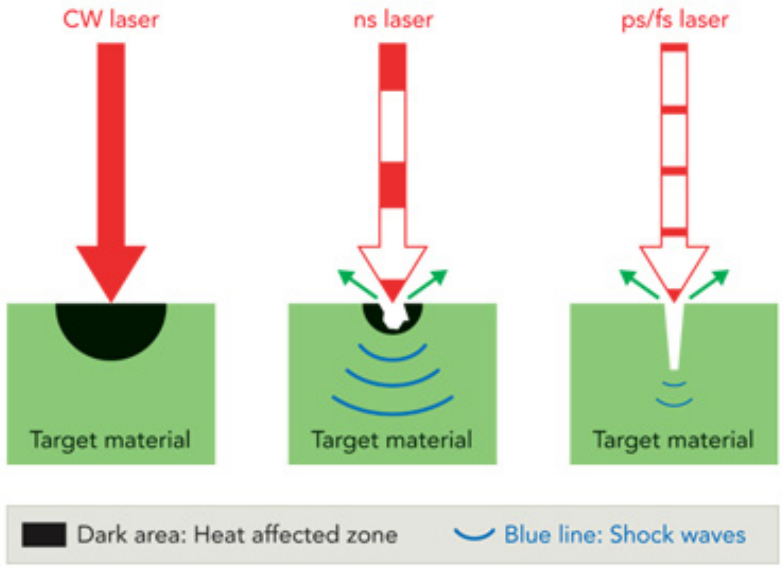

Fig. 1.3 - Different effects of a laser beam in function of different pulse durations (ref.15).

For all laser assisted material processing applications, the first stage involves the coupling of laser radiation to electrons within the metal and, initially, photon interaction with matter occurs through the excitation of valence and conduction band electrons throughout the wavelength band from infrared (10 μm) to UV (0.2 μm) regions. Absorption of wavelength between 0.2 and 10 μm leads to intraband transition (free electrons only) in metals and interband transition (valence to conduction) in semiconductors. Conversion of the absorbed energy to heat involves the excitation of valence and/or conduction band electrons, the excited electron–phonon interaction within a span of 10-11–10-12 s, the electron–electron or electron–plasma interaction and the electron–hole recombination within 10^{-9}–10^{-10} s (Auger process). Since free carrier absorption (by conduction band electrons) is the primary route of energy absorption in metals, beam energy is almost instantaneously transferred to the lattice by electron–phonon interaction.
Similarly, transition in semiconductor or polymers having ionic/covalent bonding with energy gap between conduction and valence bands is marginally slower.

1.4 Laser-matter processing

The laser processes may be classified into three major classes:

1) heating (without melting/vaporizing).
2) melting (no vaporizing).
3) vaporizing.

While the transformations such hardening, bending and magnetic domain control which rely on surface heating without melting require low power density laser, surface melting, glazing, cladding, welding and cutting (melting involving) require high power density laser. Similarly, cutting, drilling and similar machining operations which remove material as vapour hence, need delivery of a substantially high-power density within a very short interaction/pulse time. The different industrial applications, in function of the laser parameters, are shown in Fig. 1.4.

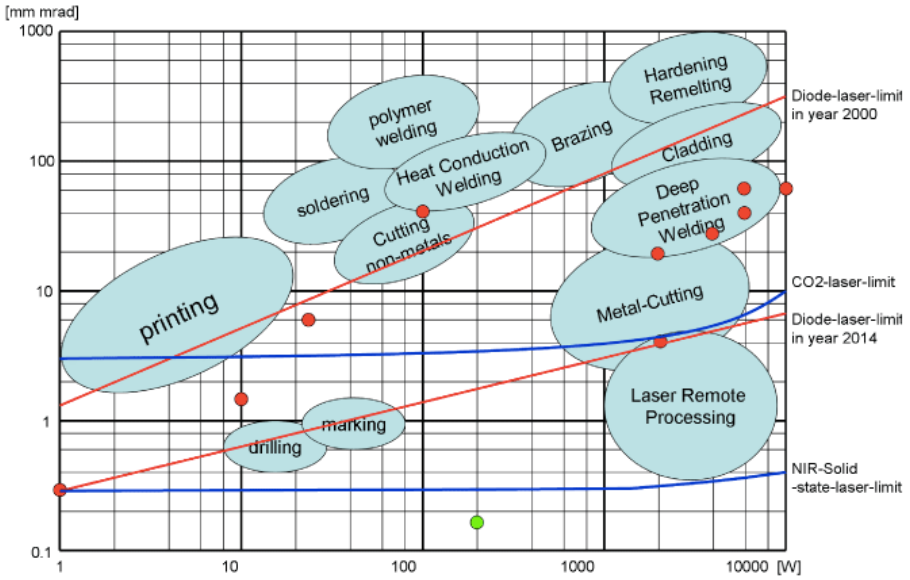

Fig. 1.4 - Beam parameter product vs. laser power for different applications and laser types. Red circles indicate commercially available diode-lasers. Green circle: 200W green solid-state-laser.

Beam configuration and beam profile also play an important factor in determining the energy distribution at the interaction zone during laser processing. Four types of beam profiles are commonly used for material processing: Gaussian, multimode, square (or rectangular) and Top -Hat [16].

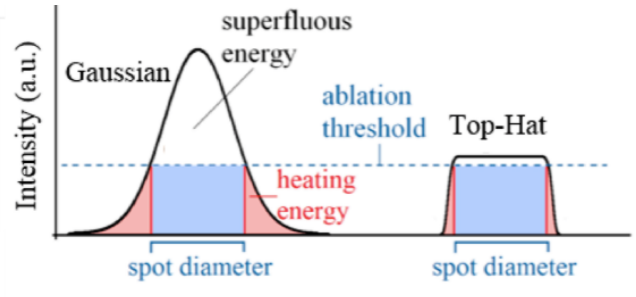

Fig. 1.5 - Difference between Gaussian and Top-Hat beam profiles (ref. 18).

A Gaussian beam is most suitable for cutting and welding applications rather than for surface treatment because, being a 'sharp tool,' it tends to vaporize and melt the substrate deeply. In contrast, multimode, top hat and square profiles ('blunt tools') are preferred for surface engineering. Beam shaping is the process of altering an input beam to produce an output beam with a desired spatial or irradiance profile while beam shaping plays an important role in determining the quality of hardening, welding and laser micro-processing [17,18].
Laser heating with fluence below the threshold of melting can activate a variety of temperature-dependent processes within the solid material: in fact, the high temperatures generated may enhance diffusion rates promoting impurity doping, the reorganization of the crystal structure [19], and sintering of porous materials [20].
Also, the rapid generation of large temperature gradients can induce thermal stresses and thermo-elastic excitation of acoustic waves [21]: these stresses may be responsible of the mechanical behaviour of the material such as work hardening, warping, or cracking.
A fluence above the threshold of melting can lead to the formation, on the surface, of molten material transient pools which may support much higher atomic mobility and solubility than in the solid phase, resulting in rapid material homogenization.
High self-quenching rates with solidification front velocities up to several m/s can be achieved by rapid dissipation of heat into the cooler surrounding bulk material [22, 23] and this rapid quenching can freeze in defects and supersaturated solutes [24] as well as form metastable material phases. Slower re-solidification rates can allow recrystallization of larger grains than the original material: use of shaped beam profiles has also been shown to allow control of the re-crystallization dynamics [25].

Laser ablation
Laser ablation is the removal of material from a substrate by direct absorption of laser energy and it occurs above a threshold fluence, depending on the absorption mechanism, material properties, microstructure, morphology, the presence of defects, and on laser parameters such as wavelength and pulse duration. Typical threshold fluences for metals are between 1 and 10 J/cm^2, for inorganic insulators between 0.5 and 2 J/cm^2, and for organic materials between 0.1 and 1 J/cm^2 [26]. With multiple pulses, the ablation

thresholds may decrease due to accumulation of defects: above the ablation threshold, thickness or volume of material removed per pulse typically shows a logarithmic increase with fluence, according to the Beer–Lambert law.
A variety of mechanisms may be active during laser ablation depending on the material system and laser processing parameters such as wavelength, fluence, and pulse length [27]; at low fluence, photo-thermal mechanisms for ablation include material evaporation and sublimation.
For multicomponent systems, the more volatile species may be depleted more rapidly, changing the chemical composition of the remaining material [28-30]. With higher fluence, heterogeneous nucleation of vapour bubbles leads to normal boiling and, if material heating is sufficiently rapid to approach its thermodynamic critical temperature, rapid homogenous nucleation and expansion of vapour bubbles lead to explosive boiling (phase explosion) carrying off solid and liquid material fragments [31].
When in the matter excitation time is shorter than thermalisation time, non-thermal photochemical ablation mechanisms can occur: with ultrafast pulses, for instance, direct ionization and formation of dense electron-hole plasmas can lead to a thermal phase transformation, direct bond-breaking, and explosive disintegration of the lattice through electronic repulsion (Coulomb explosion) [32].

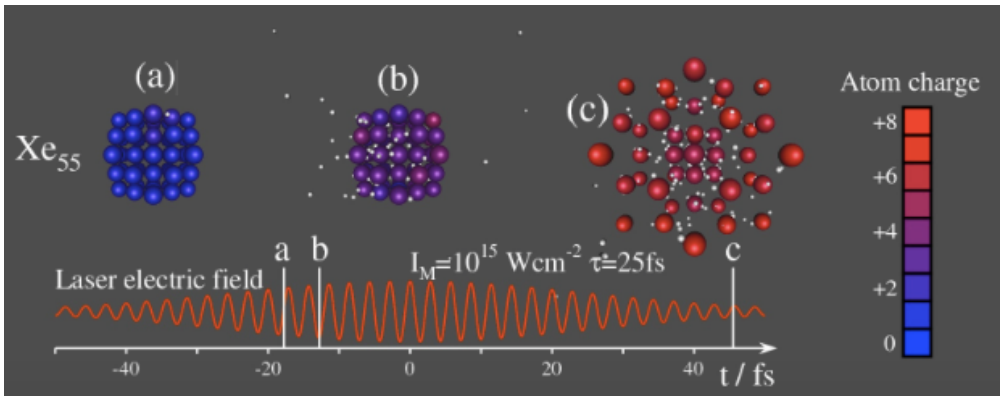

Fig. 1.6 - The ionization and Coulomb explosion process, demonstrated for a small cluster (Xe55, ion charges are colour coded, electrons in light grey) irradiated by a 25 fs Gaussian laser pulse (peak intensity $I_M = 10^{15}$ Wcm^{-2}). (a) Initial tunnel ionizations, generating the first ion-electron pairs in the cluster, increasing the local electric field and facilitating further ionizations, (b) nanoplasma formation by classical barrier suppression and electron impact ionization, constituting the main inner ionization channels, (c) outer ionization and Coulomb explosion. The instants of the three snapshots of the time evolution together with the oscillating laser electric field are given on the time axis (ref. 31).

In some non-metal materials such as polymers and biological materials with relatively long irradiation times, photochemical ablation can still occur with short wavelength nanosecond lasers, producing well defined ablated regions with small Heat Affected Zone (HAZ) [33].
In all cases, material removal is accompanied by a highly-directed plume ejection from the irradiated zone. The dense vapor plume may contain solid and liquid clusters of material and, at high intensities, a significant fraction of the species may become ionized, so producing a plasma. Laser material processing offers the possibility of realizing the sequent manufacturing finished components directly from the raw materials without any elaborate intermediate operation [34-37].

1.5 Laser manufacturing in the industrial field

Laser assisted bending involves the curvature of sheet metal modifying by thermal residual stresses induced by laser assisted heating without any externally applied mechanical forces [38- 44].
Bending angle and properties of the bent zone may be influenced by controlling parameters such as laser beam radius, power density, interaction/pulse time, material properties (thermal, physical or chemical) and dimension/geometry of the workpiece (thickness, curvature, etc.).
Schuocker [45] developed a mathematical model to predict the temperature and stress distribution during laser assisted deep drawing, showing a considerable reduction in drawing force: the bending angle, stress–strain relation, temperature and residual stress distribution were predicted by the simulation for different materials, sheet thicknesses, scanning speeds and laser powers and the experimental results were suitably compared with the theoretical prediction.
Laser rapid prototyping is the development of small, complex and intricate components by coupling laser with computer controlled positioning stages and computer aided engineering design [46-50] based on repetitive deposition and processing of material layers known as additive free-form fabrication technique [51-54].
The advantages offered by these techniques include the capabilities to produce components of intricate shape with a greater accuracy, faster processing speed, economy in energy and material consumption. Laser engineered net shaping is a process in which near net shape metal structures are built from powdered metal layer by layer from computer generated designs.
Laser joining is a directed energy beam assisted fusion joining technique which involves the application of a high-power laser beam as a source of heat to fuse and join two solids of similar or dissimilar natures. The advantages of laser joining over conventional fusion or arc welding processes include high welding speed, narrow HAZ, low distortion, ease of automation, ability for single pass joining of thick sections and better design flexibility with controlled bead size. The special interest in laser joining lies in its capability of

fusion joining of dissimilar materials with different section thicknesses, compositions and/or physical/chemical properties for industry scale applications particularly in automotive and aerospace industry [55-62].
Laser welding, because of the sheer volume/extent of work and advancement over the years, constitutes the most important operations among the laser joining processes [63-68]. There are two fundamental modes of laser welding depending on the beam power/configuration and its focus with respect to the workpiece: conduction welding and keyhole or penetration welding, as shown in Fig. 1.7.

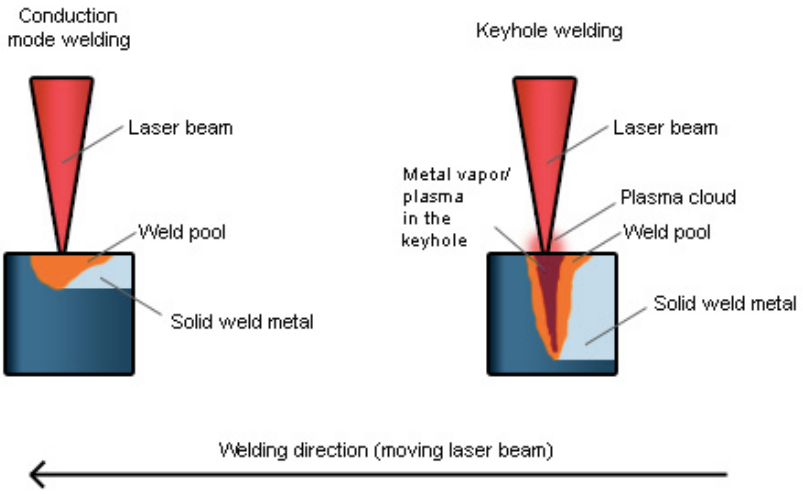

Fig. 1.7 - Difference between the "Conduction mode welding" and the "Keyhole welding" (ref. 64).

Conduction welding occurs when the beam is out of focus (above the surface) and the power density is low/insufficient to cause boiling at the given welding speed. In deep penetration or keyhole welding, the beam focus lies below the surface so that sufficient energy per unit area is available to cause evaporation and formation of a hole in the melt pool. The 'keyhole' behaves like an optical black body in that the radiation enters the hole and is subjected to multiple reflections before being able to escape. The transition from conduction mode to deep penetration mode occurs with increasing laser intensity and duration of laser pulse applied to the workpiece.
Laser cutting does have a diversified application starting from thin sheet metal cutting for general purpose equipment (such as household appliances, electrical cabinets and automotive components) to thick section metal cutting (for trucks, buildings, stoves, construction equipment, ship building…). Research efforts that have been successfully conducted on laser assisted machining of engineering materials (both metallic and non-metallic) have been reported in the literatures [69-74].

Laser drilling is a machining operation by melting and evaporation of the workpiece using a high-power laser beam. Metals/alloys, polymers and ceramics may be drilled by laser assisted drilling [75-86]. It can be done both in pulsed and CW modes with suitable laser parameters. The advantage of using laser is that it can drill holes not only vertically but also at an angle inclined to the surface (e.g. fine lock pinholes in Monel metal bolts). Mechanical drilling is slow and causes extrusions at both ends of the hole that must be cleaned.

Laser micromachining is the ability to machine very small features such as holes into a metal, ceramic, semiconductor or polymer sheet/film by laser ablation with an unmatched precision, accuracy and speed has opened a very useful scope application of laser material processing in microelectronic industry.

The combination of a high-energy laser pulse for melting coupled with a properly tailored high intensity laser pulse for liquid expulsion results in efficient drilling of metal targets. The improvement in drilling is attributed to the recoil pressure generated by rapid evaporation of the molten material by the second laser pulse.

Laser cleaning is the removal of small particles or continuous layers from a metal surface and it can be carried out by laser beam using a selected area irradiation at an optimum combination of incident power, interaction/pulse time and gas flowrate (that sweeps the dislodged atoms from the surface) [87-95].

At the initial stage, a plasma plume is formed due to ionization of the atoms vaporized from the surface and blocks the beam/surface contact. As the irradiation stops, the temporary compression on the surface changes into tension and causes spallation of the oxidized layer. A dramatic improvement in cleaning efficiency in terms of area and energy is possible when laser beam irradiates the workpiece at an oblique or glancing angle of incidence rather than direct or perpendicular irradiation of the surface.

Laser marking may be used in metallic, polymeric and glassy materials [96-103].

Laser ablation can be applied as a means for direct marking on plastics or polymer compounds as it is fast, economical and ecofriendly compared with the conventional marking processes.

Besides embossing a mark/design on a surface for identification or aesthetics, laser marking is also useful in non-contact and dry etching and printing of polypropylene or polyethylene plastics using a 532 nm laser pulse.

Similarly, laser irradiation can produce controlled micro-cracking or fracture of soda lime and borosilicate glasses.

Laser scribing involves laser ablation of a groove or row of holes that form perforation lines to separate a large substrate into individual circuits. Laser scribing is extensively used for machining of ceramics in the microelectronics industry. The quality of scribing, particularly for silicon chips and alumina substrates is judged by the amount of debris produced and size of HAZ (the smaller the better for both). Laser scribing needs a very low power so as not to melt the surface and the mechanisms responsible for improvement include magnetic domain refinement, stress relaxation and inhibition of domain wall movement. Laser scribing also relieves the stresses that are induced in the material during

manufacture. The scribe lines increase the surface resistivity of the material, resulting in reduced eddy current loss. Laser scribing of polycrystalline thin films used for solar cells can eliminate the frequently observed problem of ridge formation along the edges of scan wavelength range [104].

Chapter 2

Laser-Tissue Interactions

2.1 Experimental models for energy deposition prediction

The prediction of light energy deposition in human tissues is essential during various biological applications [105-113] and for this reason much efforts are being made in the study of light interaction with biological tissue due to the development and wide use of lasers for surgical and therapeutic applications. The rapidly increasing use of light in diagnostic and therapeutic medicine has created the need of exact determination of light distribution in tissues [114-119].

If a laser beam strikes biological tissue, a specific distribution of the laser light inside the irradiated volume is observed. Part of the radiation is absorbed by the tissue and, consequently, may be therapeutically active while another part will be transmitted either directly at or after multiple scattering, this depending on the layer thickness while a further fraction of the photons will be scattered in the tissue and leave it as re-emission.

Only a small percentage will be directly reflected at the surface, due to a step in the value of the refractive index.

The measurable quantities of re-emission, reflection and transmission are often called macroscopic optical properties and are in function of wavelength, tissue type and layer thickness. The distribution of the laser light inside the tissue and the resulting macroscopic optical properties are determined by three processes, absorption, scattering and refraction. If during the laser irradiation the tissue structure changes, as in the case of bleaching by coagulation or blackening by carbonization, the optical properties may considerably change.

Numerous models for the prediction of the fluence rates in tissue, or reflection and transmission of light by tissue have been developed. The accuracy of these models ultimately depends upon how well the optical properties of the tissue are known. Optical parameters are obtained by converting measurements of observable quantities (e.g., reflection) into parameters which characterize light propagation in tissue. The conversion process is based on the theory of light transport in tissue.

In past years, most of the studies have reported values for the total attenuation coefficient, the effective attenuation coefficient, the effective penetration depth, the absorption and scattering coefficients and the scattering anisotropy factor for a variety of tissues at a variety of light wavelengths and their results are based upon approximations to the radiative transport theory (e.g., diffusion theory). Yet sufficient variations in model assumptions (e.g., isotropic-anisotropic scattering or matched-mismatched boundaries), measurement techniques, experimental apparatus, calibration schemes, and biological heterogeneities exist that efforts to extract average values for different tissue types is complicated.

The Monte Carlo simulation technique, which is based on the statistical nature of radiation interactions, has been widely applied in laser radiation transport studies. This mathematical modeling may provide a better understanding of the interaction between tissue and laser depending on the wavelength and help to determine the effective wavelength as a function of penetration in tissue. When the photon is launched, if there is a mismatched boundary at the tissue surface, some specular reflectance will occur. The specular reflectance depends on the average refractive index and on the surface texture [120]. The photon weight after the specular reflection is transmitted into the tissue.

The step size of each launched photon(s) and the azimuthal angle Φ are calculated based on a random sampling of the probability distribution for the photon's free path, the computer's random number generator yields a random variable from 0 to 1:

$$S = -\ln \zeta / \mu_t$$
$$\Phi = 2\pi\zeta$$

where ζ is a random number equally distributed between 0 and 1 ($0 < \zeta \leq 1$). μ_t is the extinction coefficient ($\mu_t = \mu_a + \mu_s$) where μ_a is the absorption coefficient and μ_s is the scattering coefficient [121].

In case of multi-layered tissue, the photon may hit a boundary between each tissue layers during the simulation. The photon can be either internally reflected by the boundary or escape as observed reflectance. Four steps are involved in the simulation when the photon hits a boundary of the layer:

1) The distance between the photon point and the boundary is calculated.

2) Next step decides whether the step size is greater than distance between the photon point and the boundary.

3) If the photon hit a boundary, probability of a photon is computed whether photon being internally reflected, which depends on the angle of incidence onto the boundary [122].

If the angle of incidence is larger than the critical angle, the internal reflectance is set to 1.

4) To determine whether the t photon is reflected by the boundary or transmits into lower tissue, a random number *(ζ)* is generated: if $\zeta \leq R(\theta_i)$, the photon is reflected while if $\zeta > R(\theta_i)$ the photon is transmitted [123].

Some of the transmitted light will re-emerge through the air-skin interface into the air. The re-emergence of light will result in the observed diffuse reflection. Their weights are accordingly scored into the diffuse reflectance or diffuse transmittance depending on where the photon packet exits. The diffuse reflectance comprises photons which enter the tissue and subsequently are scattered back through the irradiated tissue surface. Therefore, the diffuse reflectance determines the probability that a photon is backscattered by either single or multiple scattering interactions, and absorption along its optical path within the tissue depending on the tissue scattering coefficient and scattering anisotropy [124].

As we showed in the study [125] performed in the Photonic Devices Lab of the Department of Engineering and Architecture by using a supercontinuum source on different kinds of rat tissues, generally, each irradiated tissue had no transmission in two wavelength intervals, the first one (350-600 nm) in the visible section of the "therapeutic window" due to the presence of chromophores, the other one in the infra-red portion (1300-1700) due to the water absorption peak (Fig. 2.1)

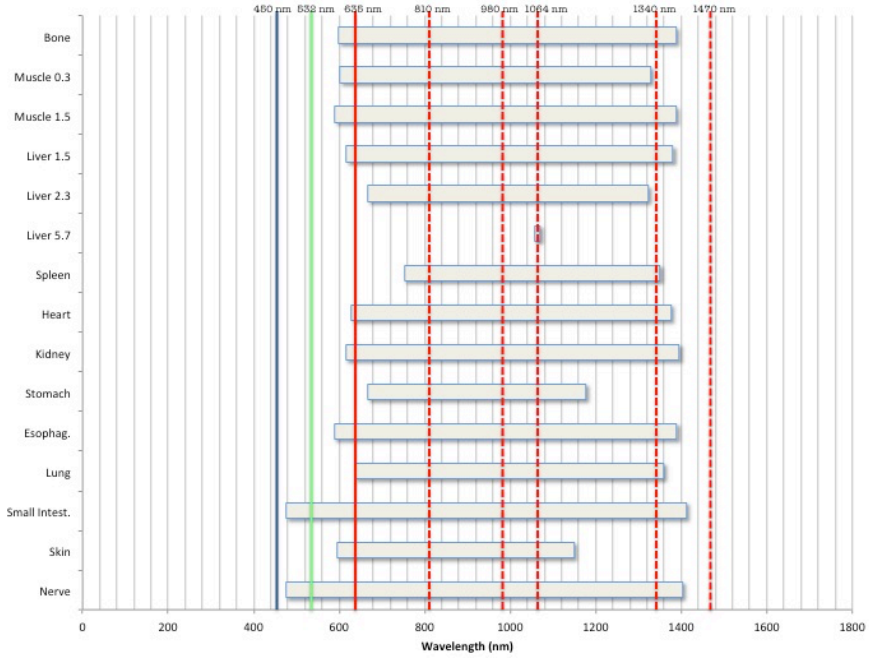

Fig. 2.1 - Graphic visualization of the wavelengths transmitted by the different samples in relationship with the most commonly used laser in surgery and LLLT (in increasing order: Blue diode, KTP, red diode, IR diode, Nd:YAG, Nd:YAP and IR diode) (ref. 125).

2.2 Role of the chromophores in the energy absorption

Chromophores are all the tissue elements absorbing a certain wavelength or spectrum of light energy to a high degree.
In biological tissues the chromophores are predominantly coupled to cellular components (e.g. to membranes), or they are present in the form of a cellular substructure like the nucleic bases of DNS/RNS. In the NIR and MIR, tissue absorption is dominated mainly by the absorption in water. Absorption by molecules, e.g. glucose, plays an insignificant role. Besides low-energy electronic transitions, mainly higher harmonics and combination vibrations will be excited. The combination bands are composed of hydrogen tensile vibrations contributed mainly by molecular groups like N-H (amino), O-H (hydroxyl) and C-H (hydrocarbon).
The scattering behaviour of biological tissue is also important because it determines the volume distribution of light intensity in the tissue. This is the primary step for tissue interaction, which is followed by absorption and heat generation. Scattering of light in tissue is caused by inhomogeneity such as cell membranes or intracellular structures. Scattering arises due to a relative refractive index mismatch at the boundaries between two such media or structures, e.g. between the extracellular fluid and the cell membrane. Scattering of a photon is accompanied by a change in the propagation direction without loss of energy and the scattering structures of the tissue can be:

1) macroscopic like muscle fibers, skin layers, or dentin tubules.
2) microscopic like cells or intracellular structures.
3) sub-microscopic, considering macromolecules or nanoparticles.

Scattering, is expressed by the scattering coefficient μ_s (cm^{-1}). The inverse parameter, $1/\mu_s$ (cm), is the mean free path length until a next scattering event occurs. For red light in the human skin, the mean free path length for absorption is 50 μm, and the mean free path length for scattering is 5 mm: this means that, statistically, a photon is scattered 100 times until it is absorbed.
The energy states of molecules are quantized; therefore, absorption of a photon takes place only when its energy, $E = h\nu$, corresponds to the energy difference between such quantized states.
Absorption of a photon by a chromophore causes either a quantized change in the distance between charges (electron transition, ultraviolet or visible spectrum) or a quantized change of vibrational modes of the molecule (vibration transition, near infrared [NIR]).
Absorbing molecular components of the tissue are porphyrin, haemoglobin, melanin, flavin, retinol, nuclear acids, deoxyribonucleic acid (DNA)/ribonucleic acid (RNA), and reduced nicotinamide adenine dinucleotide, where electronic transitions are excited, leading to discrete and intense (broad) absorption bands. In the NIR and mid-infrared (MIR) region, tissue absorption is dominated by water absorption, with the maximum at 3 μm, as shown in Fig. 2.2.

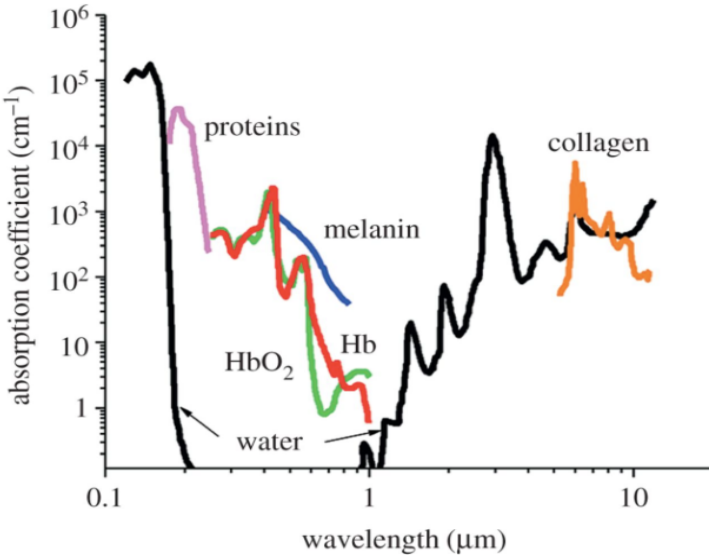

Fig. 2.2 - Absorption coefficients of the main chromophores in tissues (ref. 126).

The absorption coefficient α characterizes the absorption and it is the product of absorber concentration c_a (cm^{-3}) and absorption cross-section σ (cm^2), measured in cm^{-1}.
In general, different absorbers contribute at one wavelength, consequently μ_a must be considered the sum of all substances involved:

$$\mu_a = \Sigma c_a \, \sigma_a$$

Biological tissues typically display absorption coefficients in the range 0.01 cm^{-1} < μ_a < 100 cm^{-1} [126, 127] and generally, in tissue optics the absorption coefficient is given in mm^{-1} (1 mm^{-1} = 10 cm^{-1}).
For exclusively absorbing materials the intensity of the part I_T transmitted through a layer of thickness d (cm) can be easily calculated according to Beer-Bouger-Lambert law.
If I_0 is the intensity on entry into the substrate:

$$I_T = I_0 \exp(-\mu_a d)$$

The variety of interaction mechanisms that may occur when applying laser light to biological tissue is multifarious, depending both by the tissue characteristics (reflection, absorption and scattering coefficients, heat conduction and capacity) both by the laser parameters (wavelength, exposure time, applied energy, focal spot size, power density and fluence).

Although the number of possible combinations for the experimental parameters is unlimited, most of authors agree that the three main categories of laser- tissue interactions are: Photochemical interactions, Photothermal interactions, Photomechanical interactions (Fig. 2.3).

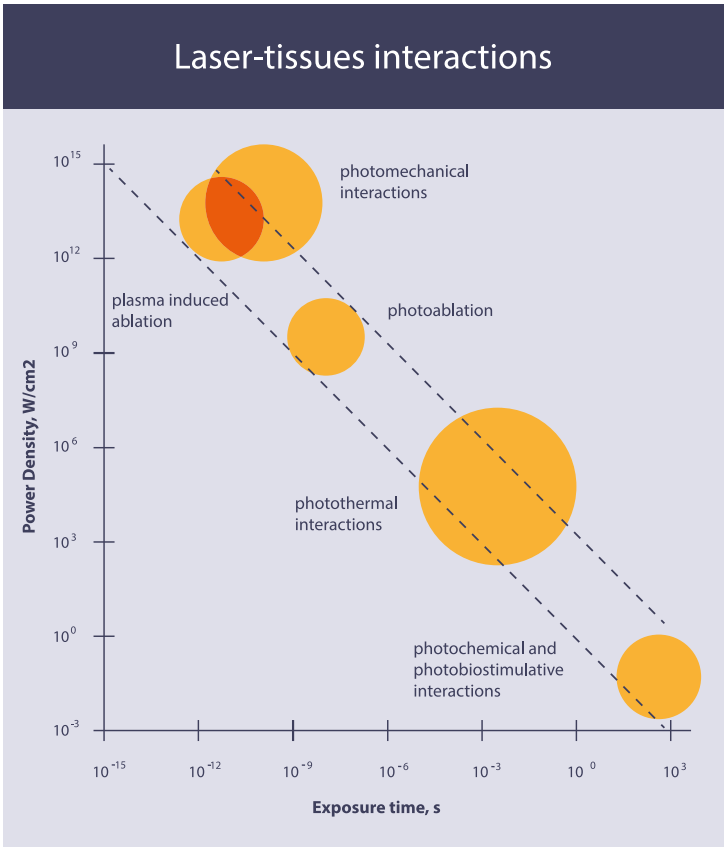

Fig. 2.3 - The main laser-tissue interactions in function of the PD and time of irradiation (ref. 106).

2.3 Photochemical interactions

The group of photochemical interactions stems from empirical observations that light can induce chemical effects and reactions within macromolecules or tissues and the most popular example, created by the evolution itself, it is represented by the photosynthesis. In the field of medical laser physics, the two main applications of the photochemical interactions are the photodynamic therapy (PDT) and the biostimulation or Low Level Laser Therapy (LLLT) and both take place at very low power densities, typically 1W/cm^2, and require long exposure times ranging from seconds to CW.

PDT was first developed at the beginning of the twentieth century in Munich when Oscar Raab and his professor, Herman von Tappeiner, noticed the effects of photosensitivity on paramecia. Raab observed the rapid death of the protozoon *Paramecium caudatum* after light exposure in the presence of acridine dye. The presence of light, which modified the effect of the dye, led to the identification of a photosensitizer. Subsequently, Professor von Tappeiner went on to carry out other experiments and discovered that the presence of oxygen was necessary for the reaction occurring, thus creating the term PDT.
PDT involves the administration of a photosensitizing agent into the tissue of a tumor, followed by the activation of this agent using light at a specific wavelength. The treatment consists of two stages. In the first stage, the photosensitizing agent is accumulated, particularly in the tumor cells, following topical or systemic administration. In the second stage, the photosensitized tumor is exposed to light at a wavelength that coincides with the absorption spectrum of the photosensitizing agent. As shown in Fig. 2.4, this activated agent transfers energy to molecular oxygen, generating reactive oxygen species (ROS); the subsequent oxidation of the lipids, amino-acids and proteins induces necrosis and apoptosis. In addition, ROS indirectly stimulate the transcription and release of inflammatory mediators [128].

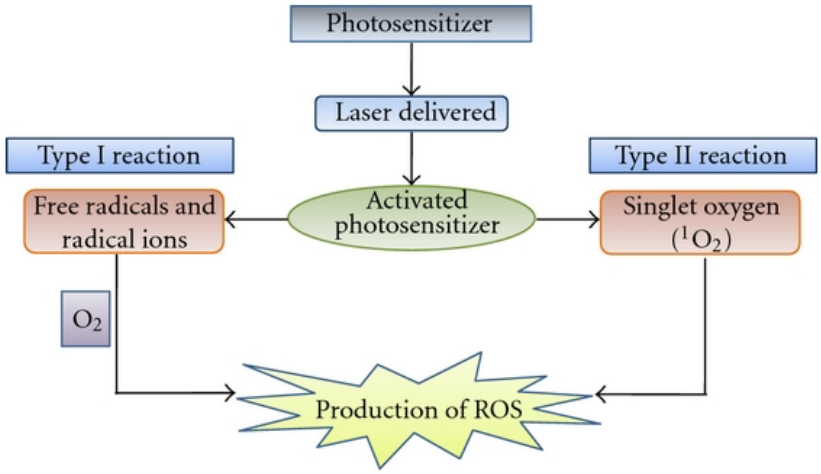

Fig. 2.4 - Main reactions involved in Photo Dynamic Therapy (ref. 128).

Oxidation of the cell constituents by ROS damages the plasma membranes and the cell organelles, with a subsequent alteration in permeability and transport function between the intra- and extracellular media. Inhibition of mitochondrial enzymes appears to represent a key event in cell death by PDT [129]. An apoptotic response to PDT was reported by Agarwal et colleagues in 1991 [130]. This response may be directly induced by PDT without any need for the transduction of intermediary signs that may be lacking in certain drug- resistant neoplastic cells. Cell death by PDT does not appear to depend on the phase of the cell cycle or on genetic factors (e.g. p53 gene) [131].

PDT targets include tumor cells, tissue micro- vasculature and the host's inflammatory and immune systems. It appears clear that the combination of all these components is required to achieve long term control of the tumor. The main characteristic of the inflammatory process is the release of vasoactive substances, components of the complement, proteinases, peroxidases, cytokines, growth factors and other immuno-regulators. There is evidence of an increase in the regulation of interleukin-1-beta (IL1beta), interleukin-2 (IL-2), tumor necrosis factor alpha (TNF alpha) and granulocyte colony-stimulating factor (G-CSF) [132].

Biomodulation was born in Hungary in 1967 when Endre Mester noticed the ability of the He-Ne laser to increase hair growth [133] and stimulate wound healing in mice [134], and, shortly afterward, he began to use lasers to treat patients with non-healing skin ulcers [135]. Since those early days, the use of low-power lasers (as opposed to high-power lasers that can destroy tissue by a photothermal effect) has steadily increased in diverse areas of medical practice that require healing, prevention of tissue death, pain relief, reduction of inflammation, and regenerative medicine.

Low-Level Laser Therapy (LLLT) uses low-powered laser light in the range of 1-1000 mW, at wavelengths from 632-1064 nm, to stimulate a biological response. These lasers emit no heat, sound, or vibration. Instead of generating a thermal effect, LLLT acts by inducing a photochemical reaction in the cell.

Mitochondria are considered the power generators of the eukaryotic cell, converting oxygen and nutrients through the oxidative phosphorylation process and electron transport chain into adenosine triphosphate (ATP). The basic idea behind cellular respiration is that high-energy electrons are passed from electron carriers, such as reduced nicotinamide adenine dinucleotide (NADH) and the reduced form of flavin adenine dinucleotide (FADH2), through a series of transmembrane complexes (including cytochrome c oxidase [CCO]) to the final electron acceptor, generating a proton gradient. The gradient is used by FOF1 ATP synthase to produce ATP. Various in vitro experiments, such as those that use rat liver isolates, found that cellular respiration was upregulated when mitochondria were exposed to a He-Ne laser or other forms of illumination. Laser irradiation caused an increase in mitochondrial products (such as ATP [136, 137], NADH, protein, ribonucleic acid [RNA] [138]) and a reciprocal augmentation in oxygen consumption. As shown in Fig. 2.5, a similar effect is produced when tissue that contains mitochondria is exposed to low-level radiation. Visible and near-infrared (NIR) light is absorbed by the organelle, and an upregulation of cellular respiration is observed [139].

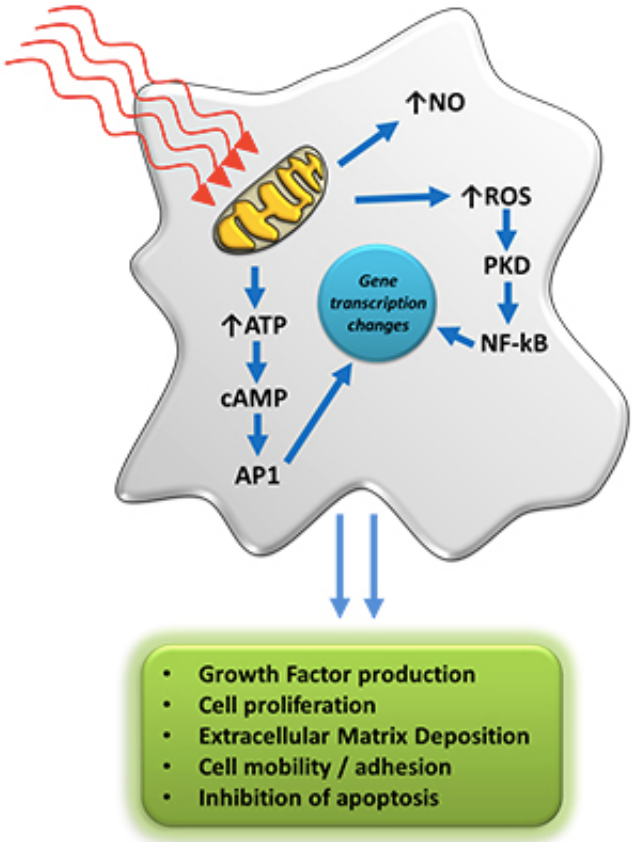

Fig. 2.5 - Action of biomodulation on mitochondria and consequent biochemical effects activation (ref. 139).

LLLT promotes the synthesis of deoxyribonucleic acid (DNA) and RNA [140] and increases the production of proteins [141]. It also modulates enzymatic activity [142], affects intracellular and extracellular pH [143] and accelerates cell metabolism [144]. The expression of multiple genes related to cellular proliferation, migration, and the production of cytokines and growth factors also have been shown to be stimulated by low-level light [145].

Today, LLLT is used by physical therapists to treat a wide variety of acute and chronic musculoskeletal aches and pains, by dentists to treat inflamed oral tissues and to heal diverse ulcerations [146, 147], by dermatologists to treat oedema, non-healing ulcers, burns, and dermatitis [148, 149], by orthopedists to relieve pain and treat chronic inflammations and autoimmune diseases [150], and by other specialists, as well as general practitioners. Laser therapy is also widely used in veterinary medicine [151] (especially in racehorse-training centres), and in sports-medicine and rehabilitation clinics [152] to

reduce swelling and hematoma, relieve pain, improve mobility, and treat acute soft-tissue injuries.

2.4 Photothermal interactions

The term "phototermal interactions" stands for a large group of laser-tissue interaction types where the increase in local temperature is the significant parameter change, induced by either CW or pulsed laser radiation.
Photothermal interaction is a complex process resulting from three distinct phenomena: conversion of light to heat, transfer of heat and the tissue reaction, which is related to the temperature and the heating time [153].
This interaction leads to denaturation or to the destruction of a volume of tissue. The known factors are the parameters of the laser (wavelength, power, time and mode of emission, beam profile and spot size) and the tissue being treated (optical coefficients, thermal parameters and coefficients of the reaction of thermal denaturation).
Thermal action of a laser beam can be described as one of these types, depending on the degree and the duration of tissue heating [154]:
Hyperthermia: meaning a moderate rise in temperature of several ºC, corresponding to temperatures of 41º to 44º for some tens of minutes and resulting in cell death due to changes in enzymatic processes. This is a difficult procedure to control and so it is little used in practice.
Coagulation: refers to an irreversible necrosis without immediate tissue destruction. The temperature reached (50º to 100º C) for around a second, produces desiccation, blanching, and a shrinking of the tissues by denaturation of proteins and collagen.
Vaporization: means a loss of material. The various constituents of tissue disappear in smoke at above 100º C, in a relatively short time of around one tenth of a second. At the edges of the vaporization zone there is a region of coagulation necrosis: there is a gradual transition between the vaporization and healthy zones. The haemostatic effect is due to this region of coagulation necrosis. If the vaporized zone has a large area of some millimetres in diameter, it is possible to destroy tumours bigger than those treated by a simple coagulation. If the vaporized region is narrow, a cutting effect is then obtained.
Carbonization: at temperature above approximatively 100° the tissue starts to carbonize leading to a blackening in colour. In surgery, even if carbonization may reduce visibility during the intervention, it should be avoided in any case, since tissue already becomes necrotic also at lower temperatures.
Melting: in the teeth irradiated at high power, the temperature may reach a few hundred degrees Celsius: it is possible to observe melted and afterwards down-cooled tooth substance as well as gas bubbles like solidified lava.

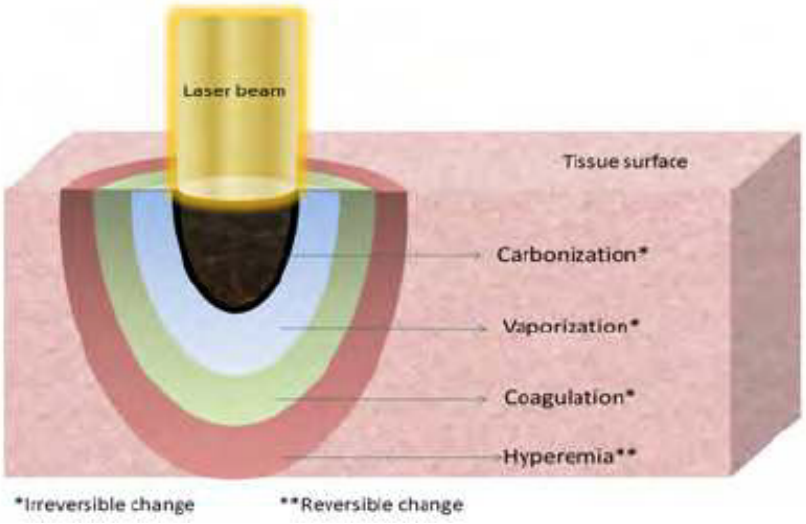

Fig. 2.6 - Laser photothermal effects (ref. 107).

Frequently, not only one but several effects are induced in biological tissue, ranging from carbonization at the tissue surface to hyperthermia a few millimetres inside the tissue and depending on the laser parameters.
Reversible and irreversible tissue damage can be distinguished: while carbonization, vaporization and coagulation are certainly irreversible processes because they induce irreparable damage, hyperthermia can turn out to be able a reversible or irreversible process, depending on the type of tissue and the laser parameters [155].

2.5 Photomechanical interactions

Mechanical effects can result from either the creation of a plasma, an explosive vaporization, or the phenomenon of cavitation, each of which is associated with the production of a shock wave.
With nano- or pico-second pulsed lasers, a very high intensity of luminous flux over a small area (around 1010 W/cm^2) ionizes atoms and creates a plasma [156]. At the boundary of the ionized region, there is a very high-pressure gradient which causes the propagation of a shock wave. It is the expansion of this shock wave which causes the destructive effect. These lasers are used principally in ophthalmology for breaking the membranes which often develop after the implanting of an artificial lens. The protection of the retina is possible by two different mechanisms: firstly, the plasma produced is self-absorbing, so preventing the light from reaching the retina (plasma shielding); in addition, the wide angle of focusing results in a very divergent beam after the focal point and the

light reaching the retina has too low a power density to represent a significant danger [157].

When the exposure time of the laser is lower than the characteristic time of thermal diffusion in the tissue, it produces a thermal containment, with an accumulation of heat without diffusion and an explosive vaporization of the target: this is the mechanism involved in selective photothermolysis; if a mechanical containment is added to a thermal containment, the explosive vaporization does not occur, and a gas bubble is created which will implode when the laser beam is interrupted, creating the phenomenon of cavitation: this is the mechanism which is used for fragmentation of urinary calculi by a laser emitting micro-second pulses [158].

Photoablation, discovered by Srinivasan and Mayne-Banton in 1982, is defined by as a pure ablation of material without thermal lesions at the margins and the typical threshold values for this type of interaction are around 108 W/cm^2. It occurs because of the principle of dissociation: with very short wavelengths (190 to 300 nm), the electric field associated with the light is higher than the binding energy between molecules. The molecular bonds are broken and the tissue components are vaporized, without generation of any heat at the edges [159]. Photoablation can be summarized as a two-steps process, considering the two atoms A and B:

Excitation: $AB + hv \longrightarrow (AB)^*$

Dissociation: $(AB)^* \longrightarrow A+B+ E_{kin}$

This effect is obtained with lasers of very energetic wavelengths such as those emitting in the ultra-violet (excimer lasers emit at 193 nm (ArF), 248 nm (KrF) or 308 nm (XeCl)). The action is very superficial, only over several microns, because light at these wavelengths is very strongly absorbed by tissue.

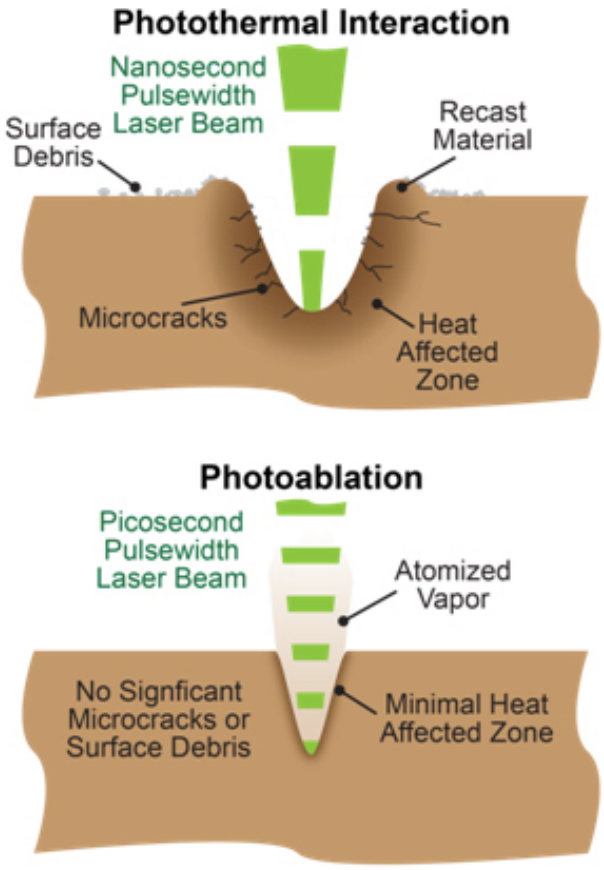

Fig. 2.7 - Difference between photothermal interaction and photoablation (ref. 159).

The photodisruption (from Latin: ruptus= ruptured) may be regarded as a multi-cause mechanical effect starting with optical breakdown and including shock wave generation, cavitation and jet formation and all these effects take place at different time scale [160]. In fact, while plasma formation begins during the laser pulse and lasts for a few nanoseconds afterwards (the time needed for the free electron diffusion into the surrounding medium), shock wave generation is associated with the expansion of the plasma and, 30-50 ns later, slows down to an ordinary acoustic wave; finally, cavitation, which is a macroscopic effect, starts 50-150 ns after the laser pulse and, after several oscillations of expansion and collapses within a period of a few hundred microseconds, generates a jet formation of a speed up to 156 m/sec [161] in the bubbles near a solid boundary.

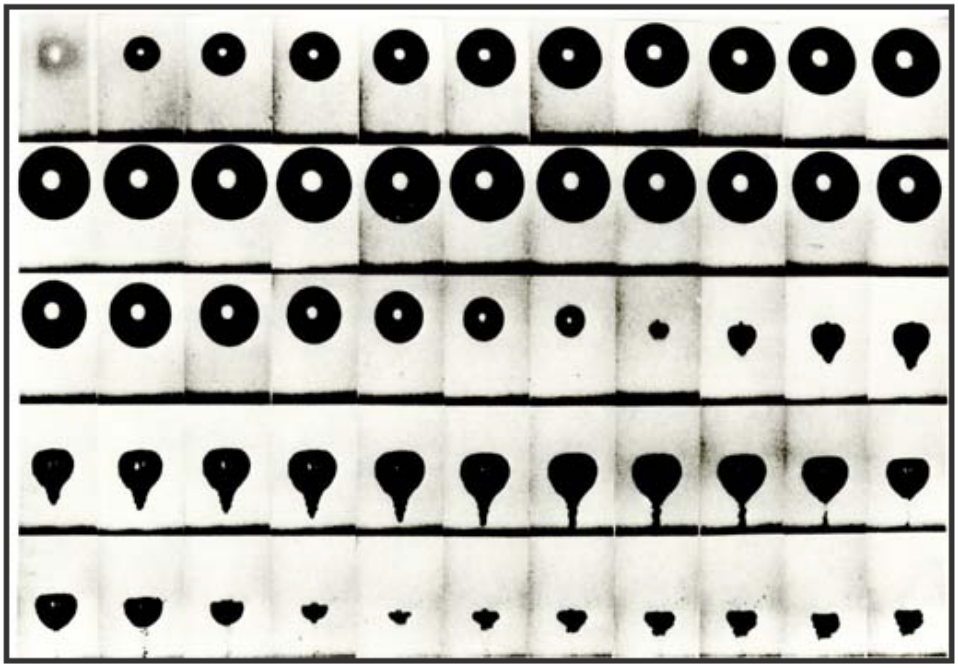

Fig. 2.8 - High-speed micro-cinema-graphic sequence of laser-induced cavitation near a solid surface shows the formation of a micro-jet impact with a velocity of approximately 400 km per hour (ref. 107).

The typical parameters of the photodisruption may be considered a pulse duration between 100 fs and 100 ns and a power density between 1011 and 1016 W/cm^2.

Chapter 3

Laser in Dentistry

3.1 History of laser in medicine

The laser medicine started in 1960 when some pioneers, such as dr. Leon Goldman, began research on the interaction of laser light on biologic systems, including early clinical studies on humans [161]. Interest in medical applications was intense, but the difficulty controlling the power output and delivery of laser energy, as well as the relatively poor absorption of these red and infrared wavelengths led to inconsistent and disappointing results in early experiments. The exception was the application of the ruby laser in retinal surgery in the mid-1960s [162]. In 1964, the Argon Ion laser was developed: this continuous wave 488 nm (blue-green) gas laser was easy to control, and its high absorption by haemoglobin made it well suited to retinal surgery, soon making clinical systems for treatment of retinal diseases available.
In 1964, Nd:YAG (Neodymium: Yttrium Aluminum Garnet) laser and CO_2 (Carbon Dioxide) laser were developed at Bell Laboratories, this last laser emitting a CW infrared beam at 10600 nm in an easily manipulated and focused beam well absorbed by water. Because soft tissue consists mostly of water, researchers found that CO_2 laser beam could cut tissue like a scalpel, but with minimal blood loss. The surgical uses of this laser were investigated extensively from 1967-1970 by pioneers such as Dr. Thomas Polanyi and dr. Geza Jako and, in the early 1970s, use of the CO_2 laser in ENT (ears, nose, and throat) and gynecologic surgery became well established, though limited to academic and teaching hospitals [163].
Dye lasers became available in 1969 and Excimer lasers, in 1975. Since then, many other different laser systems have become available for industrial scientific and telecommunications applications, as well as medical uses.

In the early 1980s, smaller but more powerful lasers became available, and were soon appearing in community hospitals and even physicians' offices. Most of these systems were CO_2 lasers used for cutting and vaporizing, and Argon lasers for ophthalmic use. Nd:YAG and KTP laser systems were used by larger hospitals for the new field of laparoscopic surgery. These "second generation" lasers were all continuous wave, or CW systems, which means to cause non-selective heat injury, and the proper use required a long "learning curve" and experienced laser surgeons.
The single most significant advance in the use of medical lasers was the concept of "pulsing" the laser beam, which allowed selective destruction of abnormal or undesired tissue, while leaving surrounding normal tissue undisturbed. The first lasers to fully exploit it were the pulsed dye lasers introduced in the late 1980s for the treatment of port wine stains and strawberry marks in children, followed by the first Q-switched lasers for tattoo removal [164, 165]. Another major advance was the introduction of scanning devices in the early 1990s, enabling precision computerized control of laser beams. Scanned, pulsed lasers revolutionized the practice of plastic and cosmetic surgery by making safe, consistent laser resurfacing possible, as well as increasing public awareness of laser medicine and surgery.
Medical lasers have made it possible to treat conditions previously considered untreatable, or difficult to treat. Patients benefit by improved results and less cost. In the last few years, the main focus of research and development of medical lasers has been on laser hair removal, the treatment of vascular lesions including leg veins, and vision correction. The thrust of current research is directed towards non-ablative laser resurfacing ("laser skin toning"), "no-touch" computerized vision correction, and improved photodynamic therapy for treatment of skin cancer and for hair removal [166].

3.2 Early applications of laser in dentistry

The first application of laser technology in dentistry was described by Goldman in 1964, four years after the realization of the first laser device, the "Ruby Laser", by Maiman in 1960 [167].
The main reasons of this delay are, on the one hand the difficulty of the beam delivering in a small cavity such the mouth which was solved only by the finalizing of efficient delivery systems and, on the other hand the necessity to utilize different wavelengths due to the different target tissues present into the oral cavity.
Another problem found by the first researchers who used laser technology in oral applications was the need of limit thermal elevation under values compatible with the biological integrity of the tissues.
For this last reason the first studies, including those by Goldman, Kinersly, Morrant, Stern and Taylor may be reminded only for their historical relevance [168, 169] by considering the paper by Frame in 1984 as the first which described an "in vivo" oral surgery intervention using a CO_2 laser without collateral biological damages [170].

Further work in the 1970's focused on the effects of neodymium (Nd:YAG) and carbon dioxide (CO_2) lasers on dental hard tissues. Early researchers found that CO_2 and Nd:YAG lasers produced cracking and disruption of enamel rods, incineration of dentinal tubule contents, excessive loss of tooth structure, carbonization and fissuring and increased mineralization caused by the removal of organic contents [171]. It was also reported that the use of the CO_2 laser was unfavourable because of the loss of the odontoblastic layer [172].

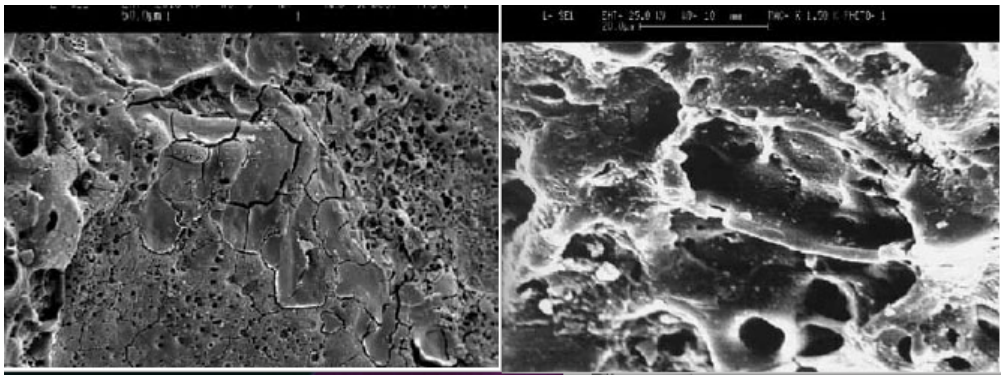

Fig. 3.1- Effects of Nd:YAG irradiation on human dental enamel. (Left: 500X, Right: 1500X): micro-cracks, melting and craters are present.

Therefore, for many years, the utilization of laser in dentistry was limited only to the soft tissue surgery.

3.3 Use of laser in hard dental tissues

In 1990 laser technology was introduced in conservative dentistry by Hibst and Keller, who described the possibility to use an Er:YAG laser as alternative to conventional instruments, such as the turbine and micro-motor [173, 174]. Widespread interest in employing this new technology stems from the number of significant advantages, as described in several scientific studies. Thanks to the affinity of the Er:YAG laser wavelength (2940 nm) to water (absorption peak = 3000nm) and hydroxyapatite (absorption peak = 2800nm), as shown in Fig. 3.2, laser technology allows for efficient ablation of hard dental tissues without the risk of micro- and macro-fractures, as have been observed with the use of conventional rotating instruments [175, 176]. The dentin surface treated by laser appears clean, without a smear-layer and with the tubules open and clear [177].

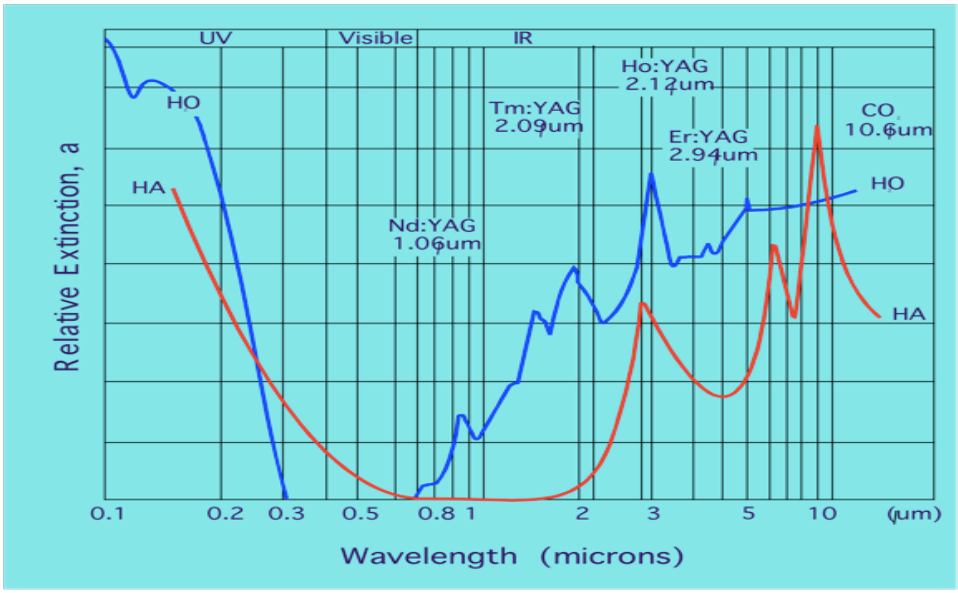

Fig. 3.2 - Absorption spectra of water and hydroxyapatite (ref. 175).

Thermal elevation in the pulp, recorded during Er:YAG laser irradiation, is lower than that recorded by using a turbine and micro-motor with the same conditions of air/water spray [178, 179]. This wavelength also has an antimicrobial decontamination effect on the treated tissue, which destroys both aerobic and anaerobic bacteria [180]. The most interesting aspects of this new technology are related to the goals of modern conservative dentistry: i.e. minimally invasive treatments and adhesive dentistry. Er:YAG lasers can reach spot dimensions smaller than 1 mm which enables a selective ablation of the affected dentin while preserving the surrounding sound tissue to produce highly efficient restorations [181]. Several in vitro studies have demonstrated that the preparation of enamel and dentine by Er:YAG laser, followed by orthophosphoric acid-etching, enhances effectiveness in terms of reduced micro-leakage and increased bond strength [182].

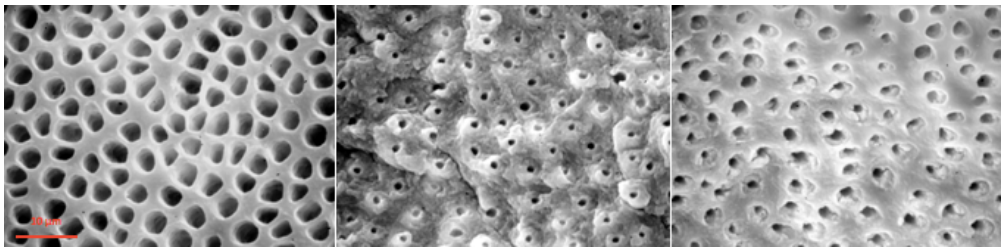

Fig. 3.3 - Dentine conditioning: bur + orthophosphporic acid (left), Laser (centre), Laser + orthophosphoric acid (right).

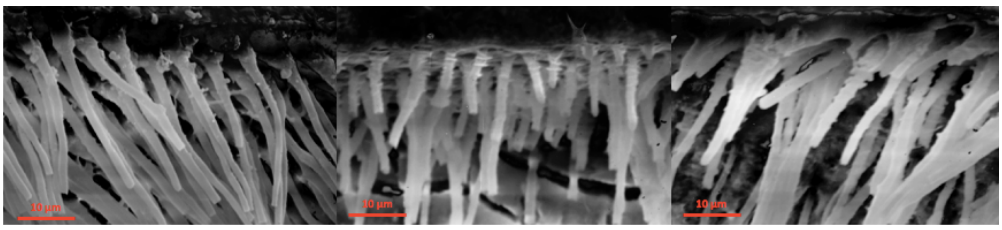

Fig. 3.4 - Resin tags into the dentine prepared by bur + orthophosphporic acid (left), Laser (centre), Laser + orthophosphoric acid (right).

3.4 Diode lasers in dentistry

A great improvement was reached in 2000's with the introduction of the diode lasers: in fact, this family of lasers, based on the semiconductor technology, and allowing to reduce size, costs and the necessity of maintenance, made the utilization of the coherent light in dentistry very popular.
While for many years the diode laser wavelengths used in dentistry have been around 1000 nm, thanks to the great absorption in haemoglobin and so able to give a good haemostasis of the operative field, in the last years a great interest was focused on the lasers emitting in the visible portion, particularly the blue, and in the far infrared, 1500 and 2000 nm, to get all the advantages derived by a great absorption in the water.
Unfortunately, the main limit of the diode laser utilization in dentistry are related to the possibility to treat only the oral soft tissues: in fact, it results very effective when used in oral surgery but it cannot be utilized on the teeth for conservative dentistry.
The employment of laser in dentistry may be up to day summarized in three main targets:
-hard dental tissues (teeth, bone): the clinic utilization includes mainly the conservative dentistry and the bone surgery and it may be performed only by the Erbium family lasers (Er:YAG and Er, Cr:YSGG).
-soft dental tissues (vascularized and keratinized gum): its applications consist of the oral surgery interventions and normally Nd:YAG, CO_2 and diodes are the first choice lasers.
-ceramics surfaces (etchable and non etchable porcelain): its employing is related to the characterization of the internal surfaces of ceramic prosthetics to enhance the adhesion to the teeth and the CO_2, Nd:YAP and Nd:YAG laser are utilized.
By these considerations, it arises that the possibility to have wavelength able to be effective in all the three targets described might be a great success.

3.5 Fiber lasers and their possible role in dentistry

Fiber lasers, a new generation of lasers that has recently become commercially available, present important advantages as compared with previous technologies in terms of source brilliance, stability of the oscillating mode, efficiency, possibility of a monolithic packaging and low-maintenance costs. There are a lot of features that differentiate fiber lasers from the other existing laser technologies and give them superior overall performance. Due to large surface-to-volume ratio, fiber lasers provide better thermal management and almost total elimination of thermal lensing, which plagues solid-state crystal counterparts. The well controlled spatial distribution of the signal, provided by the continuous guidance, results in superior beam quality and stability, while small quantum defect, as well as, low cavity and transmission losses result in record wall-plug efficiencies. Also, fiber lasers show turn-key operation and small foot print. Their unique properties, particularly the output power stability and unparalleled beam quality at high output powers, have increased their market penetration and have enabled a great number of new applications. The amorphous nature of glass host in the fiber core produces inhomogeneously broadened active-ion emission and absorption spectra, which are wider than they would be in crystals. This enables fiber lasers to be widely tuned and work efficiently from continuous-wave (CW) operation to ultra-short optical pulses. They show high gain, which enables master- oscillator power amplifier (MOPA) and cascaded amplifier con- figurations and makes them suitable for average power scaling. However, the small saturation energy, associated with the relatively small—compared to solid-state rod counterparts—fiber core diameter compromises the energy storage capabilities and high energy operation.

Fiber lasers are sources where the active medium is an optical fiber with core doped by active ions such as Nd (neodymium), Yb (ytterbium), Er (erbium), Tm (thulium) [183]. Even if the first fiber laser was constructed in 1963 by Elias Snitzer [184, 185], for several years rare earth doped fiber lasers have been able to produce only few mW of output power [186]. It was in fact only two decades later, in the 1980s, that the first commercial fiber laser using single mode diode pumping and emitting a few tens of mW appeared in the market. Since then, this kind of laser has become very popular, due to its large gain and the feasibility of single-mode continuous wave operation not achievable in the common crystal laser versions [187]. The fundamental difference between traditional solid-state lasers and fiber lasers lies in the form of the gain medium. In fact, while bulk crystal lasers are typically based on conventional rod or slab geometries, in fiber lasers active ions are added into the core of an optical fiber, often with a length of many metres [188]. This laser family emits in a wide range of wavelengths, depending on dopants and host materials, operates in continuous wave (CW) or pulsed mode. CW output powers of several kW [189] and pulse energies up to around 30 mJ [190] can be currently obtained with Yb-doped fiber lasers. When compared to other sources, fiber lasers have a great number of advantages, such as high efficiency (>30% pump to signal conversion), high

brightness, excellent beam quality, high output powers and easy coupling into other fibers or systems [191-195].

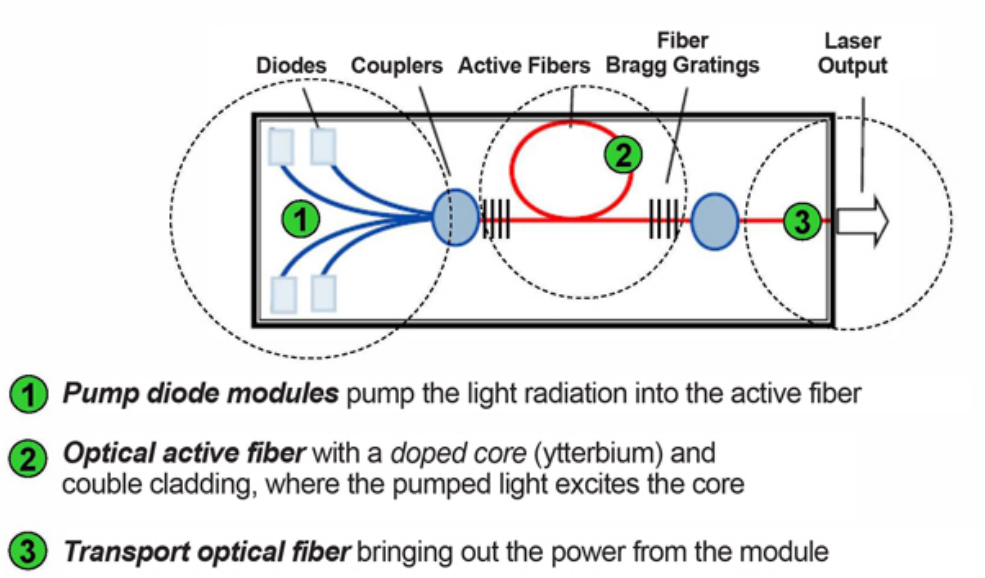

Fig. 3.5 - Scheme of a fiber laser (ref. 187).

The most common applications of fiber lasers regard the industrial field, where they are used mainly for material processing (i.e., for cutting and marking). The main utilizations of fiber lasers in medicine are related to the lithotripsy [196], the surgical treatment of vascular lesions [197], the non-surgical skin aesthetic procedures [198, 199], the urinary surgery [200], and the eye surgery [201].
The aim of this study was to evaluate the effectiveness of the use of fiber lasers for dental applications, particularly on soft tissues, hard tissues and ceramic surfaces.

Chapter 4

Fiber lasers and soft tissue surgery

4.1 Introduction

As reported in the previous chapter, the first application of laser technology in medicine was described by Goldman in 1964, four years after the realization of the first laser device, the "Ruby Laser", by Maiman in 1960.
One of the main problems found by all the first researchers who used laser technology for biological tissues was the need of limit thermal elevation under values compatible with their biological integrity.
To avoid the tissues overheating, and the consequent thermal damage, more and more solutions have been provided by the laser manufacturers. For example, there is the possibility to get an air-water spray directed in the same point of the laser-tissue interaction [202]. As an alternative, very low output powers can be used [203], or the laser source can be operated in chopped or pulsed mode, with short irradiation times and long pauses to favour the thermal relaxation [204].
The aim of this *ex vivo* study on fresh beef tongue samples was to estimate the performance of fiber lasers for the soft tissue oral surgery, by the tissue modifications evaluation with a qualitative microscopic observation, and the thermal elevation during the irradiation using a Fiber Bragg Grating (FBG) temperature sensor connected to an interrogator. A FBG is a wavelength-dependent reflector obtained by introducing a periodic refractive index modulation within the core of an optical fiber [205]. Whenever a broad-spectrum light beam impinges on the grating, a portion of its energy is transmitted through, and another reflected off. The reflected light signal is very narrow and centred at the Bragg wavelength. Any change in the grating refractive index or length caused by strain or temperature results in a Bragg wavelength shift [206]. As consequence, FBGs

have the potential for the measurement of strain/deformation and of temperature, with successful applications reported in many different fields, including monitoring of highways, bridges, aerospace components, and in chemical and biological sensors.
Different tests have been performed with a pulsed fiber laser emitting at 1070 nm, with maximum average output power of 20 W and fixed pulse duration of 100 ns. Experimental results have demonstrated that the best properties in term of cutting capability and the lowest heat-induced damages to the tissue can be obtained with a peak power of 2 kW, a repetition rate of 50 kHz and a speed of 5 mm/s.

4.2 Materials and Methods

Fiber laser device
The device used, was a 1070 nm pulsed fiber laser (AREX 20) provided by Datalogic, Italy. The source has a maximum average output power of 20 W and a fixed pulse duration of 100 ns, while the repetition rate ranges from 20 kHz to 100 kHz. By using a dedicated software, it is possible to determine in advance the shape and the dimension of the irradiation area (line, square, etc), as well as the number of passages (Fig. 4.1).

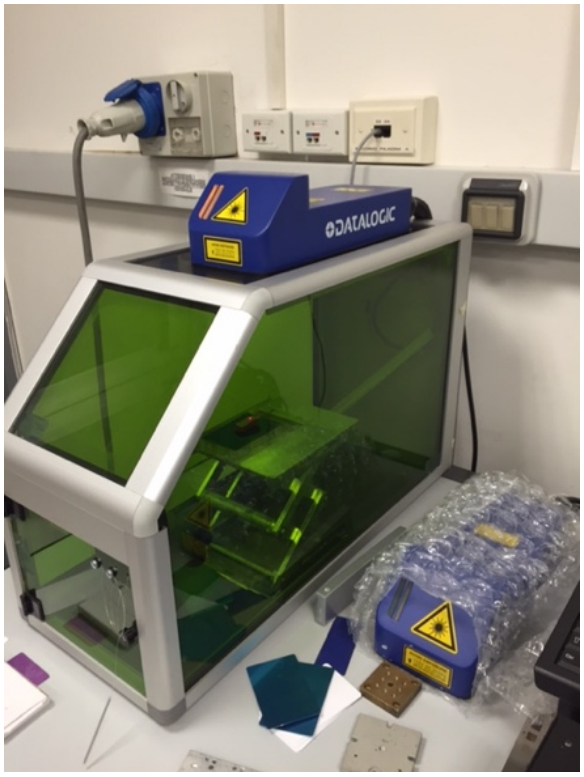

Fig. 4.1 - The pulsed fiber laser (AREX 20, Datalogic, Italy) used for the tests.

FBG Interrogator

Differently to our previous "ex vivo" studies, where we used thermocouples to investigate the temperature variations due to laser irradiation [207-209], in these tests we employed a FBG-based sensor to measure temperature during all the irradiation time and the relaxation time. To monitor the thermal elevation, a 25 mm-long FBG with centre wavelength of 1550 nm, reflectivity of 96% and acrylate coating, imprinted in a standard SMF (AOS GmbH, Germany), has been connected to an interrogator. The device used was the Dynamic Optical Sensing Interrogator sm130-500 (Micron Optics Inc, Atlanta, USA) (Fig. 4.2), which is a compact, industrial grade, dynamic optical sensor interrogation module, field proven for robust, reliable, and long term operation. The software included with the sensing interrogator system provides a single suite of tools for data acquisition, computation, and analysis of optical sensor networks. A temperature-induced wavelength shift of about 13 pm/°C has been considered for the FBG at 1550 nm [205]. In biological field, the use of FBG sensors have several advantages thanks to their valuable characteristics, i.e., acceptable accuracy and sensitivity, and robustness. Moreover, the use of non-metallic probes is advisable to reduce thermal conduction along the sensor itself.

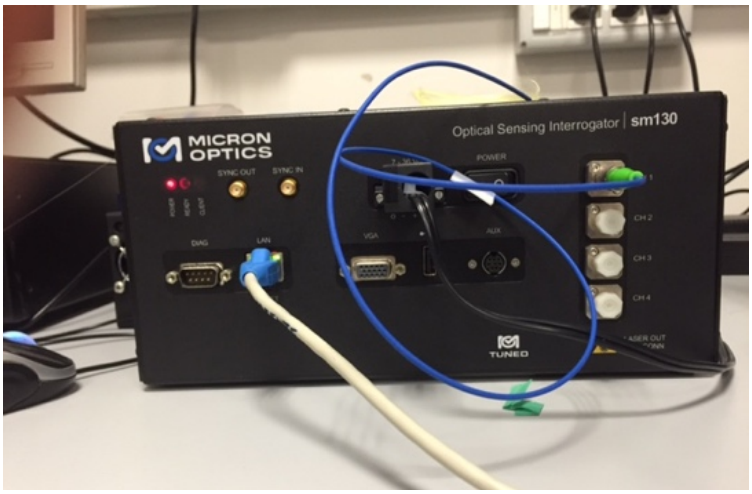

Fig. 4.2 - The Dynamic Optical Sensing Interrogator sm130-500 used for the temperature recording.

Samples collection

The tests were performed on 16 samples obtained by two fresh beef tongues. They were provided by a local abattoir, following the pertinent Italian legislation. From the ventral side of each tongue samples of 15 x 10 mm dimension and 4 mm of thickness obtained.

To avoid the tissue degradation, all the specimens were kept at a temperature of 2-4°C and 100% humidity and, just before the test, they were kept at room temperature until reaching 22-24° C. They were divided in 4 groups with 4 samples for each of them, processed with different parameters.
The optical fiber sensor, connected at one end to the FBG interrogator, was fixed longitudinally in the centre of each sample. Three linear laser irradiations were performed on the left and the right side of the optical fiber sensor, at 1, 2 and 3 mm of distance.
The peak powers utilized were: 10 kW (group 1) 7.5 kW (Group 2), 5 kW (Group 3) and 3 kW (Group 4) (Figs. 4.3 and 4.4).
On all the irradiated samples, the repetition rate was 50 kHz on the left side and 20 kHz on the right side, while the speed has been keep fixed to 5 mm/s, based on a pilot study not reported and not published. Only one passage for each test was performed.
Two of the irradiated samples are shown in Fig. 4.5, where the three laser cuts performed are visible as light-coloured parallel lines.

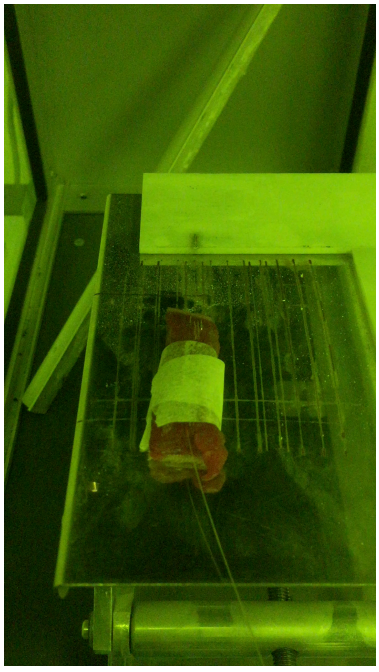

Fig. 4.3 - One of the samples during laser irradiation: it may be appreciated the optical fiber in the centre of the specimen.

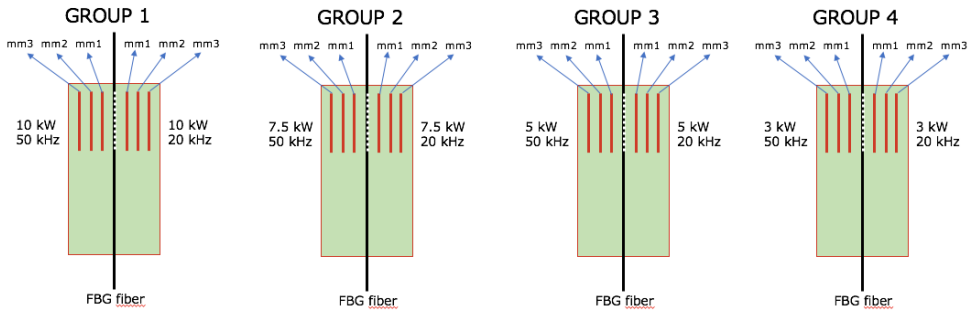

Fig. 4.4 - The setup of the temperature tests on the four sample groups.

Fig. 4.5 - Two of the samples after laser irradiation and before formalin buffering.

Histological analysis

After the laser irradiation, all the specimens were fixed in a 10% buffered formalin solution, cut into slices, and embedded in paraffin blocks, according to the conventional methods. Sections with thickness of 5 μm were obtained for haematoxylin and eosin staining. The histopathological sections were evaluated under low and high-power light microscopy (Nikon Lab Phot) by a pathologist unaware of the laser parameters used. Specimens were observed at two different magnifications (40× and 100×) for

measurement of tissue injuries widths. The extension of tissue injuries was measured with an ocular micrometer (Olympus BX 51). The area with the most evident damage, perpendicular to the cut margin, was chosen for the evaluation. Changes grossly exceeding the average width of the damage and presumptively associated to manipulation artefacts were excluded from the evaluation.
Tissue modifications were evaluated on the basis of the following histological features:
1) epithelial changes in proximity of the resection margin, evaluated from the edge of the margin to a depth of 1,000 μm. Variables evaluated include nuclear changes (presence of picnotic, spindle-shaped and hyperchromic nuclei), cytoplasmatic and cell membrane changes (hyperchromic cytoplasm, cell fusion and/or loss of normal cell adhesion), possible intraepithelial or subepithelial loss of attachment on the basis of a cut-off value of 10% of altered tissue in the whole resection margin.
2) connective tissue modifications, evaluated from the edge of the margins to a depth of 1,000 μm. Variables evaluated included carbonization (thermal necrosis), desiccation (presence of dense eosinophilic layer underlying the possible carbonization area and mainly consisting of collagen denaturation and tissue hyalinization).
3) presence or absence of vascular modifications, analysed by considering a cut-off value of 10% of the above-mentioned changes in the observed area (from the edge of the margin to a depth of 1,000 μm), presence of thrombosed or collapsed blood and lymphatic vessels (including presence of intraluminal clotted erythrocytes, presence of vascular stasis (not-collapsed vessels associated to the presence of gathered erythrocytes).
4) incision morphology, sub classified into regular (presence of a linear, smooth edge for more than 90% of the whole resection margin) and irregular (presence of a rough, uneven edge for more than 90% of the whole resection margin).
The pathologist assigned also a score to the epithelial and stromal modification, based on these criteria: 1 = Light alterations; 2 = Medium alterations; 3 = High alterations.
It was also evaluated, by assigning a score, the quality of the cut, based on these criteria: 0= not evaluable; 1= extremely irregular; 2= very irregular; 3= irregular; 4= poorly irregular; 5= regular; the score 5 was considered that obtained by a cold blade.

4.3 Results

The results, both from the point of view of the microscopic observation and by the FBG temperature recording, were very homogeneous inside each group of samples.

Histological evaluation
The samples evaluation of the different laser parameters made by the blind pathologist are resumed in Tab. 4.1. Notice that incision morphology was irregular for all the laser parameters used and no modified vessels were found for any condition. The best results have been reached with a pulse peak power of 3 kW and a repetition rate of 50 kHz, since by these parameters degree 0 of modifications for both epithelial and stromal level has

been obtained, as well as the best score (3) was also assigned by the pathologist to the quality of the incision.
By keeping fixed the average output power and by decreasing the repetition rate to 20 kHz, even if no epithelial and stromal modifications (degree 0) were noticed, in this case the pathologist was not able to appreciate the cut and, for this reason, a score of 0 was assigned to the quality of the incision. So, these parameters must be considered not sufficient to perform an effective incision on the soft tissues tested.
Conversely, the worst scores are the ones related to the laser cut made with the highest peak power, 10 kW, for both the two values of repetition rate used (50 and 20 kHz).

PARAMETERS	EPITHELIAL MOD.	SCORE*	STROMAL MOD.	SCORE*	VESSELS	INCISION	SCORE**
Peak power 10 kW - Repetition rate 50 kHz	Nuclear hypercromasia and cytoplasmatic alterations by thermal effect with partial detachement of epithelium and stroma	3	Eosinophilia and thermal necrosis	3	No modified vessels	Irregular	1
Peak power 10 kW - Repetition rate 20 kHz	Nuclear hypercromasia and cytoplasmatic alterations by thermal effect	3	Eosinophilia and thermal necrosis	2	No modified vessels	Irregular	1
Peak power 7.5 kW - Repetition rate 50 kHz	Nuclear hypercromasia and cytoplasmatic alterations by thermal effect	2	Eosinophilia and thermal necrosis	2	No modified vessels	Irregular	1
Peak power 7.5 kW - Repetition rate 20 kHz	Nuclear hypercromasia and cytoplasmatic alterations by thermal effect	2	Eosinophilia and thermal necrosis	1	No modified vessels	Irregular	1
Peak power 5 kW - Repetition rate 50 kHz	Nuclear hypercromasia and cytoplasmatic alterations by thermal effect	1	Eosinophilia and thermal necrosis	0	No modified vessels	Irregular	2
Peak power 5 kW - Repetition rate 50 kHz	Nucleus and cytoplasma well readable	0	Eosinophilia and thermal necrosis	1	No modified vessels	Irregular	2
Peak power 3 kW - Repetition rate 50 kHz	Nucleus and cytoplasma well readable	0	Slight eosinophilia	0	No modified vessels	Irregular	3
Peak power 3 kW- Repetition rate 20 kHz	Cut not evaluable, no alterations on the tissue	0	No modification	0	No modified vessels	Not evaluable	0
* Ephitelial and stromal modifications: 1 = Light alterations; 2 = Medium alterations; 3 = High alterations							
**Quality of the incision: 0= not evaluable; 1= extremely irregular; 2= very irregular; 3= irregular; 4= poorly irregular; 5= regular (cold blade)							

Tab. 4.1 - The samples evaluation of the different laser parameters and the scores assigned by the blind pathologist.

Temperature analysis

The temperature variation, recorded in all the sample groups, is reported in Tab. 4.2.

	50 kHz 1 mm	50 kHz 2 mm	50 kHz 3 mm	20 kHz 1 mm	20 kHz 2 mm	20 kHz 3 mm
10 kW	19.20	9.20	5.30	18.80	8.30	5-00
7.5 kW	14.80	8.50	4.50	14.10	7.90	4.50
5 kW	14.60	8.20	4.30	14.00	6.00	4.10
3 kW	6.70	4.50	2.60	6.30	4.10	2.50

Tab. 4.2 - The average of thermal elevation peaks (in C degrees) during the irradiation with different parameters.

The variation of the temperature recorded by the FGB interrogator during and after the laser irradiation with repetition rate of 20 kHz, speed of 5 mm/s and peak power of 10 kW, 7.5 kW, 5 kW and 3 kW is shown in Fig. 4.6.

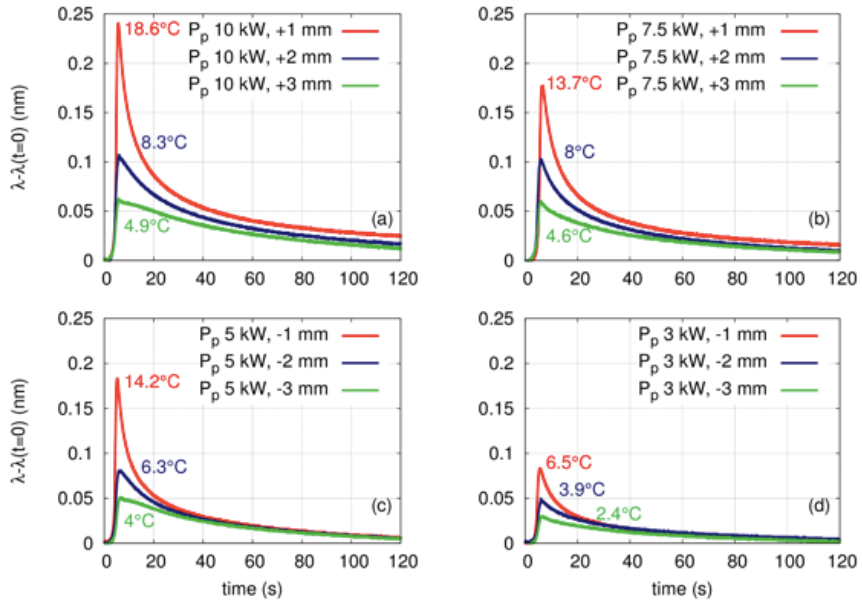

Fig. 4.6 - FBG wavelength shift recorded during and after the laser irradiation of a sample with 20 kHz repetition rate, 5 mm/s speed and peak power of (a) 10 kW, (b) 7.5 kW, (c) 5 kW and (d) 3 kW, at different distances from the fiber sensor.

As we may see, the thermal elevation, measured in the time interval of 120 s by the FBG wavelength shift, had the same behaviour in all the irradiated samples: it started with the laser irradiation, had an abrupt increase during the tissue cut and slowly decreased to its initial value in 120 sec.

The variation of the temperature was most important when the laser irradiation was close to the fiber, also in function of both the power and the repetition rate increase.
The slight differences were recorded between the groups 3 and 4 where, by the peak power decreasing, it was appreciated in all the samples a modest reduction of the temperature variation, with both the repetition rates used.

4.4 Discussion

The term "photothermal interactions" stands for a large group of laser-tissue interaction types where the increase in local temperature is the significant parameter change, induced by either CW or pulsed laser radiation. It is a complex process resulting from three distinct phenomena: conversion of light to heat, transfer of heat and tissue reaction, which is related to temperature and heating time [206].
From the beginning of the utilization of laser technology in surgery newer and newer wavelengths were proposed to improve the effectiveness of the cut minimizing at the same time the side effects on the tissue.
In different previous *ex vivo* studies performed by thermocouples recording [207-209] we analysed the thermal effects produced by different wavelengths, both emitting in the infrared portion and visible, on animal models.
In all these tests, we employed lasers in CW or in pulsed regime or in chopped mode with pulses of μsec. Results demonstrated that thermal elevation significantly changes as a function of the wavelength used and the parameters utilized in the irradiation.
This study presents three aspects which may be considered original. The first one is the employ of a laser with the active medium formed by an optical fiber: the advantages of this kind of devices have been described in the "Introduction" section.
The second one is the utilization of ns pulses: this short duration allows to reach very high peak powers without causing an excessive thermal elevation. The third one is the use of a FBG interrogator to record the temperature during all laser irradiation with high precision. Histological analysis demonstrated that the biological structures of the irradiated tissues had a very low thermal damage coupled with a good quality of the incision, at 3 kW power with a repetition rate of 50 kHz.

4.5 Conclusion

This *ex vivo* study shows that 1070 nm Yb-doped pulsed fiber laser can be very useful in oral surgery, since it provides a reduced thermal elevation in the irradiated tissues, thus consequently respecting their biological structures. Moreover, this work demonstrates that FBG sensor, based on the optical fiber technology as the laser source considered for the tests, may be a good instrument to record thermal elevation when applied to the *ex vivo* studies on animal models.

Chapter 5

Fiber lasers and di-silicate ceramics

5.1 Introduction

The request of ceramic prosthetic restorations has increasingly become common in daily dentistry as well as the continuous need of precisions, particularly in cosmetic dentistry. where new materials, such feldspathic ceramics, play an important role in prosthetic rehabilitations. Unfortunately, failure resulting from porcelain fracture has been described as ranging from 2.3% to 8%, and, nevertheless it seems to have a multifactorial cause [210-212], with the key role attributed to the composite resin adhesion with porcelain: for this reason, the conditioning methods of ceramic surface are very interesting [213].
The inside surface of the ceramic prosthetics must be conditioned for optimizing micro-mechanical retention by the resin penetration into the ceramic micro-roughness: this treatment enlarges the surface in contact with the tooth structure through micro-porosities creation, so enhancing the cement mechanical retention. [214, 215]. To produce surface roughness and to promote micro-mechanical retention, different treatment methods have been proposed, such as diamond roughening, air-particle abrasion with aluminium oxide and acids etching [214, 215]. All these techniques have been investigated under *in vitro* conditions [216-218].
The use of laser technology for surface treatment has been successfully applied in many industrial fields by the utilization of high power sources and it today represents a controllable and flexible way for the surface properties modification of different materials [219, 220], being laser processing parameters during matter modifications able to influence the surface microstructure [221].
The different techniques used for ceramic surface conditioning have demonstrated several limits as well as the utilisation of laser had controversial results. Particularly, some tests

made on lithium-di-silicate [222] and CAD-CAM ceramics [223] with CW CO_2 laser at 10.6 μm showed the presence of micro-cracks and melting textures, due to the thermal effect of the laser irradiation, at output powers higher than 10 W CW (3184.7 W/cm²). Moreover, the observation of the ceramics structure irradiated by a 10 W (14185 W /cm²) pulsed Nd:YAP laser at 1340 nm showed the presence of holes, micro-cracks and melting grains [224, 225]. This is probably caused by the effect of high quantities of radiation energy given in a well-defined portion of the ceramic surface over a short period, this leading to a very high energy density accumulation. Micro-cracks formation on ceramics after CO_2 and Nd:YAP laser irradiations may be related to the high thermal effects of laser processing which leads to an extreme physical stress in the re-hardening ceramic surface [226]. Also Er:YAG laser was used for surface treatment of feldspathic porcelain, but its effect resulted significantly weaker than that of the HF surface treatment. The achievable assumption is that the laser energy from an Er:YAG laser is not enough absorbed in porcelain and so not sufficient to create a micro-mechanical retention pattern for more favourable bonding [227]. In agreement with this study, some Authors affirmed that, even at a very high energy (500 mJ), Er:YAG laser is not able to cause a roughness on the porcelain surface sufficient to promote reliable adhesion to the resin composite [228]. Recently, the so-called "ultra-short pulses" lighted up a great interest in the field of laser dentistry. Some studies confirmed that Ti:Sapphire femtoseconds laser produced a very high mean roughness value [229]. However, this source is very expensive and for this reason, to date, it is still utilized only in few laboratories.
The *in vitro* study here reported has the aim to verify the possibility of performing the surface treatment of Lithium di-silicate ceramic specimens by the irradiation of a 1070 nm pulsed fiber laser.
The surface modifications obtained by irradiating the Lithium di-silicate samples using different laser parameters were analysed by optical microscope, Scanning Electron Microscope (SEM) and Energy Dispersive Spectroscopy (EDS). Moreover, a FBG temperature sensor recorded the temperature increase during the tests. Results obtained with the different analysis have demonstrated that fiber laser processing with optimized parameters can be considered a good technique to increase the adhesion of Lithium di-silicate ceramics.

5.2 Materials and Methods

The circular faces of twelve cylinders of Lithium di-silicate ceramics (e.max Press, Ivoclar, Italy) with 10 mm diameter and 8 mm height (Fig. 5.1) were processed in three 3 x 3 mm square zones by using a 1070 nm pulsed fiber laser (AREX 20) provided by Datalogic, Italy (see Chapter 4).

Fig. 5.1 - Samples used in the tests (center and right) and metal cylinder used to check the focus of the laser beam (left). Notice the groove for placing the FBG sensor in the centre of the sample surface.

Each square zone on the sample faces has been processed with different laser parameters. In particular, the output power has been changed from 100% to 30% and the speed from 50 to 5 mm/s (Fig. 5.2).

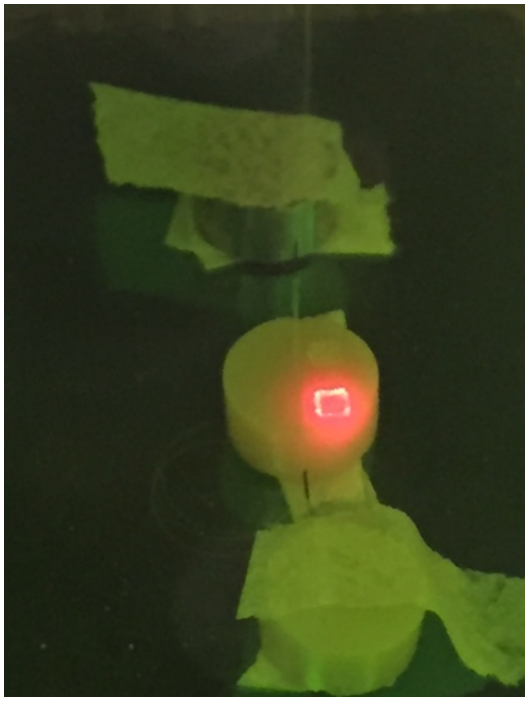

Fig. 5.2 - The ceramic sample during the laser irradiation.

After a preliminary pilot study with different parameters it was decided to maintain for all the tests a repetition rate of 20 kHz (Fig. 5.3).

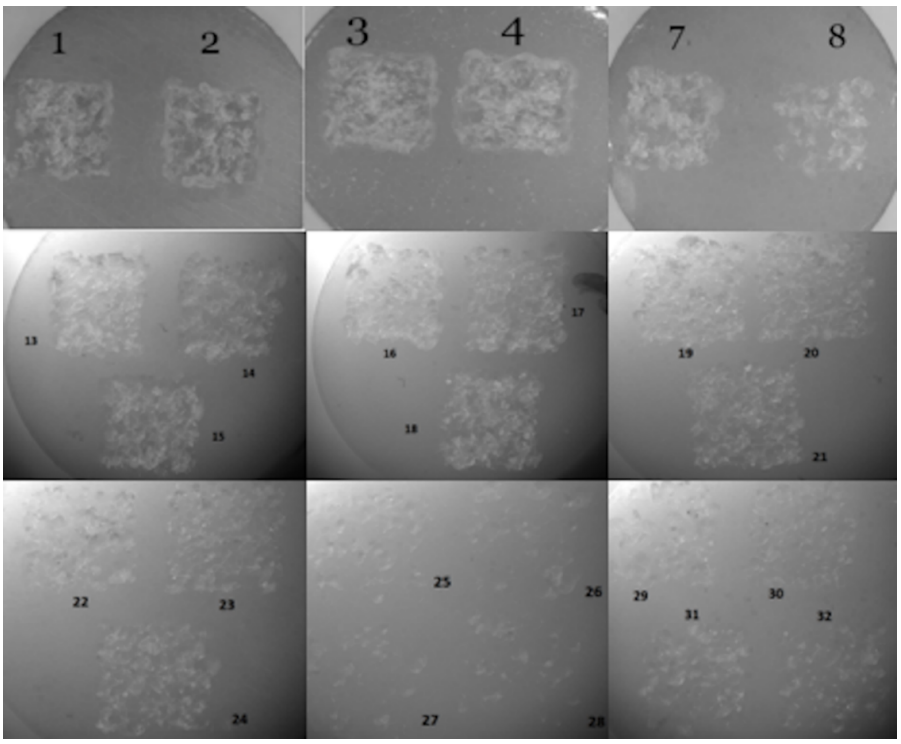

Fig. 5.3 - Some irradiated samples of the pilot study to determine the proper repetition rate to use in the tests.

The lens used with the AREX 20 laser has a focal length of 160 mm. In this configuration, the laser beam has a spot-size of 80 μm. Each square zone on the sample surface has been processed with a meshed filling pattern with a distance between lines of 0.03 mm.
The laser beam focalization was checked by a metal cylinder of the same dimension of the samples.
The specimens were subsequently observed by an optical microscope (Olympus MTV-3, Japan), then metallized and analysed by a SEM (Ion sputter Jeol JFC 1100E, USA) and an EDS system (JSM-35CF, Jeol Ltd., Japan).
During the irradiation of the sample with the best laser parameters, according to the results of SEM and EDS analysis, the thermal elevation was recorded by a FBG-based temperature sensor connected to an interrogator. The fiber sensor was positioned into the groove in the middle of the sample. The device used to measure the FBG wavelength shift induced by the temperature increase was the Dynamic Optical Sensing Interrogator sm130-500 (Micron Optics Inc, Atlanta, USA).

5.3 Results and Discussion

SEM observation
By comparing at higher magnification, the control group (non-irradiated samples) and the cylinders processed by the fiber laser, great differences can be noted (Fig. 5.4).

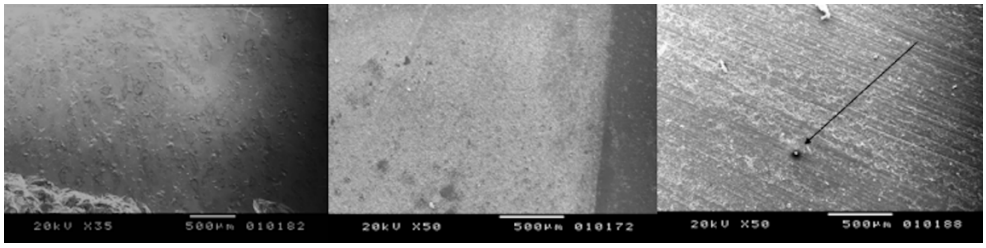

Fig. 5.4 - (Left): Non-irradiated sample. (Centre): peak power of 7.5 kW and 50 mm/sec speed. (Right): peak power of 7.5 kW and 10 mm/sec speed with a carbonization spot (left: X35; centre and right: X50).

In fact, all the treated samples show a rough surface with a great number of holes and irregularities. The comparison of the samples irradiated with different laser parameters evidenced some areas of melting and burning when the highest energy was used, due to the cumulative effect of the laser energy. The presence of some cracks with variable intensities, also due to the thermal effects of laser irradiation, has also been noted (Figs. 5.5 - 5.6 – 5.7 – 5.8).

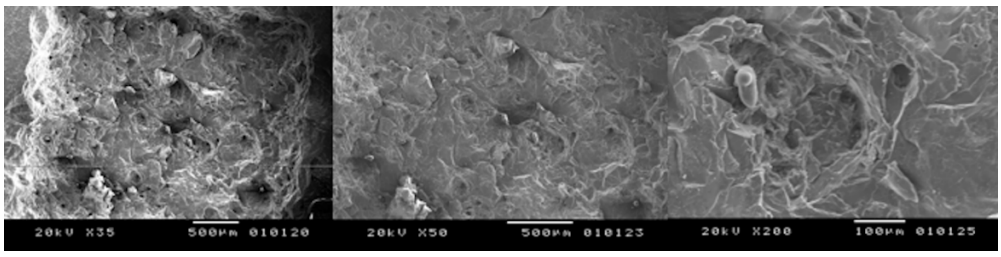

Fig. 5.5 - Peak power of 10 kW, speed of 10 mm/s: many zones with melting and carbonization are shown (left: X35, centre: X200, right: X500).

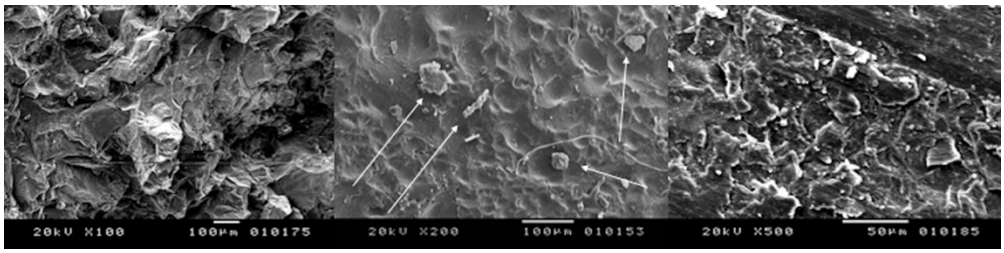

Fig. 5.6 - Peak power of 10 kW, speed of 50 mm/s: some points with melting are shown (left: X100, centre: X200, right: X500).

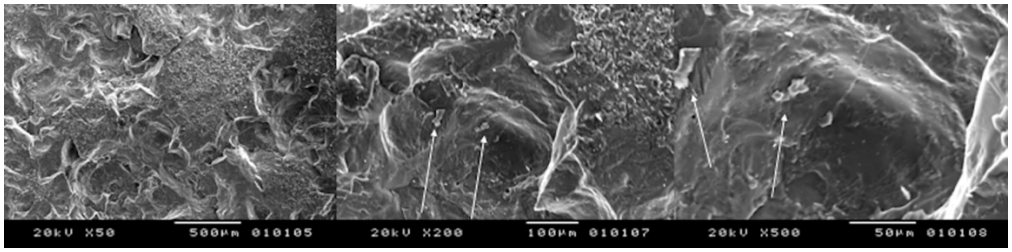

Fig. 5.7 - Peak power of 7.5 kW, speed of 50 mm/s: presence of melting and carbonization in some areas of the sample (left: X35, centre: X50, right: X200).

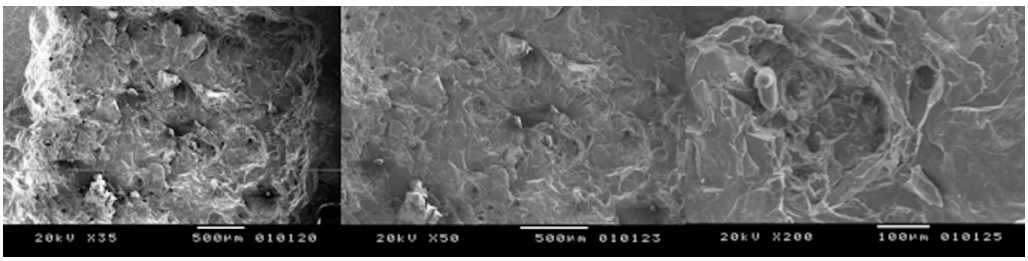

Fig. 5.8 - Peak power of 5 kW, speed of 10 mm/s: evidence of some zones with melting (left: X50, centre: X100, right: X500).

The laser parameters which seem to be the most effective for surface conditioning without damages for the material are peak power of 5 kW, repetition rate of 20 kHz and speed of 50 mm/sec. In fact, the samples irradiated with these parameters revealed a rough surface with holes, irregularities, cavities and recesses, while the presence of thermal damaging effects, such as melting, burning and cracks, was not shown (Fig. 5.9).

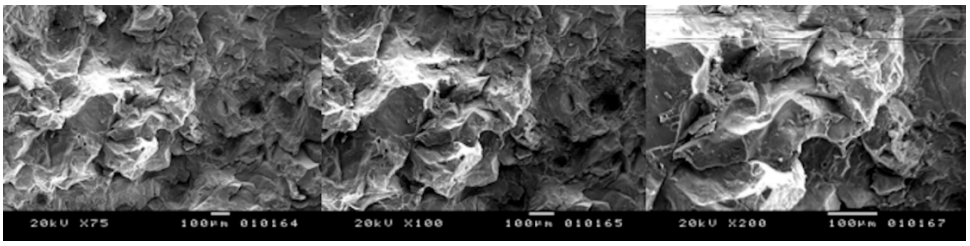

Fig. 5.9 - Peak power of 5 kW, speed of 50 mm/s: no evidence of carbonization and melting zones (left: X75, centre: X100, right: X200).

EDS analysis

The EDS analysis consists in the percentage recording of chemical elements in the point where the probe is placed. Analysed samples showed, in general, slight differences in the chemical composition between control groups and irradiated samples, even if some variations were detected by changing the laser parameters, thus confirming the information shown by the SEM observation.

The differences of elemental composition between the non-irradiated areas in the different samples may be explained by the structure of the ceramic which is not homogeneous, this resulting in structural variations of the tested zones (Fig. 5.4, left).

The samples treated with laser operating at peak power of 10 kW, repetition rate of 20 kHz and speed of 50 mm/s evidenced in some zones (red spots) a lower percentage of C when compared to the control group. Conversely, O and Al elements were slight higher in the affected zones (Fig. 5.10).

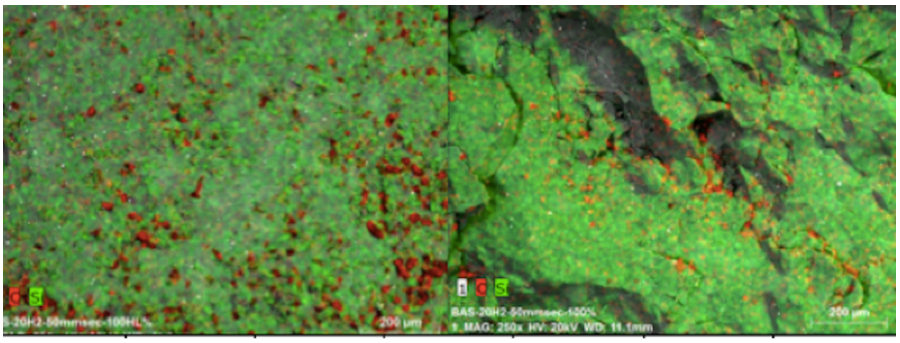

Concentration (%) of some elements before and after laser irradiation (10 kW, 50 mm/sec)

	C	O	Si	K	Al	Na
non-irradiated	16.70	41.40	25.70	6.10	4.30	3.40
irradiated	7.40	44.40	23.70	8.00	6.70	5.50

Fig. 5.10 - (left) Control group and (right) samples irradiated with peak power of 10 kW and speed of 50 mm/s: in red the C concentration.

The samples irradiated with peak power of 7.5 kW, repetition rate of 20 kHz and speed of 50 mm/s showed that only the Carbon concentration was higher in the control group (13.6%), while all the other elements considered, that is O, Si, K, Al and Na, presented higher concentration values in the treated surfaces (Fig. 5.11).

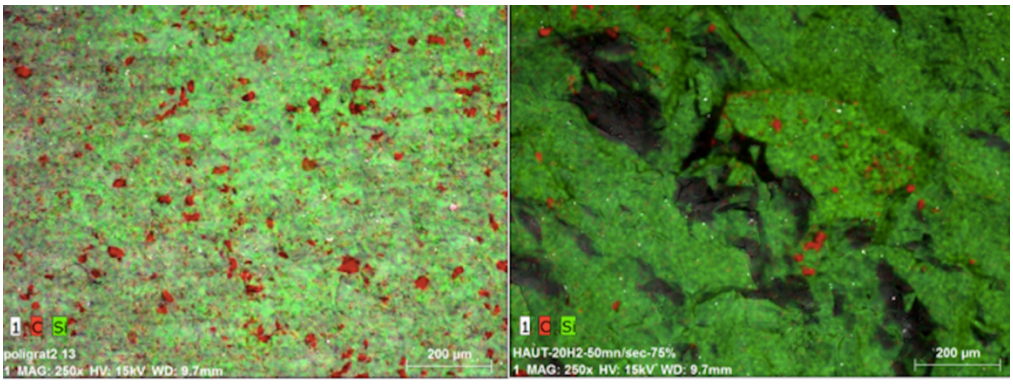

Concentration (%) of some elements before and after laser irradiation (7.5 kW, 50 mm/sec)

	C	O	Si	K	Al	Na
non-irradiated	13.60	41.20	27.10	7.40	4.50	3.40
irradiated	3.80	44.40	27.10	8.90	5.90	4.70

Fig. 5.11 - (Left) Control group and (right) samples irradiated with peak power of 7.5 kW and speed of 50 mm/s: in red the C concentration.

Carbon is one of chemical ceramic composition of lithium di-silicate. The presence of carbon on ceramic surface is due to the high energy of laser irradiation that leads obtain burning and melting ceramic surface.
On the samples irradiated with the parameters which demonstrated the best results by the SEM observations (peak power of 5 kW, repetition rate of 20 kHz and speed of 50 mm/s), the analysis was conducted in four different zones. Results showed very slight differences for all the elements concentration in each zone analysed. These data, confirmed also by SEM observation, demonstrated a poor modification of the ceramic chemical structure caused by laser operating with the optimum parameters (Fig. 5.12).

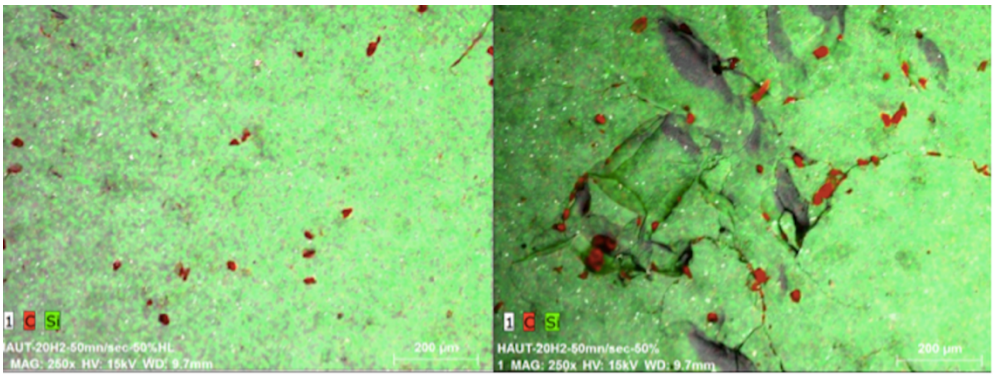

Concentration (%) of some elements before and after laser irradiation (5 kW, 50 mm/sec)

	C	O	Si	K	Al	Na
non-irradiated	5.70	43.10	27.50	9.50	6.10	4.40
irradiated	4.30	43.50	28.00	9.50	6.40	4.50

Fig. 5.12 - (Left) Control group and (right) samples irradiated with peak power of 5 kW and speed of 50 mm/s: in red the C concentration.

Thermal analysis

The temperature increase during the laser irradiation has been measured only when the source operates with the best parameters according to the results of SEM and EDS analysis. The aim of this measurement was to provide the maximum value of the temperature increase, due to the laser processing, that the di-silicate ceramic material can stand, without being damaged. Higher energy laser treatments provide a more significant temperature change, which is associated with the detrimental surface modifications shown by SEM and EDS analysis.

The thermal elevation of the sample during the irradiation with the laser operating at a peak power of 5 kW, repetition rate of 20 kHz and speed of 50 mm/s, has been recorded with a FBG connected to an interrogator. The FBG wavelength shift obtained in a time interval of 120 s, starting with the laser processing, is reported in Fig. 5.13.

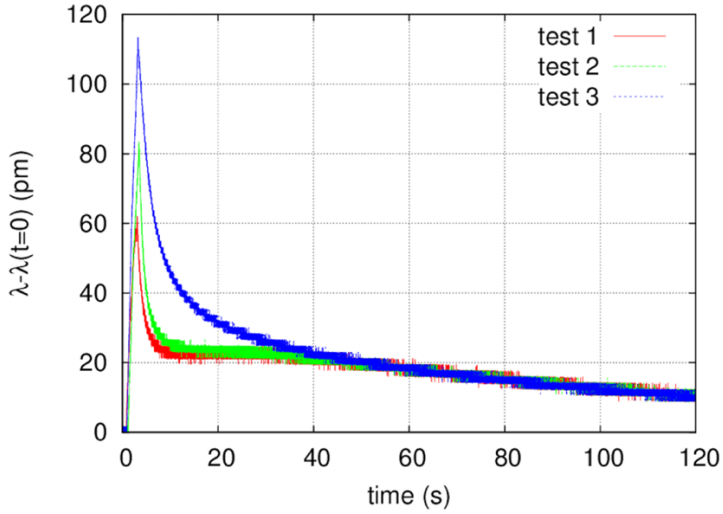

Fig. 5.13 - FBG sensor wavelength shift induced by temperature variations during and after the laser irradiation with the best parameters (peak power of 5 kW, repetition rate of 20 kHz, speed of 50 mm/s).

The temperature measurement has been repeated three times, by processing three square regions on the sample surface. The fiber sensor was placed in the centre of the sample, approximately at the same distance from all the areas irradiated by the laser. Notice that the wavelength shift measured by the interrogator is between 65 pm and 115 pm, obtained, respectively, in the first and the third test. Consequently, the temperature increase due to the laser processing is between 5°C and 9°C. The slight growth of the temperature value measured in the second and the third test can be due to a gradual heating of the sample, due to the previous laser processing. Moreover, slight differences in the distance of the three zones irradiated by the laser with respect to the sensitive part of the fiber sensor must be taken into account.

The measure of temperature rise during laser irradiation may give more explanation of crack formations: micro-cracks formation on ceramics after laser irradiations could be explained through the high thermal effects of laser processing, with the consequence of an extreme physical stress in the re-hardening ceramic surface.

It must be underlined also the importance of the very short pulse duration utilized by the fiber laser used in this study (100 ns) which may explain the great difference between the fluences of these tests, compared to those given in the cited works where irradiation had been performed in CW or in μs.

5.4 Conclusion

As mentioned in the "Introduction", different surface treatment methods have been proposed to provide roughness and promote micro-mechanical retention, such as diamond roughening, air-particle abrasion with aluminium oxide, acids etching and laser irradiation. In current study, laser irradiation could roughen ceramic surfaces which increases the surface in contact with the tooth structure, creating micro-porosities and enhancing the potential for mechanical retention of the cement.
According to several cited Authors and to the data reported here, irradiated surfaces showed higher roughness values than non-irradiated surfaces liable to enhance mechanical retention due to the extreme physical stress created in the re-hardening ceramic surface by the characteristic photo-ionization.
This *in vitro* study demonstrated that the utilization of 1070 nm pulsed fiber lasers for the Lithium di-silicate ceramics surface conditioning is effective and damage-free. In fact, the results obtained using the proper laser parameters (peak power of 5 kW, repetition rate of 20 kHz and speed of 50 mm/s) show that it is possible to create an important ceramic rough surface, ready to incorporate in its cavities the bonding agent. Moreover, thermal elevation recorded during irradiation was very low, thus explaining the few damages evidenced and, overall, the poor modifications in the ceramic structure shown by the EDS analysis.
The use of a pulsed fiber laser at 1070 nm represents a new approach in prosthetic dentistry, opening new perspectives, which shall be confirmed by further *ex vivo* studies. The next analysis will regard the mechanical properties of irradiated ceramic surface (micro-hardness, roughness) and the adhesion characteristics after ceramic sealing (wettability, shear bond strength and micro-leakage), to confirm the capacity of improving the adhesion of laser processed di-silicate ceramics to the dental tissues.

Chapter 6

Fiber lasers and hard dental tissues

6.1 Introduction

The use of laser technology in dentistry was reported for the first time in the mid-1960s [172] but it was only after 1990 that the number of scientific publications dealing with laser-assisted dentistry increased enormously [230]. One of the main reasons for this rapid interest increase in the field can be attributed to the possibility of hard tissue ablation by the Erbium family of lasers (Er:YAG and Er,Cr:YSGG) [175, 176]. This indication was also clinically tested in conservative dentistry, suggesting that the laser was a good alternative to conventional instruments such as the turbine and micro-motor [231].
However, Erbium lasers have still some disadvantages and unsolved problems, such as the cost of the device and the large size of the systems due to the complexity of the device, particularly related to the necessity of a water cooling system very efficient to minimize the high temperature provoked by the optic pumping system consisting in a flash-lamp. In addition, with this technology, the treatment time is longer compared to the use of traditional instruments. Articulated arm delivery systems ensure low energy loss, but these have very poor ergonomics and flexibility.
For these reasons, several other wavelengths have been investigated for ablation of hard dental tissues (i.e, CO_2 [232], Nd:YAG [233], Excimer [234] and Argon [235] lasers). However, no promising results have been obtained yet.
In a previous study performed in the Photonic Devices Lab of the Department of Engineering and Architecture [204], we investigated the effectiveness of dental hard tissue ablation using a picosecond pulsed diode pumped solid-state (DPSS) laser. Several *in vitro* tests on extracted human teeth were undertaken, followed by the evaluation of the ablation quality and temperature increase inside the teeth. Results showed the presence of

cracks and fissures even if the temperature inside the pulp chamber didn't reach 5.5°, which is considered the limit for maintaining the tooth vitality.
The aim of this study was to evaluate the capacity of a 1070 nm pulsed fiber laser of ablating the enamel and dentine without causing thermal effects such carbonization and cracks in the surrounding zones and, eventually, to determine the best parameters for obtaining the best and faster cut, coupled to minimal side effects.

Material and Methods
Seventy-three human extracted third molars were used for this study (Fig. 6.1, left).
They were stored in 0.5% chloramines solution before the experiment to inhibit microbial growth for 1 h until being ready for use. They were maintained for a maximum of 10 days before the tests in those conditions and then placed in distilled water according to ISO standards 11405. Only dental caries free teeth were selected and, before the experiment, the teeth were cleaned with ultrasonic scaling. Teeth labial surfaces of the crowns were polished using pumice and water slurry in a rubber cup. Then the teeth were rinsed with water for 15 seconds and blown dry with oil-free compressed air (Cattani Compressor). The teeth with defects were removed and, at the end, sixty cylinders of 5 mm thickness were obtained (Fig. 6.1, right).

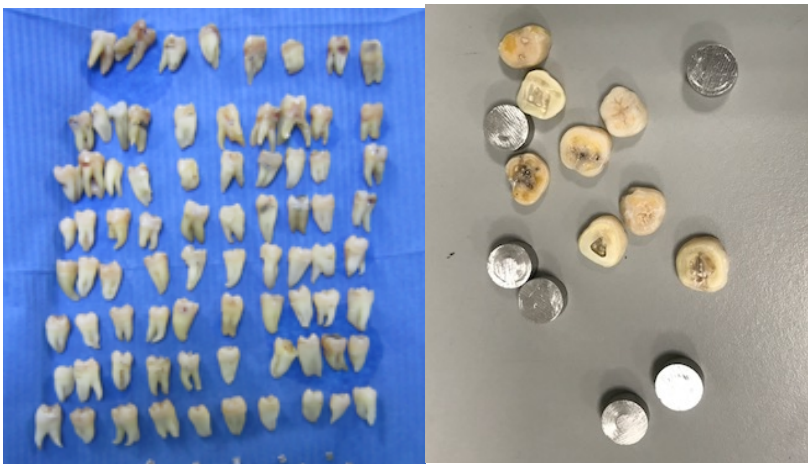

Fig. 6.1 - (left): the extracted human teeth used for the test; (right): sections obtained and steel cylinders used for laser focal distance adjustment.

Each sample was processed in three 3 x 3 mm square zones with a 1070 nm fiber pulsed fiber laser (AREX 20) provided by Datalogic, Italy (see Chapter 4) with different laser parameters. Particularly, the average power has been changed from 100% (peak power of 10 kW) to 30% (peak power of 3 kW), the repetition rate from 100 to 20 kHz and the speed from 50 to 5 mm/s. The laser beam focalization was checked by a metal cylinder of the same dimension of the samples.

The microscopic observation showed a large amount of thermal damages consisting in cracks, fissures and melting zones with all the laser parameters used (Fig. 6.2). Consequently, for decreasing the thermal elevation provoked by the laser beam, a small cooling system consisting of an air/water spray delivering device was located inside the safety box, with the possibility to be oriented exactly at the impact point of the laser on the target (Fig. 6.3). It was connected, by a pipeline, to a compressor located outside the box.

Fig. 6.2: Optical microscope observation sample irradiated with a peak power of 7.5 kW without air/water spray: a great amount of melting and carbonization can be appreciated.

Fig. 6.3 - The air/water spray sprinkler.

A sequence of tests including all the parameters used in the previous ones was repeated using the air/water spray, but results were the same.
The interesting phenomenon noticed was the formation, in some of the irradiated samples, of a great amount of melting without carbonization.
For this reason, we decided to perform some more tests to verify the possibility to use this device for enamel and dentine welding in the fractured teeth.
The first step was to choose the best parameters for obtaining a large part of melting with minimal carbonization and. After many tests, it was established that this was possible only with a peak power of 3 kW, a repetition rare of 20 kHz and a speed of 5 mm/s on the basis that, with all the other parameters, the teeth were carbonized (Fig. 6.4).

Fig. 6.4 - Some carbonized samples after laser irradiation.

For this purpose, 18 samples with the same dimensions of those used in the previous tests were prepared (Fig. 6.5, left) and subsequently cut, by a steel disc, perpendicularly to the plane face to obtain two parts by each specimen (Fig. 6.5, centre). The two parts of each tooth were put near each other and laser irradiated to reach a welding between them (Fig. 6.5, right).
Samples were divided in three groups:
irradiated with a peak power of 3 kW without filler;
irradiated with a peak power of 3 kW with apposition of Hydroxyapatite (powder);
irradiated with a peak power of 3 kW with apposition of Hydroxyapatite (nanoparticles).

Fig. 6.5 - The samples used for dentine welding tests.

6.2 Results and Discussion

Cavity preparation
Microscopic analysis revealed, in all the samples and with all the parameters used, a great number of cracks, melting and fissures, not compatible with the integrity of the tooth preservation (Fig. 6.6).

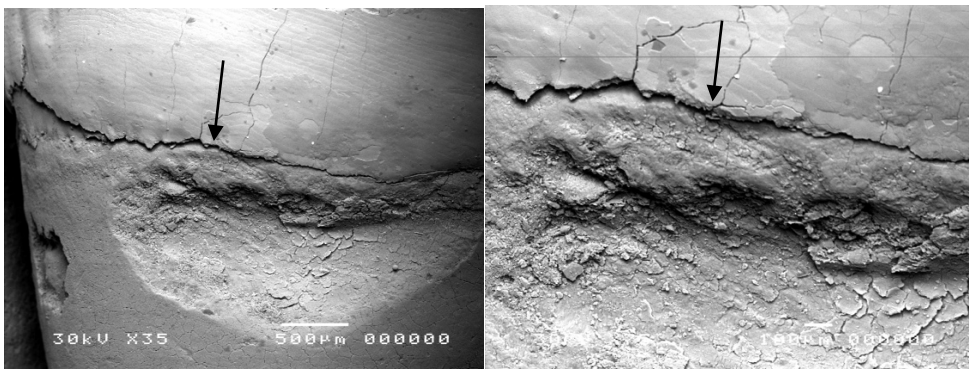

Fig. 6.6 - SEM observation of a sample irradiated with a peak power of 7.5 kW without air/water spray: it is possible to appreciate some zones of melting, some cracks and an extended fissure interesting all the observed area (Left: X35, Right: X100).

The addition of an air/water spray did not change the results obtained in the first sequence of tests. In fact, also in all the samples processed in this way it was observed the presence of several zones with thermal damages with no differences with respect to the images appreciated in the teeth irradiated without the spray (Fig. 6.7).

Fig. 6.7 - SEM observation of a sample irradiated with a peak power of 5 kW with air/water spray: presence of zones with melting and cracks; in the left picture, it is possible to appreciate a great and deep fissure (Left: X35, Centre: X75, Right; X100).

Enamel and dentine welding

In all the three groups of samples (a, b, c) the microscopic observation showed a process of welding with formation of melted dentine inside the gap.

However, the best results were seen in group c, where the welding process seemed to be more important (Fig. 6.8).

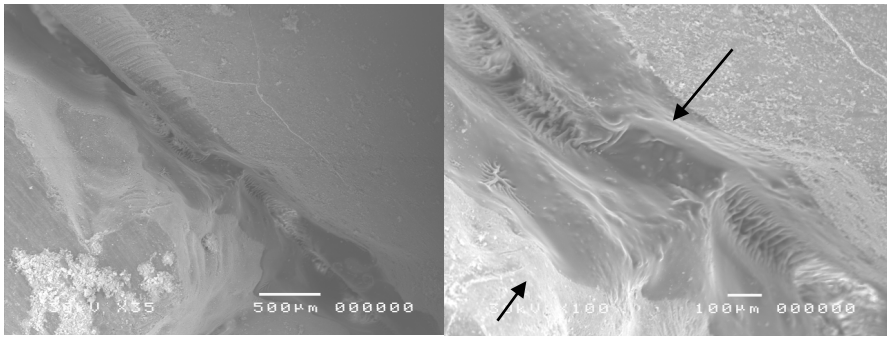

Fig. 6.8 - SEM observation of one of the group c samples: evident the melted dentine filling the gap between the two parts (Left: X35, Right: X100).

6.3 Conclusion

While the utilisation of the 1070 pulsed fiber laser seems to be not possible in the dental cavity preparation, due the too high temperature which is not compatible with the integrity of the tooth vitality, very interesting and promising is the use of this source to realize an effective welding of enamel and dentine by inducing a melting of them.

Several further tests will be necessary to investigate the quality of the process, particularly by the point of view of the strength bond and the depth of the link. However, this procedure opens new clinical perspectives for the treatment of fractured teeth which, at this moment, cannot be treated and are candidate to removal from the mouth.

Chapter 7

Project for an “at home” intraoral device based on Random Laser technology

7.1 Introduction

A laser is usually constructed from two basic elements: a material that provides optical gain through stimulated emission and an optical cavity that partially traps the light. When the total gain in the cavity is larger than the losses, the system reaches a threshold and lases: it is the cavity that determines the modes of a laser, that is, it determines the directionality of the output and its frequency.
Random lasers work on the same principles, but the modes are determined by multiple scattering and not by a laser cavity [236]. The difference between traditional and random lasers are shown in Fig. 7.1.

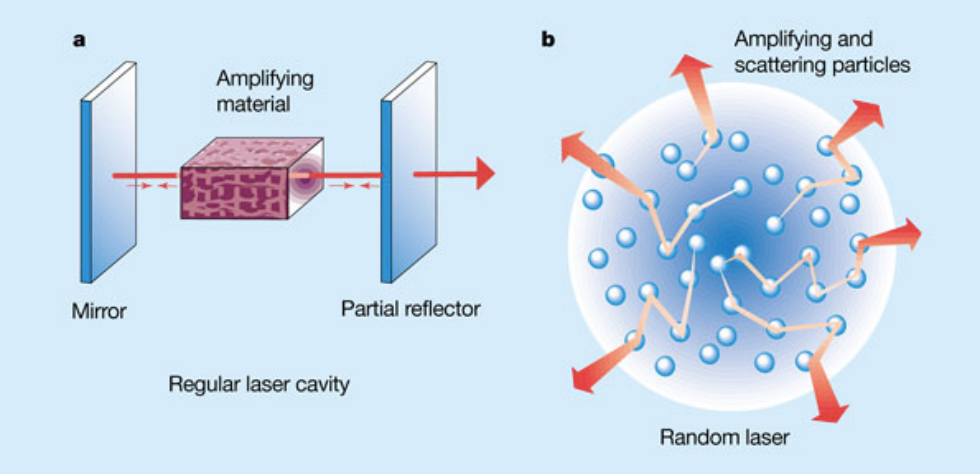

Fig. 7.1- Difference between traditional and random lasers: a- In a regular laser the light bounces back and forth between two mirrors that form a cavity. After several passes through the amplifying material in the cavity, the gain amplification can be large enough to produce laser light; b - In a random laser the cavity is absent but multiple scattering between particles in the disordered material keeps the light trapped long enough for the amplification to become efficient, and for laser light to emerge in random directions (ref. 236).

As theoretically predicted by Letokhov [237] and later demonstrated by Lawandy [238], the presence of a disorder pattern combined with the amplification given by an active material can be exploited to create this new class of lasers with particular properties. Inside a disordered active material, the light is forced to travel through longer paths, so reaching the lasing threshold with an emission spectrum characterized by narrow peaks apparently not correlated with each other’s [237]. Comparing to a traditional laser, the feedback mechanism is due to the strong scattering and not to the action of an optical cavity.

There has been tremendous interest in random lasers research over the past decades. Laser-like emission has been observed in dye lasers based on solutions containing nano-particles and in laser crystal powders [239-246].

Our interest on random lasers arose from one of their more particular properties, consisting on the demonstration that laser emission from the powder could be, from the spatial point of view, omni-directional [247].

The aim of this work is to prototype of intra-oral random laser to be used by the patient himself for the treatment of several diseases of the mouth.

The characteristics, advantages and indications of biomodulation have been described in the Chapter 2.

Recently, a new laser device, which can be used at home by the patient himself for inflammation and pain reduction, has been proposed (Fig. 7.2)

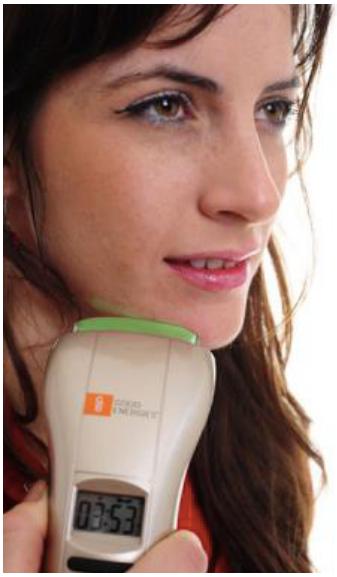

Fig. 7.2 - The laser device used for the “at home” LLLT treatment (ref. 248).

This laser is characterized by reduced dimensions and class II, according the ANSI classification, and it is able to solve some problems related to the utilization of traditional diode laser for the LLLT treatments.
In fact, one of the problems related to the LLLT is represented by the necessity, for the patients, to go to the therapist twice/three times weekly for treatments of some minutes. The arrival on the market of new LLLT appliances, cheaper, smaller and able to be used at home by the patients themselves might represent a solution to this problem, giving the possibility for the patients to receive daily LLLT treatment, avoiding the risk of overpower, as this device has only a power setting [248, 249].
Unfortunately, this kind of device cannot find application for treating the intra-oral lesions: in fact, even if its dimension is very small, it cannot be introduced into the mouth. Moreover, due to the laser beam is collimated, for treating lesions which are distributed all over the oral mucosa it is necessary to irradiate sequentially each area corresponding to the spot size for at least 5 min, resulting on a very long session.
It is evident that the opportunity of a laser device spatially emitting in each point of the oral cavity might represent a real new therapeutic possibility for operator and patient and, for this reason, we started an experimental setup with the final aim to realize a random laser to use intraorally.

7.2 Material and Methods

According to the literature [250, 251], we decided to excite a solution of Rhodamine 6G, Ethylene Glycol and Antimony oxide nanoparticles (Fig. 7.3) by a pumping system consisting in a laser emitting around 500 nm.
In fact, the absorption peak of Rhodamine 6G is at 530 nm while its emission peaks are at 555-585 nm (Fig. 7.4).

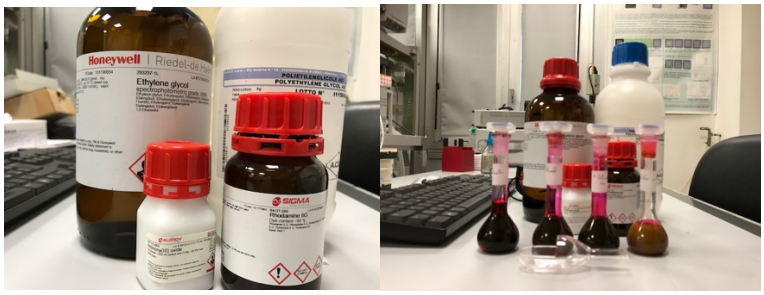

Fig 7.3 - Reagents used (left) and some of the solutions with different reagents’ concentrations tested (right).

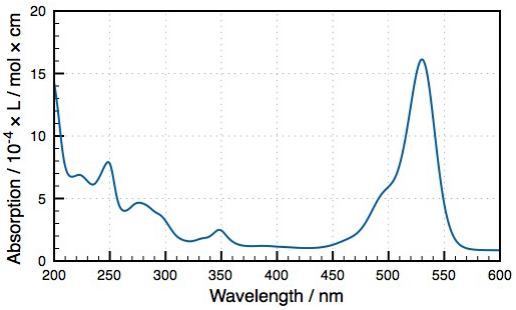

Fig 7.4 - Absorption spectrum of Rhodamine 6G.

The pumping system utilized was a fiber laser located in the Laboratory of our Department (Boreas, Eolite Lasers, USA) with these parameters:

Diode Current:	23A
Frequency:	60 kHz
Green Power:	0.3 W
Pulse duration:	10 ns

It emits both at 1030 and 515 nm; given that we decided to use only the visible beam, the first step was the positioning of a filter to eliminate the infra-red portion of the emission.

Subsequently, by means of some mirrors, the beam was directed on a Power-meter (Coherent LabMax top, Transcat, USA) and the energy was adjusted, after several tests at 10% of the maximum (168mW recorded by the PM).

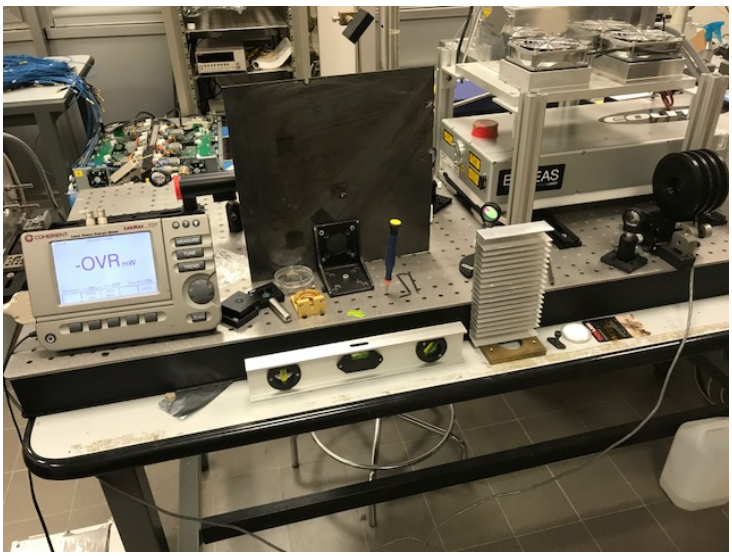

Fig. 7.5 - The set-up for the random emission laser.

A cuvette was then put before the power-meter.

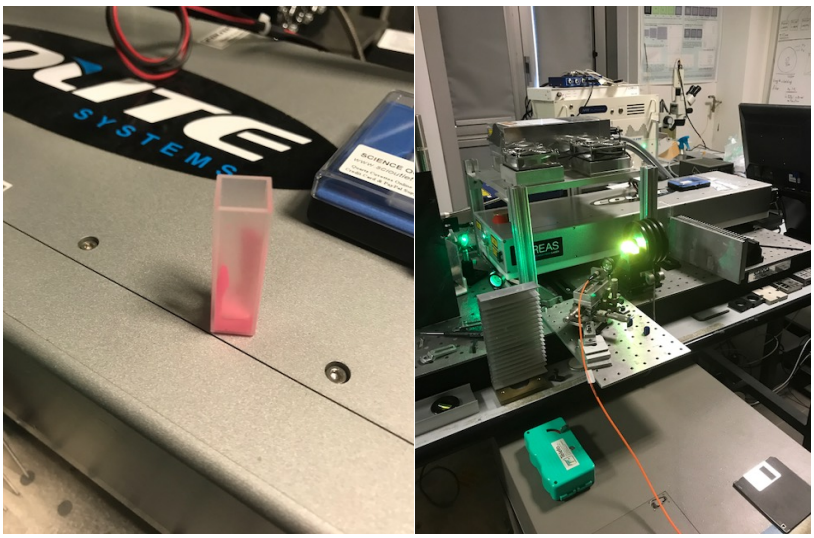

Fig. 7.6 - Left: the cuvette containing the rhodamine solution; Right: the cuvette put behind the power-meter, stimulated by the pumping laser and randomly emitting.

The cuvette was filled with a solution so composed:

Rhodamine 6G	10 g/l
Solvent (ethylene glycol)	10 g/l
number of nanoparticles (antimony oxide)	5.1 X 10^{11} X cm^{-3}

To record the coherent emission from the cuvette, an Optical Spectrum Analyzer was posed at 45° and a lens provided, to guide the beam inside a fiber connected to the device. The setup is shown in Figs. 7.5 and 7.6.
The graph resulting by the OSA analysis shows two peaks, the first at 515 nm, corresponding to the pump emission, and the second between 550-580 nm, which is the energy emitted by Rhodamine 6G (Fig. 7.7).

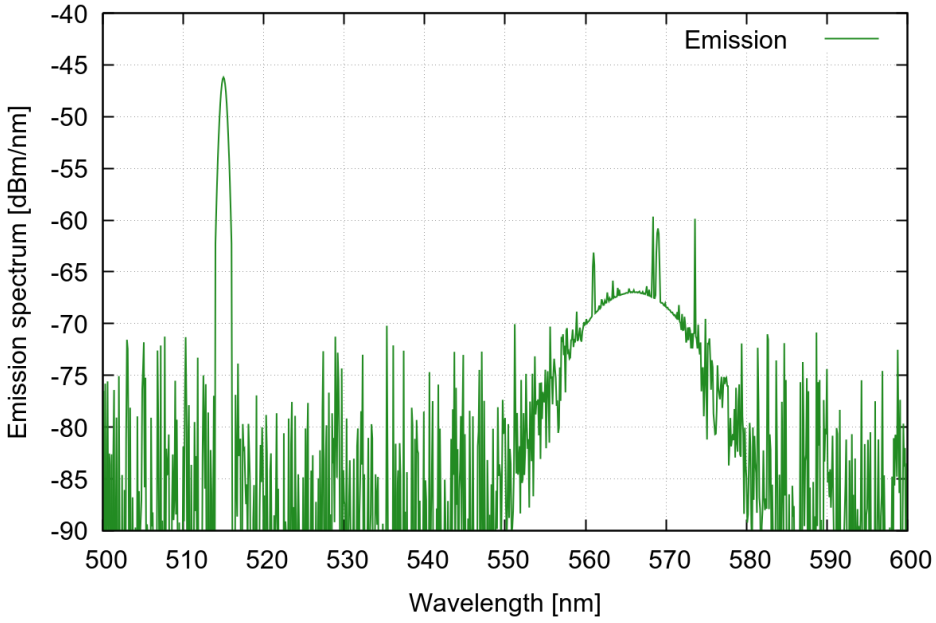

Fig. 7.7 - The graph resulting by the OSA analysis.

After this preliminary sequence of laboratory tests, we projected the prototype of the device (Fig. 7.8).

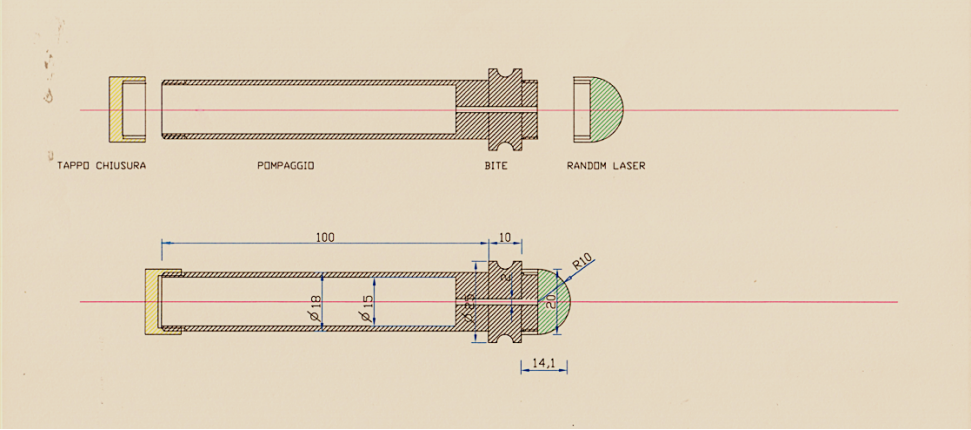

Fig. 7.8 - The prototype project.

It is a plastic cylinder, able to be put in the hand, and inside the posterior part is located the pumping system emitting toward the anterior portion with the rhodamine, which is inside the mouth and which represents the unit “random” emitting in all the directions, thanks to the plastic transparency.
The two portions are separated by a sort of bite and, in this way, the device may be maintained firmly by the teeth and at the same time it allows to the mouth to be opened and in this way the irradiation may reach all the surfaces inside the oral cavity.
Posteriorly, a screw top is provided for changing the discharged batteries, and the anterior portion, too, is changeable, to assure the perfect efficacy of the emitting solution.

7.3 Conclusion

The utilization of this laser may regard its utilization in the LLLT field, to treat some inflammatory diseases such apthae, Herpes and other gingival diseases. Moreover, it may increase the bone formation, so favouring the teeth movement in orthodontics and to reduce the osteo-integration time in implantology.
It may be used after the oral surgery to speed the healing process and to reduce the discomfort, so avoiding the use of painkillers.
The therapist may also decide to employ it in the PDT field, to treat the periodontal diseases: it will be sufficient, for the patient, to rinse some minutes before the irradiation with a solution containing a proper cromophore able to absorb the laser wavelength.
Once the device will be constructed and tested by *in vivo* test on cell cultures, it will start the process for patenting it.

Conclusion and future perspectives

In this study we investigated, by several *in vitro* and *ex vivo* tests, the possibility to employ fiber lasers in the different dental fields.
The first sequence of experiments was performed on samples obtained by bovine tongues to evaluate the quality of incision as well as the thermal elevation at different distances from the irradiated zone.
Moreover, the degree of the tissue damages was observed by a blind pathologist who assigned a score to each observed sample, so determining the best parameters able to minimize the intra- and extra-cellular modifications.
The tests demonstrated that the fiber laser device used is very effective on oral soft tissues samples, coupling a high quality of the incision with a lower increasing of the temperature which speedy decreases at the end of the irradiation.
In term of histologic modifications, the blind pathologist assigned the best score to samples irradiated at 3kW, 50 kHz which showed slight modifications, even when compared to the previous studies done by Authors with different diode and solid state lasers.
The second series of tests, performed on di-silicate ceramic samples for making the surface rough to improve the adhesion, demonstrated the capacity of the fiber laser device used to modify, with proper parameters, the samples surface with minimal or absent thermal damages, as confirmed by SEM observation, and with minimal chemical structure perturbation, as shown by the EDS analysis.
Even if the results will have to be confirmed by other different kinds of test, such profilometric and mechanical, this laser may represent a good instrument for this type of treatment.
The last sequence of tests was made on human extracted molars to verify the capacity of the fiber laser device to create cavities on dental enamel and dentine without reaching a thermal elevation dangerous for the vitality of the pulp.
Unfortunately, all the tests performed, with and without air/water spray showed that the temperature reached during irradiation was very high and not biologically compatible with the pulp tissue integrity.
All these sequences of experiments demonstrated that, even if for the moment the device used cannot be employed both in soft and hard dental tissues, however it may represent a

new opportunity in the dental field, thanks to its advantages, when compared to the gas and solid state laser or diode normally used in dentistry.
Particularly, very interesting results the poor thermal elevation in the target tissue during the irradiation which speedy decreases just after the laser beam emission.
The main reason of this behaviour may be explained by the pulsed mode consisting in a train of very short pulses (ns): their short duration, coupled with a rest time, allows to the target tissue to reach the so-called "relaxation pause", so avoiding the risk of overheating.
We must remind that the device used in the study was projected and realized for material marking and so, for using it in the dental field it will be necessary to make some changes.
Firstly, both for safety reasons and for working in "contact mode" the free beam must be launched into an optic fiber with the possibility, through a proper handpiece, to distribute the energy at the impact point.
It will be necessary also, due to the infra-red emission of the device, to add a visible aiming beam (green, red or blue) to show to the operator the zone of irradiation.
Regarding the intraoral "at home" LLLT device, the future research will be focused on the construction of the laser prototype.
We think to supply the energy for the pump by a little device, such a pointer, emitting around 500 nm, but our laboratory tests were performed with a ps pulsed laser and it will be necessary to check the thermal elevation around the pointer, which emits in CW, and, in case of overheating, to add a chopper to provide some rest times during the irradiation.
Once the prototype construction will be completed, the first sequence of tests will be conducted on cell cultures to verify the biomodulating effects and, at the same time, will start the process for patenting the device.

Figures Captions

Fig. 1.1 - The four major types of interactions of light with matter: transmission, reflection, scattering and absorption.

Fig. 1.2 - The behaviour of an incident light beam when reflected and refracted.

Fig. 1.3 - Different effects of a laser beam in function of different pulse durations.

Fig. 1.4 - Beam parameter product vs. laser power for different applications and laser types. Red circles indicate commercially available diode-lasers. Green circle: 200W green solid-state-laser.

Fig. 1.5 - Difference between Gaussian and Top-Hat beam profiles.

Fig. 1.6 - The ionization and Coulomb explosion process, demonstrated for a small cluster (Xe55, ion charges are colour coded, electrons in light grey) irradiated by a 25 fs Gaussian laser pulse (peak intensity IM = 1015 Wcm-2). (a) Initial tunnel ionizations, generating the first ion-electron pairs in the cluster, increasing the local electric field and facilitating further ionizations, (b) nanoplasma formation by classical barrier suppression and electron impact ionization, constituting the main inner ionization channels, (c) outer ionization and Coulomb explosion. The instants of the three snapshots of the time evolution together with the oscillating laser electric field are given on the time axis.

Fig. 1.7 - Difference between the “Conduction mode welding” and the “Keyhole welding”.

Fig. 2.1 - Graphic visualization of the wavelengths transmitted by the different samples in relationship with the most commonly used laser in surgery and LLLT (in increasing order: Blue diode, KTP, red diode, IR diode, Nd:YAG, Nd:YAP and IR diode).

Fig. 2.2 - Absorption coefficients of the main chromophores in tissues.

Fig. 2.3 - The main laser-tissue interactions in function of the PD and time of irradiation.

Fig. 2.4 - Main reactions involved in PhotoDynamic Therapy.

Fig. 2.5 - Action of Biomodulation on mitochondria and consequent biochemical effects activation.

Fig. 2-6 - Laser photothermal effects.

Fig. 2.7 - Difference between Photothermal interaction and Photoablation.

Fig. 2.8 - High-speed micro-cinema-graphic sequence of laser-induced cavitation near a solid surface shows the formation of a micro-jet impact with a velocity of approximately 400 kilometres (250 miles) per hour.

Fig. 3.1 - Effects of Nd:YAG irradiation on human dental enamel. (left: 500X, right: 1500X): micro-cracks, melting and craters are present.

Fig. 3.2 - Absorption spectra of water and hydroxyapatite.

Fig. 3.3 - Dentine conditioning: bur + orthophosphporic acid (left), Laser (centre), Laser + orthophosphoric acid (right).

Fig. 3.4 - Resin tags into the dentine prepared by bur + orthophosphporic acid (left), Laser (centre), Laser + orthophosphoric acid (right).

Fig. 3.5 - Scheme of a fiber laser.

Fig. 4.1 - The pulsed fiber laser (AREX 20, Datalogic, Italy) used for the tests.

Fig. 4.2 - The Dynamic Optical Sensing Interrogator sm130-500 used for the temperature recording.

Fig. 4.3 - One of the samples during laser irradiation: it may be appreciated the optical fiber in the centre of the specimen.

Fig. 4.4 - The setup of the temperature tests on the four sample groups.

Fig. 4.5 - Two of the samples after laser irradiation and before formalin buffering.

Fig. 4.6 - FBG wavelength shift recorded during and after the laser irradiation of samples with 20 kHz repetition rate, 5 mm/s speed and peak power of (a) 10 kW, (b) 7.5 kW, (c) 5 kW and (d) 3 kW, at different distances from the fiber sensor.

Fig. 5.1 - Samples used in the tests (centre and right) and metal cylinder used to check the focus of the laser beam (left). Notice the groove for placing the FBG sensor in the centre of the sample surface.

Fig. 5.2 - The ceramic sample during the laser irradiation.

Fig. 5.3 - Some irradiated samples of the pilot study to determine the proper RR to use in the tests.

Fig. 5.4 - (Left): Non-irradiated sample. (Centre): peak power of 7.5 kW and 50 mm/sec speed. (Right): peak power of 7.5

Fig. 5.5 - Peak power of 10 kW, speed of 10 mm/s: many zones with melting and carbonization are shown. (left: X35, centre: X200, right: X500)

Fig. 5.6 - Peak power of 10 kW, speed of 50 mm/s: some points with melting are shown. (left: X100, centre: X200, right: X500)

Fig. 5.7 - Peak power of 7.5 kW, speed of 50 mm/s: presence of melting and carbonization in some areas of the sample. (left: X35, centre: X50, right: X200)

Fig. 5.8 - Peak power of 5 kW, speed of 10 mm/s: evidence of some zones with melting. (left: X50, centre: X100, right: X500)

Fig. 5.9 - Peak power of 5 kW, speed of 50 mm/s: no evidence of carbonization and melting zones. (left: X75, centre: X100, right: X200)

Fig. 5.10 - (left) Control group and (right) samples irradiated with peak power of 10 kW and speed of 50 mm/s: in red the C concentration.

Fig. 5.11 - (left) Control group and (right) samples irradiated with peak power of 7.5 kW and speed of 50 mm/s: in red the C

Fig. 5.12 - (left) Control group and (right) samples irradiated with peak power of 5 kW and speed of 50 mm/s: in red the C concentration.

Fig. 5.13 - FBG sensor wavelength shift induced by temperature variations during and after the laser irradiation with the best parameters (peak power of 5 kW, repetition rate of 20 kHz, speed of 50 mm/s).

Fig. 6.1 - (left): the extracted human teeth used for the test; (right): sections obtained and steel cylinders used for laser focal distance adjustment.

Fig. 6.2 - Optical microscope observation sample irradiated without air/water spray: a great amount of melting and carbonization may be appreciated.

Fig. 6.3 - The air/water spray sprinkler.

Fig. 6.4 - Some carbonized samples after laser irradiation.

Fig. 6.5 - The samples used for dentine welding tests.

Fig. 6.6 - SEM observation of a sample irradiated at 7.5 kW without air/water spray: it is possible to appreciate some zones of melting, some cracks and an extended fissure interesting all the observed area. (Left: X35, Right: X100)

Fig. 6.7- SEM observation of a sample irradiated at 5 kW with air/water spray: presence of zones with melting and cracks; in the left picture, it is possible to appreciate a great and deep fissure. (Left: X35, Centre: X75, Right; X100)

Fig. 6.8 - SEM observation of one of the group c samples: evident the melted dentine filling the gap between the two parts (Left: X35, Right: X100)

Fig. 7.1 - Difference between traditional and random lasers. In a regular laser the light bounces back and forth between two mirrors that form a cavity. After several passes through the amplifying material in the cavity, the gain amplification can be large enough

to produce laser light. b, in a random laser the cavity is absent but multiple scattering between particles in the disordered material keeps the light trapped long enough for the amplification to become efficient, and for laser light to emerge in random directions.

Fig. 7.2 - The laser device used for the “at home” LLLT treatment

Fig. 7.3 - Reagents used (left) and some of the solutions with different reagents’ concentrations tested (right).

Fig. 7.4 - absorption spectrum of Rhodamine 6G.

Fig. 7.5 - The set-up for The Random emission

Fig. 7.6 - Left: the cuvette containing the Rhodamine solution; Right: the cuvette put behind the power-meter, stimulated by the pumping laser and randomly emitting.

Fig. 7.7 - The graph resulting by the OSA analysis

Fig. 7.8 - The prototype project

Tables captions

Tab. 4.1 - The samples evaluation of the different laser parameters and the scores assigned by the blind pathologist.

Tab. 4.2 - The average of thermal elevation peaks (in C degrees) during the irradiation with different parameters.

List of publications

A list of the publications on international journals, international and national conference proceedings, related to the work presented in this thesis is reported below:

International Journal Papers

Fornaini C, Poli F, Merigo E, Brulat-Bouchard N, El Gamal A, Rocca J-P, Selleri S, Cucinotta A: Disilicate Dental Ceramic Surface Preparation by 1070 nm Fiber Laser: Thermal and Ultrastructural Analysis. Bioengineering 2018, 5, 10.

Carlo Fornaini, Elisabetta Merigo, Federica Poli, Chiara Cavatorta, Jean-Paul Rocca, Stefano Selleri, Annamaria Cucinotta: Use of 1070 nm fiber lasers in oral surgery: preliminary ex vivo study with FBG temperature monitoring.
Laser Therapy, vol. 27 (2018) No.1

Ahmed EL Gamal, Jean Paul Rocca, Carlo Fornaini, Etienne Medioni, Nathalie Brulat-Bouchard: Microhardness evaluations of CAD/CAM ceramics irradiated with CO_2 or Nd:YAP laser.
Laser Therapy, vol. 26 (2017) No.1

El Gamal A, Medioni E, Rocca JP, Fornaini C, Muhammad OH, Brulat-Bouchard N. Shear bond, wettability and AFM evaluations on CO_2 laser-irradiated CAD/CAM ceramic surfaces.
Lasers Med Sci. 2017 May;32(4):779-785.

Carlo Fornaini, Michele Sozzi, Elisabetta Merigo, Piergiorgio Pasotti, Stefano Selleri, Annamaria Cucinotta. Supercontinuum source in the investigation of laser-tissue interactions: *ex vivo* study.
J. Biomed 2017; 2(1): 12-19. doi:10.7150/jbm.17059

Fornaini C, Merigo E, Sozzi M, Rocca JP, Poli F, Selleri S, Cucinotta A: Four different diode lasers comparison on soft tissues surgery: a preliminary ex vivo study.
Laser Ther. 2016 Jun 29;25(2):105-114.

El Gamal A, Fornaini C, Rocca JP, Muhammad OH, Medioni E, Cucinotta A, Brulat-Bouchard N: The effect of CO_2 and Nd:YAP lasers on CAD/CAM Ceramics: SEM, EDS and thermal studies.
Laser Ther. 2016 Mar 31;25(1):27-34.

Fornaini C, Lagori G, Merigo E, Rocca JP, Chiusano M, Cucinotta A: 405 nm diode laser, halogen lamp and LED device comparison in dental composites cure: an *in vitro* experimental trial.
Laser Ther. 2015 Dec 30;24(4):265-74.

Sozzi M, Fornaini C, Cucinotta A, Merigo E, Vescovi P, Selleri S: Dental ablation with 1064 nm, 500 ps, Diode pumped solid state laser: A preliminary study.
Laser Ther. 2013;22(3):195-99.

International Conference Papers

Fornaini C, Merigo E, Poli F, Rocca JP, Brulat N, El Gamal A, Cucinotta A: 1070 nm fiber laser and di-silicate dental ceramic surface conditioning: thermal and ultrastructural analysis.
29th Laserflorence Int. Congress, Florence, 9-11 November 2017

C. Fornaini, F. Poli, E. Merigo, S. Selleri, C. Cavatorta, A. Cucinotta: 1070 nm fiber laser and soft tissues oral surgery: *ex vivo* study with FBG temperature recording. CLEO Europe 2017, June 25-29, 2017, Monaco, Ger (poster)

C Fornaini, E. Merigo, H Raybaud, J-P Rocca, S Selleri, A Cucinotta: Use of fiber lasers in the oral soft tissue surgery: preliminary ex vivo study.
ASLMS Congress 2016. Boston (USA) 30 March-03 April 2016

C Fornaini, E Merigo, S Selleri and A Cucinotta: Radiation absorption in different kinds of tissue analysis: ex vivo study with supercontinuum laser source.
Photonics West 2016, S. Francisco (USA) February 2016

C Fornaini, Elisabetta Merigo, S Selleri and A Cucinotta: Blue diode laser: a new approach in oral surgery?
Photonics West 2016, S. Francisco (USA) February 2016

Fornaini C, Merigo E, Rocca Jp, Sozzi M, Selleri S, Cucinotta A: Four different diode laser wavelengths comparison: a preliminary "ex vivo" study on animal models.
28th Laserflorence Int. Congress, Florence, 5-7 November 2015

C Fornaini: Use of blue laser in oral surgery.
6th IPTA International Congress. Nice (France) 9-10 July 2015

Ahmed EL Gamal, Jean Paul Rocca, Carlo Fornaini, Omid H Muhammad, Etienne Medioni, Annamaria Cucinotta, Nathalie Brulat-Bouchard: CO_2 and Nd:YAP lasers irradiation on CAD/CAM Ceramics: SEM, EDS and thermal studies.
Biophotonics 2015. Florence, 20-22 May 2015

C. Fornaini, M. Sozzi, E. Merigo, F. Poli, S. Selleri, P. Pasotti, A. Cucinotta: Different wavelengths absorption in different tissue kinds: *ex vivo* study with a supercontinuum broadband source.
ASLMS Congress 2015. Kissimmee (USA) 22-26 April 2015

C Fornaini, E Merigo, M Sozzi, S Selleri, P Vescovi, A Cucinotta: 810nm, 980nm, 1470nm and 1950nm diode laser comparison: a preliminary *ex vivo* study on oral soft tissues.
Photonics West 2015, S. Francisco (USA) February 2015

M Sozzi, G Lagori, E Merigo, A Cucinotta, P Vescovi, S Selleri: Dental composite polymerization: a three different sources comparison.
Photonics West 2015, S. Francisco (USA) February 2015

National Conference Papers

C. Fornaini, F. Poli, E. Merigo, S. Selleri, A. Cucinotta
Ultrastructural analysis of dental ceramic surface processed by a 1070 nm fiber laser.
3rd PARMA NANO-DAY, Parma July 12-14th 2017

C Fornaini, F Poli, E Merigo, S Selleri, A Cucinotta: 1070 nm fiber laser for dental ceramic surface processing: ultrastructural analysis.
FOTONICA 2017 19a Edizione - Convegno Italiano delle Tecnologie Fotoniche, Padova, 3-5 maggio 2017

C Fornaini, F Poli, E. Merigo, M. Sozzi, J-P Rocca, S Selleri, A Cucinotta: Choice of the proper laser wavelength in the soft tissues oral surgery: *ex viv*o study. FOTONICA 2016 18a Edizione - Convegno Italiano delle Tecnologie Fotoniche. Roma, 6-8 giugno 2016

References

[1] Anisimov S.I, Bonch-Bruevich AM, Elyashevich MA, Imas Ya A, Pavlenko NA and Romanov GS: Effect of powerful light fluxes on metals. Sov. Phys.–Tech. Phys., 11, 945 (1967).

[2] Ready JF: Effects due to absorption of laser radiation. Journ. Appl. Phys., 36, 462 (1965).

[3] Anisimov SI: Evaporation of light-absorbing metals. High Temperature, 6-110 (1968).

[4] Aleshin IV, Bonch-Bruevich AM, Imas Ya A, Libenson MN, Rubanova GM and Salyadinov VS: Laser-induced evaporation of nonlinearly absorbing dielectrics. Sov. Phys.–Tech. Phys., 22, 1400 (1977).

[5] Ready JF: Effects of High-Power Laser Radiation, Academic Press, New York (1971).

[6] Anisimov SI, Imas Ya A, Romanov GS and Khodyko Yu V: Action of High-Power Radiation on Metals. Natl. Tech. Inform. Service, Springfield, VA (1971).

[7] D. Bäuerle: Laser Processing and Chemistry. Springer, Berlin (2000).

[8] J. Heller, J.W. Bartha, C.C. Poon, A.C. Tam: Temperature dependence of the reflectivity of silicon with surface oxide at wavelengths of 633 and 1047 nm Appl. Phys. Lett. 75(1), 43 (1999).

[9] M. Toulemonde, S. Unamuno, R. Heddache, M.O. Lampert, M. Hageali, P. Siffert: Time-resolved reflectivity and melting depth measurements using pulsed ruby laser on silicon. Appl. Phys. Mater. Sci. Process. 36(1), 31 (1985).

[10] C.B. Arnold, M.J. Aziz, M. Schwarz, D.M. Herlach: Parameter-free test of alloy dendrite-growth theory. Phys. Rev. B 59(1), 334 (1999).

[11] J.C. Weeber, J.R. Krenn, A. Dereux, B. Lamprecht, Y. Lacroute, JP. Goudonnet: Near-field observation of surface plasmon polariton propagation on thin metal stripes. Phys. Rev. B 64(4) (2001).

[12] R.E. Slusher, B.J. Eggleton: Non-linear Photonic Crystals, 1st ed. Springer, Berlin (2004).

[13] N. Ghofraniha, C. Conti, G. Ruocco, S. Trillo: Shocks in nonlocal media. Phys. Rev. Lett. 99(4) (2007).

[14] W. Staudt, S. Borneis, K.D. Pippert: TFT Annealing with Excimer Laser. Technology and Market Outlook. Phys Status Solidi Appl Res 166(2), 743 (1998).

[15] C. W. White and M. J. Aziz: Surface alloying by ion, electron and laser beams., Metals Park, OH, ASM. 19 (1987).

[16] B. L. Mordike: Materials science and technology. Vol. 15, 111; Weinheim, VCH (1993).

[17] D. Shealy: Historical perspective of laser beam shaping. Proc. SPIE, 4770, 28-47 (2002).

[18] F. Dickey, L. Weichman and R. Shagam: Laser beam shaping techniques. Proc. SPIE, 4065, 338–348 (2000).

[19] A.J. Hick: Rapid surface heat treatments-a review of laser and electron beam hardening. Heat Treat. Met., 10(1), 3 (1983).

[20] D.L. Bourell, H.L. Marcus, J.W. Barlow, J.J. Beaman: Selective laser sintering of metals and composites. Int. J. Powder Metall 28(4), 369 (1992).

[21] X. Wang, X. Xu: Thermo-elastic wave induced by pulsed laser heating. Appl. Phys. A Mater. Sci. Process. 73(1), 107 (2001).

[22] W.M. Steen: Laser Material Processing. 3rd edn, Springer, London (2003).

[23] J.C. Ion: Laser Processing of Engineering Materials. In: Principles, Procedure and Industrial Applications, Elsevier Butterworth-Heinemann, Oxford (2005).

[24] M.J. Aziz, J.Y. Tsao, M.O. Thompson, P.S. Peercy, C.W. White: Solute Trapping: Comparison of Theory with Experiment Phys. Rev. Lett. 56(23), 2489 (1986).

[25] J.S. Im, M.A. Crowder, R.S. Sposili, J.P. Leonard, H.J. Kim, J.H. Yoon, V.V. Gupta, H.J. Song, H.S. Cho: Controlled Super-Lateral Growth of Si Films for Microstructural Manipulation and Optimization. Phys Status Solidi Appl. Res. 166(2), 603 (1998).

[26] R.E. Slusher, B.J. Eggleton: Nonlinear Photonic Crystals. 1st edn, Springer, Berlin (2004).

[27] D.B. Chrisey, G.K. Hubler: Pulsed Laser Deposition of Thin Films. Wiley Interscience, New York (1994).

[28] C Fornaini: Intraoral laser welding. In: Laser Welding. Edited by Xiaodong Na, Stone, ISBN 978-953-307-129-9. Publisher: Sciyo, USA (2010).

[29] X.L. Mao, A.C. Ciocan, R.E. Russo: Preferential vaporization during laser ablation inductively coupled plasma atomic emission spectroscopy. Appl. Spectrosc. 52(7), 913 (1998).

[30] N.M. Bulgakova, A.V. Bulgakov: Pulsed laser ablation of solids: transition from normal vaporization to phase explosion. Appl. Phys. A Mater. Sci. Process. 73(2), 199 (2001).

[31] R. Stoian, D. Ashkenasi, A. Rosenfeld, E.E.B. Campbell: Coulomb explosion in ultrashort pulsed laser ablation of Al_2O_3. Phys. Rev. B 62(19), 13167 (2000).

[32] B.J. Garrison, R. Srinivasan: Laser ablation of organic polymers: microscopic models for photochemical and thermal processes. J. Appl. Phys. 57(8), 2909 (1985).

[33] W.M. Steen and K. Watkins: Laser material processing. Springer-Verlag, New York (2003).

[34] Mordike BL, In Cahn RW, Haasan P and Kramer EJ: Materials Science and Technology. VCH, Weinheim (1993).

[35] J. Mazumdar: Lasers for materials processing. North-Holland Pub. Co., New York (1983).

[36] M Duocastella, CB Arnold: Bessels and anular beams for materials processing. Laser Photonics Rev. 6, No. 5, 607–621 (2012).

[37] Laeng J, Stewart JG and Liou FW: Laser Metal Forming Processes and the Application in Rapid Prototyping of Metallic Parts. Proc. of 2nd International Conference on Advanced Manufacturing Technology", Johor Bahru, Malaysia, August, Elsevier, Amsterdam, the Netherlands (2000).

[38] Namba Y: Laser Forming in Space. Proceedings of the International Conference of Lasers and Electro-Optics (ICALEO'85), Boston, MA, September. Laser Institute of America, Orlando (1985).

[39] Namba Y: Laser Forming of Metals and Alloys. Proceedings of Laser Advanced Materials Processing (LAMP'87). Osaka, Japan, June High Temperature Society of Japan, Osaka (1987).

[40] F. Vollersten: Mechanisms and models for laser forming. In 'Laser assisted net shape engineering' ed. M. Geiger and F. Vollersten, Bamberg, Meisenbach (1994).

[41] F. Vollersten and M. Rodle: Model for the temperature gradient mechanism in laser bending. In 'Laser assisted net shape engineering' ed. M. Geiger and F. Vollersten, Bamberg, Meisenbach (1994).

[42] Vollersten F, Holzer S: Laser beam forming: Fundamentals and possible applications. VDI-Z., 1994, 136 (1994).

[43] M. Geiger and F. Vollersten: The Mechanisms of Laser Forming. Ann. CIRP, 42-1 (1993).

[44] H. Arnet and F. Vollertsen: Extending laser bending for the generation of convex shape. J. Eng. Manuf. 209, 433–442 (1995).

[45] Schuöcker D: Mathematical modeling of laser-assisted deep drawing. J. Mater. Process. Technol. 115, 104–107 (2001).

[46] W. Wang, M.R Holl, and D.T. Schwartz: Rapid prototyping of masks for through-mask electrodeposition of thick metallic components. J. Electrochem. Soc. 148, C363-368 (2001).

[47] Greco A, Licciulli A, Maffezzoli A: Stereolitography of ceramic suspensions. J. Mater. Sci., 36, 99–105 (2001).

[48] L. Lu, J. Y. H. Fuh, Z. D. Chen, C. C. Leong and Y. S. Wong: In situ formation of TiC composite using selective laser melting. Mater. Res. Bull., 35, 1555–1561 (2000).

[49] K. Daneshvar, M. Raissi and S. M. Bobbio: Laser rapid prototyping in nonlinear medium. J. Appl. Phys., 88, 2205–2210 (2000).

[50] S. Shoji and S. Kawata: Photofabrication of three-dimensional photonic crystals by multibeam laser interference into a photopolymerizable resin. Appl. Phys. Lett., 76, 2668–2670 (2000).

[51] O. Lehmann and M. Stuke: Laser-Driven Movement of Three-Dimensional Microstructures Generated by Laser Rapid Prototyping. Science, 270, 1644–1646 (1995).

[52] M. Burns: Automative fabrication: improving productivity in manufacturing. Englewood Cliffs, NJ, PTR Prentice-Hall Inc. (1993).

[53] K. Paul and S. Baskaran: Issues in fabricating manufacturing tooling using powder-based additive freeform fabrication. J. Mater. Process. Technol., 61, 168–172 (1996).

[54] Kochan D: Solid freeform manufacturing. Elsevier, Amsterdam (1993).

[55] S. Fukumoto, A. Hirose, KF. Kobayashi: An effective joint of continuous SiC/Ti-6Al-4V composites by diffusion bonding. Composites Engineering, 5-8 (1995).

[56] A. Forbis-Parrott: Laser beam welding is ready to go to work at Cadillac. Weld. J., 70, 37–42 (1991).

[57] S. T. Riches: Laser welding in automobile manufacture. Weld. Met. Fabr., 61, 79-83 (1993).

[58] R. S. Parmar: Welding engineering and technology. Khanna Publishers, New Delhi (1999).

[59] J. F. Lancaster: Metallurgy of welding. 4th ed. George Allen and Unwin, London. (1980).

[60] W. W. Duley: Laser welding, 1st ed. John Wiley & Sons, Inc, New York (1999).

[61] K. H. Leong, P. A. Kirkham and K. C. Meinert, Jr: Deep penetration welding of nickel aluminum bronze. J. Laser Appl., 12, 181–184 (2000).

[62] Hirose, H. Todaka, K. Yamaoka, N. Kurosawa and K. F. Kobayashi: Quantitative evaluation of softened regions in weld heat-affected zones of 6061-T6 aluminum alloy—Characterizing of the laser beam welding process. Metall. Mater. Trans. A, , 30A, 2115–2120 (1999).

[63] T. T. Hsu, Y. R. Wang, S. K. Wu and C. Chen: Effect of CO_2 laser welding on the shape-memory and corrosion characteristics of TiNi alloys. Metall. Mater. Trans. A, 32A, 569–576 (2001).

[64] J. M. Jouvard, K. Girard and O. Perret: Keyhole formation and power deposition in Nd:YAG laser spot welding. J. Phys. D: Appl. Phys., 34(18), 2894–2901 (2001).

[65] L. W. Tsay and C. Y. Tsay: The Effect of Microstructures on the Fatigue Crack Growth in Ti-6Al-4V Laser Welds. Int. J. Fatigue, 19, 713–720 (1997).

[66] Hirose, S. Fukumoto and K. F. Kobayashi: Joining Processes for Structural Applications of Continuous Fiber Reinforced MMCs. Key Eng. Mater., 104–107, 853–872 (1995).

[67] M. Marya and G. R. Edwards: Factors Controlling the Magnesium Weld Morphology in Deep Penetration Welding by a CO_2 Laser. J. Mater. Eng. Perform., 4, 435–443 (2001).

[68] T. Shida, M. Hirokawa and S. Sato: CO_2 Laser Welding of Aluminum Alloys. Journal of the Japan Welding Society, 43, 36 (1997).

[69] Belic and J. Stanic: A method to determine the parameters of laser iron and steel cutting. Opt. Laser Technol., 19, 309–311 (1987).

[70] S. L. Chen: The effects of gas composition on the CO_2 laser cutting of mild steel. J. Mater. Process. Technol., 73, 147–159 (1998).

[71] W. O'Neill and J. T. Gabzdyl: New developments in laser-assisted oxygen cutting. Opt. Lasers Eng., 34, 355–367 (2000).

[72] Ivarson, J. Powel, J. Kamalu and C. Magnusson: The oxidation dynamics of laser cutting of mild steel and the generation of striations on the cut edge. J. Mater. Process. Technol., 40, 359–374 (1994).

[73] K. Danisman, B. S. Yilbas, A. Gorur, R. Davies, C. Ciftlikli, Z. Yilbas and F. Begh: Study of some characteristics of the plasma generated during a CO2 laser beam cutting process. Opt. Laser Technol., 24, 33–38 (1992).

[74] J. Wang and W. C. K. Wong: A study of abrasive waterjet cutting of metallic coated sheet steels. J. Mater. Process. Technol., 95, 164–168 (1999).

[75] K. Y. Low, L. Li and P. J. Byrd: Spatter removal characteristics and spatter prevention during laser percussion drilling of aerospace alloys. Opt. Laser Technol., 32, 347–354 (2000).

[76] J. Cheng, E. J. Kahlen and A. Kar: Proc. ICALEO'00 Conf., Dearborn, MI, USA, October 2000, Laser Institute of America, 232–238 (2000).

[77] Lehane and H. S. Kwok: Enhanced drilling using a dual-pulse Nd:YAG laser. Appl. Phys. A, 73A, 45–48 (2001).

[78] X. Zhu, D. M. Villeneuve, Yu. A. Naumov, S. Nikumb and P. B. Corkum: Experimental Study of Drilling Sub-10 mm Holes in Thin Metal Foils With Femtosecond Pulses. Appl. Surf. Sci., 152, 138–148 (1999).

[79] Q. Wu, Y. Ma, J. Jie, B. Miao, R. Fang and X. Chen: Proc. ICALEO'01 Conf., Jacksonville, FL, USA, October 2001, Laser Institute of America, 150 (2001).

[80] Corcoran, L. Sexton, B. Seaman, P. Ryan and G. Byme: Proc. ICALEO'00 Conf., Dearborn, MI, USA, October 2000, Laser Institute of America, 100 (2000).

[81] T. Beck, S. Seidel and H. Weber: The multiconfiguration time-dependent Hartree (MCTDH) method: a highly efficient algorithm for propagating wavepackets. Laser Mater. Process., 87, (Part 1), C70–C79 (2000).

[82] Y. Yeo, S. C. Tam, S. Jana, Michael and W. S. Lau: A technical review of the laser drilling of aerospace materials. J. Mater. Process. Technol, 42, 15–49 (1994).

[83] M. Boutinguiza, J. Pou, F. Lusquinosa, F. Quintero, R. Soto, M. Perez-Amor, K. Watkins and W. M. Steen: Laser cutting using off-axial supersonic rectangular nozzles. Opt. Lasers Eng., 37, 15–25 (2002).

[84] T. Kurita, T. Ono and N. Morita: Study on the relationship between laser processing sound and material removal characteristics. J. Mater. Process. Technol., 97, 168–173 (2000).

[85] J. K. Lumpp and S. D. Allen: Excimer laser machining and metallization of vias in aluminum nitride. IEEE Trans. Compon. Packag. Manuf. Technol., 20, 241–246 (1997).

[86] H. Zheng, E. Gan and G. C. Lim: Investigation of laser via formation technology for the manufacturing of high density substrates. Opt. Lasers Eng., 36, 355–371 (2001).

[87] Tsunemi, K. Hagiwara, N. Saito, K. Nagasaka, Y. Miyamoto, O. Suto and H. Tashiro: Complete removal of paint from metal surface by ablation with a TEA CO_2 laser. Appl. Phys. A, 63A, 435–439 (1996).

[88] M. J. J. Schmidt, L. Li and J. T. Spencer: An investigation into the feasibility and characteristics of using a 2.5 KW high power diode laser for paint stripping. Surf. Coat. Technol., 141, 40–47 (2001).

[89] J. M. Lee, C. Curran and K. G. Watkins: Laser removal of copper particles from silicon wafers using UV, visible and IR radiation. Appl. Phys. A, 73A, 219–224 (2001).

[90] P. Meja, M. Autric, P. Alloncle, P. Pasquet, R. Oltra and J. P. Boquillon: Laser cleaning of oxidized iron samples: The influence of wavelength and environment. Appl. Phys. A, 69A, 687–690 (1999).

[91] K. Rubahn and J. Ihlemann: Excimer laser micro machining: fabrication and applications of dielectric masks. J. Appl. Phys., 86, 2847–2855 (1999).

[92] J. Zhang, K. Sugioka, S. Wada, H. Tashiro and K. Toyoda: Ablation of fused quartz by ultraviolet, visible or infrared laser coupled with VUV laser. Appl. Phys. A, 64A, 367–371 (1997).

[93] M. Verdier, S. Costil, C. Coddet, R. Oltra and O. Perret: On the topographic and energetic surface modification induced by laser treatment of metallic substrates before plasma spraying. Appl. Surf. Sci., 205, 3–21 (2003).

[94] J. Philip, T. Jayakumar and B. Raj: Laser etching of austenitic stainless steels for micro-structural evaluation. Mater. Sci. Eng. A, A338, 17–23 (2002).

[95] M. Kawasaki and H. Gijutsu: J. Surf. Finish. Soc. Jpn, 53, 490–496 (2002).

[96] Y. Feng, Z. Q. Liu and X. S. Yi: Marking carbon black/polypropylene compounds using a Nd: YAG laser. J. Mater. Sci. Lett., 20, 517–519 (2001).

[97] Y. S. Xiao and F. Yi: Etching behavior of plastics using a near infrared laser. J. Mater. Sci. Lett., 18, 245–247 (1999).

[98] Allcock, P. E. Dyer, G. Elliner and H. V. Snelling: Experimental observations and analysis of CO_2 laser-induced microcracking of glass. J. Appl. Physi., 78, 7295-7303 (1995).

[99] Beu-Zion, A. Inberg, N. Croitoru and S. A. Shalem Katzir: Hollow glass waveguides and silver halide fibers as scanning elements for CO_2 laser marking systems. Opt. Eng., 39, 1384–1390 (2000).

[100] L. Monaco, E. Gallus and M. Bianco: Lamiera, 39, 58–63 (2002).

[101] J. Bosman: Materialen (Netherlands), 17, 4–6 (2001).

[102] S. Buckley and C. M. Roland: Reversible optical data storage on polyethylene terephthalate. Polym. Eng. Sci., 37, 138–142 (1997).

[103] R. Alexander and M. S. Khlif: Laser marking using organo-metallic films. Opt. Lasers Eng., 25, 55–70 (1996).

[104] A. D. Compaan, I. Matulionis and S. Nakade: Laser scribing of polycrystalline thin films. Opt. Lasers Eng., 34, 15–45 (2000).

[105] Sadoghi P: Influence of scattering, tissue optical parametres and interface reflectivities on photon migration in human tissue. J Mod Opt. 54: 845-854 (2007).

[106] Neimz NH: Laser- tissue Interaction: Fundamentals and Applications. Springer-Verlag, New York. (2003).

[107] Sadoghi P: Discrete ordinates method for propagation of light in highly scattering vascular tissues. Opt Commun. 266: 363-359 (2006).

[108] Arridge SR, Hebden JC: Optical imaging in medicine: II. Modelling and reconstruction. Phys Med Bio. 42: 841-853 (1997).

[109] Arridge SR, Dehghani H, Schweiger M, Okada E: The finite element model for the propagation of light in scattering media: A direct method for domains with non-scattering regions. Med Phys. 27: 256-264 (2000).

[110] Cheong WF, Prahl SA, Welch AJ: A Review of the Optical Properties of Biological Tissues. IEEE J QUANTUM ELECT. 26: 2166- 2185 (1990).

[111] Welch AJ, Gardner C, Richards-Kortum R, Criswell G, Pfefer J, Warren S: Propagation of fluorescent light. Laser Surg Med. 21: 166-178 (1997).

[112] Yicong Wu, Peng Xi, Jianan Qu, Tak-Hong Cheung, and Mei-Yung Yu: Depth-resolved fluorescence spectroscopy of normal and dysplastic cervical tissue. Opt Express 13: 382-388 (2005).

[113] Arridget SR, Copet M, Delpy DT: The theoretical basis for the determination of optical pathlengths in tissue: temporal and frequency analysis. Phys Med Biol. 37: 1531-1560 (1992).

[114] N. Bashkatov, E. A. Genina, V. I. Kochubey, V. V. Tuchin: Optical properties of human skin, subcutaneous and mucous tissues in the wavelength range from 400 to 2000nm, J. Phys. D: Appl. Phys. 38 2543–2555 (2005).

[115] S.W. Lanigan: Lasers in dermatology. Springer, London (2000).

[116] R. Young: Chromophores in human skin. Phys. Med. Biol. 42 789-802 (1997).

[117] S. L. Jacques, D. J. McAuliffe: The melanosome: threshold temperature for explosive vaporization and internal absorption coefficient during pulse laser irradiation. Photochem. Photobiol. 53, 769-775 (1991).

[118] Claridge, D. Hidovic- Rowe, P. Taniere, T. Ismail: Quantifying mucosal blood volume fraction from multispectral images of the colon, Proc. SPIE. 6511, 17-22 (2007).

[119] R. Yip: Significance of an abnormally low or high hemoglobin concentration during pregnancy: special consideration of iron nutrition, Am. J. Clin. Nutr. 72 272S-279S (2000).

[120] M. C. van Beekvelt, M. S. Borghuis, B. G. van Engelen, R. A. Wevers, and W. N. Colier: Adipose tissue thickness affects in vivo quantitative near-IR spectroscopy in human skeletal muscle. Clinical Science 101, 21-28 (2001).

[121] J. S. Dam, P. E. Andersen, T. Dalgaard, and P. E. Fabricius: Determination of tissue optical properties from diffuse reflectance profiles by multivariate calibration. Appl. Opt. 37, 772-778 (1998).

[122] L. Wang, S.L. Jacques and L. Zheng: MCML-MonteCarlo modeling of light transport in multi-layered tissues. Computer Methods and Programs in Biomedicine 47, 131-146 (1995).

[123] T. J. Farrell, M. S. Patterson, B. C. Wilson: A diffusion theory model of spatially resolved, steady-state diffuse reflectance for the non-invasive determination of tissue optical properties in vivo. Med. Phys. 19, 879-888 (1992).

[124] Zeng, C. MacAulay, C. Palcic, and D. I. McLean: A computerized autofluorescence and diffuse reflectance spectro-analyser system for in vivo skin studies. Phys. Med Biol. 38, 231-240 (1993).

[125] Fornaini, M. Sozzi, E. Merigo, P. Pasotti, S. Selleri, A. Cucinotta: Supercontinuum source in the investigation of laser-tissue interactions: “ex vivo” Study. J. Biomed; 2(1):12-19 (2017).

[126] Cheong Wf, Prahl Sa, Welch Aj: A review of the optical properties of biological tissues. IEEE J Quant EI 26:2166-2185 (1990).

[127] Roggan A, Dorschel K, Minet 0, Wolff D, Muller G: The optical properties of biological tissue in the near infrared wavelength range - review and measurements. In: Muller G, Roggan A (EDS) Laser induced interstitial thermotherapy. SPIE-Press, Bellingham, 10-44 (1995).

[128] Calzavara-Pinton PG, Venturini M, Sala R: Photodynamic therapy: update 2006. Part 1: Photochemistry and photobiology. J Eur Acad Dermatol Venereol.; 21:293-302 (2007).

[129] Morton CA: Photodynamic therapy for non-melanoma skin cancer: and more? Arch Dermatol;140:116-120 (2004).

[130] Agarwal ML, Clay ME, Harvey EJ, Evans HH, Antunez AR, Oleinick NL: Photodynamic therapy induces rapid cell death by apoptosis in L5178Y mouse Lymphoma cells. Cancer Res.; 51:5993-6 (1991).

[131] Dougherty TJ, Gomer CJ, Henderson BW, Jori G, Kessel D, Korbelik M, et al: Photodynamic therapy. J Natl Cancer Inst.; 90:889-905 (1998).

[132] Goldman M, Atkin D: ALA/PDT in the treatment of actinic keratosis: spot Versus confluent therapy. J Cosmet Laser Ther.;5:107-110 (2003).

[133] Mester E, Szende B, Tota JG: Effect of laser on hair growth of mice. Kiserl Orvostud.;19:628–631 (1967).

[134] Mester E, Spiry T, Szende B, et al: Effect of laser rays on wound healing. Am J Surg.; 122:532–535 (1971).

[135] Mester E, Szende B, Spiry T, et al: Stimulation of wound healing by laser rays. Acta Chir Acad Sci Hung.; 13:315–324 (1972).

[136] Aimbire F, Albertini R, Pacheco MT, et al: Low-level laser therapy induces dose-dependent reduction of TNFalpha levels in acute inflammation. Photomed Laser Surg; 24:33–37 (2006).

[137] Karu T: Primary and secondary mechanisms of action of visible to near-IR radiation on cells. J Photochem Photobiol B; 49:1–17 (1999).

[138] Passarella S, Casamassima E, Molinari S, et al: Increase of proton electrochemical potential and ATP synthesis in rat liver mitochondria irradiated in vitro by helium-neon laser. FEBS Lett.; 175:95–99 (1984).

[139] Greco M, Guida G, Perlino E, et al: Increase in RNA and protein synthesis by mitochondria irradiated with helium-neon laser. Biochem Biophys Res Commun; 163:1428–1434 (1989).

[140] Lohr NL, Keszler A, Pratt P, et al: Enhancement of nitric oxide release from nitrosyl hemoglobin and nitrosyl myoglobin by red/near infrared radiation: potential role in cardioprotection. J Mol Cell Cardiol.;47:256–263 (2009).

[141] Kam T, Kalendo G, Lethokov V. Lobko: Biostimulation of HeLa cells by low-intensity visible light II. Stimulation of DNA and RNA synthesis in a wide spectral range. Nuevo Cimento. 309–318 (1984).

[142] Baxter GD: Therapeutic Lasers: Theory and Practice. Churchill Livingstone; London, England (1994).

[143] Longo L: Terapia Laser. USES; Firenze, Italy (1986).

[144] Cruanes CJ: Laser Therapy Today. Laser Documentation Centre. Barcelona, Spain (1984).

[145] Zhang Y, Song S, Fong CC, et al: cDNA microarray analysis of gene expression profiles in human fibroblast cells irradiated with red light. J Invest Dermatol; 120:849–857 (2003).

[146] Dostalova T, Hlinakova P, Kasparova M, Rehacek A, Vavrickova L, Navratil L: Effectiveness of physiotherapy and GaAlAs laser in the management of Temporo-mandibular Joint Disorders. Photomed Laser Surg.; 30:275-280 (2012).

[147] Fornaini C: LLLT in the Symptomatic Treatment of Oral Lichen Planus. Laser Ther. Mar 28;21(1):51-3 (2012).

[148] Bouzari N, Davis S C and Nouri K: Laser treatment of keloids and hypertrophic scars. Int J Dermatol 46(1): 80-88 (2007).

[149] Cunliffe W J and Goulden V: Phototherapy and acne vulgaris. Br J Dermatol 142(5): 855-856 (2000).

[150] Bjordal JM, Johnson MI, Lopes-Martins RA, Bogen B, Chow R, Ljunggren AE: Short-term efficacy of physical interventions in osteoarthritic knee pain. A systematic review and meta-analysis of randomised placebo-controlled trials. Musculoskelet Disord. Jun 22; 8:51 (2007).

[151] Godine RL: Low level laser therapy (LLLT) in veterinary medicine. Photomed Laser Surg. Jan;32(1):1-2 (2014).

[152] Milani L: Soft-laser therapy in the treatment of fibromyositis in sports medicine. Minerva Med. Jun 30;74(27):1689-92 (1983).

[153] Parrish JA, Deutsch TF: Laser photomedicine. IEEE J. Q. Electron. QE-20 1386-1396. (2010).

[154] Fisher JC: Qualitative and quantitative tissue effects of light from important surgical lasers: Optimal surgical principles. In: Laser Surgery in Gynecology. Wright VC, Fisher JC, eds. Philadelphia: WB Saunders Co, pp.58-81 (1993).

[155] Thomsen S: Pathologic analysis of photothermal and photomechanical effects of laser-tissue interactions. Photochem Photobiol.; 53:825–35 (1991).

[156] Vogel A, Busch S, Jungnickel K, Birngruber R: Mechanism of intraocular photodisruption with picosecond and nanosecond laser pulses. Laser Surg Med 15, 32-43 (1994).

[157] Friedman HD, Levi E: Plasma Shielding. Physics of Fluids 13, 1049 AIP. (1970).

[158] Dretler SP: Laser lithotripsy: a review of 20 years of research and clinical applications. Laser Surg Med, , 8; 341-356 (1998).

[159] Srinivasan R, Mayne-Banton V: Self-developing photoetching of polyethylene terephthalate films by far ultraviolet excimer laser radiation. Appl. Phys. Lett., 41; 576-578 (1982).

[160] Bloembergen N: Laser-induced electric breakdown in solids. IEEE J. Q. Electron., QE-10; 375-386 (1974).

[161] Vogel A, Lauterborn W, Timm R: Optical and acoustic investigation of the dynamics of laser-produced cavitation bubbles near a solid boundary. J Fluid Mech, 206; 299-338 (1989).

[162] L. Goldman and R. J. Rockwell: Lasers in Medicine. Gordand and Breach, New York (1971).

[163] Beetham WP, Aiello LM, Balodimos MC, Koncz L: Ruby laser photocoagulation of early diabetic neovascular retinopathy. Preliminary report of a long-term controlled study. Arch Ophthalmol. Mar;83(3):261-72 (1970).

[164] Geza J Jako: Laser surgery of the vocal cords. An experimental study with laser Carbon Dioxide Lasers on dogs. Laryngoscope, 82; Dec (1972).

[165] Reiken SR, Wolfort SF, Berthiaume F, Compton C, Tompkins RG, Yarmush ML: Control of hypertrophic scar growth using selective photothermolysis. Lasers Surg Med.;21(1):7-12 (1997).

[166] Scheibner A, Kenny G, White W, Wheeland RG: A superior method of tattoo removal using the Q-switched ruby laser. J Dermatol Surg Oncol. Dec;16(12):1091-8 (1999).

[167] Badawi A, Tome MA, Atteya A, Sami N, Morsy IA: Retrospective analysis of non-ablative scar treatment in dark skin types using the sub-milliseconds Nd:YAG 1,064 nm laser. Lasers Surg Med. Feb;43(2):130-6 (2011).

[168] Goldman L: Effect of laser beam impacts on teeth. J. Amer. Dent. Assoc. Mar. (1965).

[169] Kinersly T: Laser effects on tissue and materials related to dentistry. J. Amer. Dent. Assoc. (1965).

[170] Morrant G.A: Lasers: an appraisal of their possible use in dentistry. Dent. Pract. (1965).

[171] Wigdor H, Abt E, Ashrafi S, Walsh JT Jr: The effect of lasers on dental hard tissues. J Am Dent Assoc. Feb;124(2):65-70 (1993).

[172] Stern R.H.: Laser effect on dental hard tissues. A preliminary report. J. S. Calif. Dent. Assoc. (1965).

[173] Taylor R.: The effects of laser radiation on teeth, dental pulp, and oral mucosa of experimental animals. Oral Surg., (1965).

[174] Basu MK, Frame JW, Rhys Evans PH: Wound healing following partial glossectomy using the CO2 laser, diathermy and scalpel: a histological study in rats. J Laryngol Otol. Apr;102(4):322-7 (1988).

[175] Hibst R, Keller U: Experimental studies of the application of the Er:YAG laser on dental hard substances: I. Measurement of the ablation rate. Laser Surg Med. 9:338, (1989).

[176] Keller U, Hibst R: Experimental studies of the application of the Er:YAG laser on dental hard substances: II. Light microscopic and SEM investigations. Lasers Surg Med; 9:345-351 (1989).

[177] Dostálová T, Jelínková H, Krejsa O, Hamal K, Kubelka J, Procházka S, Himmlová L: Dentin and pulp response to Erbium:YAG laser ablation: a preliminary evaluation of human teeth. J Clin Laser Med Surg; 15:117-121 (1997).

[178] Pelagalli J, Gimbel CB, Hansen RT, Swett A, Winn DW: Investigational study of the use of Er:YAG laser versus dental drill for caries removal and cavity preparation--phase I. J Clin Laser Med Surg;15:109- 115 (1997).

[179] Takeda FH, Harashima T, Kimura Y, Matsumoto K: Comparative study about the removal of smear layer by three types of laser devices. J Clin Laser Med Surg; 16:117-122 (1998).

[180] Glockner K, Rumpler J, Ebeleseder K, Städtler P: Intrapulpal temperature during preparation with the Er:YAG laser compared to the conventional burr: an in vitro study. J Clin Laser Med Surg; 16:153-157 (1998).

[181] Rizoiu I, Kohanghadosh F, Kimmel AI, Eversole LR: Pulpal thermal responses to an erbium, chromium: YSGG pulsed laser hydrokinetic system. Oral Surg Oral Med Oral Pathol Oral Radiol Endod.;86:220-223 (1998).

[182] Ando Y, Aoki A, Watanabe H, Ishikawa I: Bactericidal effect of erbium YAG laser on periodontopathic bacteria. Lasers Surg Med 19:190-200 (1996).

[183] Kornblit R, Trapani D, Bossù M, Muller-Bolla M, Rocca JP, Polimeni A: The use of Erbium:YAG laser for caries removal in paediatric patients following minimally Invasive Dentistry concepts. Eur J Paediatr Dent; 9:81-87 (2008).

[184] Ceballos L, Toledano M, Osorio R, Tay FR, Marshall GW: Bonding to Er:YAG laser treated dentin. J Dent Res; 81:119 (2002).

[185] V. Tuchin: Biomedical Optics and Biophotonics. SPIE Press, USA (2012).

[186] RR. Anderson and JA. Parrish: Selective Photothermolysis: Precise Microsurgery by Selective Absorption of Pulsed Radiation. Science 220 524-527 (1983).

[187] JA. Parrish, RR. Anderson, T. Harrist, B. Paul and GF. Murphy: Selective Thermal Effects with Pulsed Irradiation from Lasers: From Organ to Organelle. Journal of Investigative Dermatology 80 75-80 (1983).

[188] MN. Zervas and C A. Codemard: High Power Fiber Lasers: A Review. IEEE Journal of selected topics in Quantum Electronics, Vol. 20, No. 5, September/October (2014).

[189] M. Pierce, S. Jackson, P. Golding, B. Dickinson, M. Dickinson, T. King, P. Sloan: Development and application of fibre lasers for medical applications, Proc. SPIE 4253, Optical Fibers and Sensors for Medical Applications 144, 4 (2001).

[190] Shiner: The Impact of Fiber Laser Technology on the World Wide Material Processing Market, CLEO: 2013. OSA Technical Digest (online) Optical Society of America, AF2J:1 (2013).

[191] Zheng, H. Zhang, P. Yan, M. Gong: Low repetition rate broadband high energy and peak power nanosecond pulsed Yb-doped fiber amplifier. Optics & Laser Technology 49 284-287 (2013).

[192] Tünnermann: High-power CW Fiber Lasers-Present and future. LTJ 2, 54-56 (2005).

[193] DJ. Richardson, J. Nilsson and WA. Clarkson: High power fiber lasers: current status and future perspectives. Journal of the Optical Society of America B -27(11) 63-92 (2010).

[194] TS. McComb, RA. Sims, CC. Willis, P. Kadwani, V. Sudesh, L. Shah, and M. Richardson: High-power widely tunable thulium fiber lasers. Applied Optics 49(32) (2010).

[195] MN. Zervas: High power ytterbium-doped fiber lasers — fundamentals and applications. Int. J. Mod. Phys B 28 (2014).

[196] LA. Hardy, CR. Wilson, PB. Irby, NM. Fried: Thulium fiber laser lithotripsy in an in vitro ureter model. J Biomed Opt. 19(12) (2014).

[197] JA. Park, SW. Park, IS. Chang, JJ. Hwang, SA. Lee, JS. Kim, HK. Chee, IJ. Yun: The 1,470-nm bare-fiber diode laser ablation of the great saphenous vein and small saphenous vein at 1-year follow-up using 8-12 W and a mean linear endovenous energy density of 72 J/cm. J Vasc Interv Radiol, 25(11) 1795-800 (2014).

[198] DC. Wu, DP. Friedmann, SG. Fabi, MP. Goldman, RE. Fitzpatrick: Comparison of intense pulsed light with 1,927-nm fractionated thulium fiber laser for the rejuvenation of the chest. Dermatol Surg. 40(2) 129-33 (2014).

[199] P. Wattanakrai, S. Pootongkam, S. Rojhirunsakool: Periorbital rejuvenation with fractional 1,550-nm ytterbium/erbium fiber laser and variable square pulse 2,940-nm erbium:YAG laser in Asians: a comparison study. Dermatol Surg. 9 (2012).

[200] R. Li, D. Ruckle, M. Keheila, J. Maldonado, M. Lightfoot, M. Alsyouf, A. Yeo, SR. Abourbih, G. Olgin, JL. Arenas, DD. Baldwin: High-Frequency Dusting Versus Conventional Holmium Laser Lithotripsy for Intrarenal and Ureteric Calculi. J Endourol 13 (2016).

[201] Morin, F. Druon, M. Hanna, P. Georges: MicroJoule femtosecond fiber laser at 1.9 μm for corneal surgery applications. Optics Letters 34(13) (2009).

[202] FF. Sperandio, DT. Meneguzzo, LS. Ferreira, PA. da Ana, LH. Azevedo, SC. de Sousa: Different air-water spray regulations affect the healing of Er,Cr:YSGG laser incisions. Lasers Med Sci 26(2) 257-65 (2011).

[203] Fornaini, E. Merigo, J-P. Rocca, G. Lagori, H. Raybaud, S. Selleri, A. Cucinotta: 450 nm Blue Laser and Oral Surgery: Preliminary ex vivo Study. J Contemp Dent Pract 17(10) 1-6 (2016).

[204] M. Sozzi, C. Fornaini, A. Cucinotta, E. Merigo, P. Vescovi, S. Selleri: Dental ablation with 1064 nm, 500 ps, Diode pumped solid state laser: A preliminary study. Laser Ther 22(3) 195-9 (2013).

[205] D. Kersey, M. A. Davis, H. J. Patrick, M. LeBlanc, K. P. Koo, C. G. Askins, M. A. Putnam, E. J. Friebele: Fiber grating sensors. J. Lightw. Technol. 15(8) 1442–1463 (1997).

[206] P. Saccomandi, E. Schena, MA. Caponero, FM. Di Matteo, M. Martino, M. Pandolfi, S. Silvestri: Theoretical Analysis and Experimental Evaluation of Laser-Induced Interstitial Thermotherapy in Ex Vivo Porcine Pancreas. IEEE Transactions on Biomedical Engineering 59(10) (2012).

[207] Merigo, F. Clini, C. Fornaini, A. Oppici, C. Paties, A. Zangrandi, M. Fontana, JP. Rocca, M. Meleti, M. Manfredi, L. Cella, P. Vescovi: Laser-assisted surgery with different wavelengths: a preliminary ex vivo study on thermal increase and histological evaluation. Lasers Med Sci. -28(2) (2013).

[208] Fornaini, E. Merigo, P. Vescovi, M. Bonanini, W. Antonietti, L. Leoci, G. Lagori, M. Meleti: Different laser wavelengths comparison in the second-stage implant surgery: an ex vivo study. Lasers Med Sci. 30(6) 1631-9 (2015).

[209] Fornaini, E. Merigo, M. Sozzi et Al: Four different diode lasers comparison on soft tissues surgery: a preliminary ex vivo study. Laser Ther 25(2) 105- 114 (2016).

[210] Ulusoy M, Toksavul S: Fracture resistance of five different metal framework designs for metal-ceramic restorations. Int J Prosthodont 15, 571-574 (2002).

[211] Kang MS, Ercoli C, Galindo DF, Graser GN, Moss ME, Tallents RH: Comparison of the load at failure of soldered and non-soldered porcelain-fused-to-metal crowns. J Prosthet Dent 90, 235-240 (2003).

[212] Michalakis KX, Stratos A, Hirayama H, Kang K, Touloumi F, Oishi Y: Fracture resistance of metal ceramic restorations with two different margin designs after exposure to masticatory simulation. J Prosthet Dent 102, 172-178 (2009).

[213] Appeldoom RE, Wilwerding TM, Barkmeier WW: Bond strength of composite resin to porcelain with newer generation porcelain repair systems. J Prosthet Dent 70, 6-11 (1993).

[214] Demirel F, Muhtaroğullari M, Yüksel G, Cekiç C: Microleakage study of 3 porcelain repair materials by autoradiography. Quintessence Int, 38, 285-290 (2007).

[215] Giordano R, McLaren EA: Ceramics overview: classification by microstructure and processing methods. Compend Contin Educ Dent, 31, 682–4 (2010).

[216] Albakry M, Guazzato M, Swain MV: Fracture toughness and hardness evaluation of three pressable all-ceramic dental materials. J Dent 31, 181–8 (2003).

[217] Chung KH, Hwang YC: Bonding strengths of porcelain repair systems with various surface treatments. J Prosthet Dent 78, 267-274 (1997).

[218] Suliman AH, Swift EJ Jr, Perdigao J: Effects of surface treatment and bonding agents on bond strength of composite resin to porcelain. J Prosthet Dent, 70, 118-120 (1993).

[219] Diaz-Arnold AM, Schneider RL, Aquilino SA: Bond strengths of intraoral porcelain repair materials. J Prosthet Dent 61, 305-309 (1989).

[220] Holand W, Schweiger M, Frank M, Rheinberger V: A comparison of the microstructure and properties of the IPS empress 2 and the IPS empress glass ceramics. J Biomed Mater Res 53, 297–303 (2000).

[221] Della Bona A, Mecholsky JJ Jr, Anusavice KJ: Fracture behavior of lithia disilicate and leucite based ceramics. Dent. Mater 20, 956–62 (2004).

[222] Piwowarczyk A, Ottl P, Lauer HC, Kuretzky T: A clinical report and overview of scientific studies and clinical procedures conducted on the 3 M ESPE lava all-ceramic system. J Prosthodont 14, 39–45 (2005).

[223] Rocca J-P, Fornaini C, Brulat-Bouchard N, Bassel Seif S, Darque-Ceretti E: CO_2 and Nd:YAP laser interaction with lithium disilicate and Zirconia dental ceramics: A preliminary study. Optics & Laser Technology 57, 216-223 (2014).

[224] El Gamal A, Fornaini C, Rocca JP, Muhammad OH, Medioni E, Cucinotta A, Brulat-Bouchard N: The effect of CO_2 and Nd:YAP lasers on CAD/CAM Ceramics: SEM, EDS and thermal studies. Laser Ther. 25(1), 27-34 (2016).

[225] Liu L, Liu S, Song X, Zhu Q, Zhang W: Effect of Nd: YAG laser irradiation on surface properties and bond strength of zirconia ceramics. Lasers Med Sci. 30, 627-634 (2015).

[226] Ural C, KalyoncuoGlu E, Balkaya V: The effect of different outputs of carbon dioxide laser on bonding between zirconia ceramic surface and resin cement. Acta Odontol Scand. 70, 541–546 (2012).

[227] Sadeghi M, Davari A, Abolghasami Mahani A, Hakimi H: Influence of Different Power Outputs of Er:YAG Laser on Shear Bond Strength of a Resin Composite to Feldspathic Porcelain. J Dent (Shiraz) 16, 30-6 (2015).

[228] Shiu P, De Souza Zaroni WC, Eduardo Cde P, Youssef MN: Effect of feldspathic ceramic surface treatments on bond strength to resin cement. Photomed Laser Surg 25, 291–296 (2007).

[229] Erdur EA, Basciftci FA: Effect of Ti:Sapphire-femtosecond laser on the surface roughness of ceramics. Lasers Surg Med. 47, 833-8 (2015).

[230] Freedman: Buyers' guide to dental lasers. Lasers entering into the mainstream of dentistry. Dent Today 27(12):92-96 (2008).

[231] Keller U, Hibst R, Geurtsen W, Schilke R, Heidemann D, Klaiber B, Raab WH: Erbium:YAG laser application in caries therapy. Evaluation of patient perception and acceptance. J Dent 26(8):649-656 (1998).

[232] Lee CS, Lee CY, Kim U, Choi SK: CO_2 laser irradiation on dental hard tissues. Taehan Chikkwa Uisa Hyoph Chi. October;23(10):881-7 (1985).

[233] Myers TD, Myers WD: In vivo caries removal utilizing Nd:YAG laser. J Mich Dent Assoc. 1985 Feb;67(2):66-9 (1985).

[234] Frentzen M, Koort HJ, Kermani O, Dardenne MU: Preparation of hard tooth structure with Excimer lasers. Dtsch Zahnarztl Z. Jun;44(6):454-7 (1989).

[235] Renneboog-Squilbin C, Nammour S, Coomans D, Barel A, Carleer M, Dourov N.J: Measurement of pulp temperature increase to externally applied heat (argon laser, hot water, drilling). Biol Buccale. Sep;17(3):179-86 (1989).

[235] D. S. Wiersma: The physics and applications of random lasers. Nat Phys, 4(5):359–367, May (2008).

[237] V. S. Letokhov: Stimulated emission of an ensemble of scattering particles with negative absorption. JETP Lett. 5, 212-215 (1967).

[238] Lawandy, N. M. & Balachandran, R. M: Random laser? Reply. Nature 373, 204 (1995).

[239] Cao, J. Y. Xu, S.-H. Chang, and S. T. Ho: Transition from amplified spontaneous emission to laser action in strongly scattering media. Phys. Rev. E 61, 1985-1989 (2000).

[240] R. C. Polson, M. E. Raikh, and Z. V. Vardeny: Universal properties of random lasers. IEEE J. Sel. Top. Quantum Electron. 9, 120-123 (2003).

[241] S. Mujumdar, V. Turck, R. Torre, and D. S. Wiersma: Chaotic behavior of a random laser with static disorder. Phys. Rev. A 76, 033807 (2007).

[242] X. Wu and H. Cao: Statistical studies of random-lasing modes and amplified spontaneous-emission spikes in weakly scattering systems. Phys. Rev. A 77, 013832 (2008).

[243] K. L. van der Molen: Experiments on scattering lasers: from Mie to random. Univ. Twente, Enschede (2007).

[244] S. Wiersma: The physics and applications of random lasers. Nature Phys. 4, 359-367 (2008).

[245] Vanneste, C. & Sebbah, P: Selective excitation of localized modes in active random media. Phys. Rev. Lett. 87, 183903 (2001).

[246] Hui Cao: Lasing in random media. Waves Random Media 13, R1-R39 (2003).

[247] M. A. Noginov: Solid-State Random Lasers. Springer, Berlin (2005).

[248] Fornaini C, Pelosi A, Queirolo V, Vescovi P, Merigo E: The "at-home LLLT" in temporo-mandibular disorders pain control: a pilot study. Laser Ther. Mar 31;24(1):47-52 (2015).

[249] Merigo E, Rocca JP, Oppici A, Cella L, Fornaini C: At-home laser treatment of oral neuronal disorders: Case reports. J Clin Exp Dent. Apr 1;9(4):595-598 (2017).

[250] J Kitur, G Zhu, M Bahoura and MA Noginov: Dependence of the random laser behavior on the concentrations of dye and scatterers. J. Opt. 12 024009 (5pp) (2010).

[251] Selanger K A, Falnes J and Sikkeland T: Fluorescence life-time studies of rhodamine 6G in methanol. J. Phys.Chem. 81 1960–3 (1977).

Acknowledgement

Author wants firstly to thank prof. Annamaria Cucinotta and prof. Stefano Selleri for their kind cooperation and help during all the steps of this work performing.

The Author would like also to thank:

Datalogic S.p.A. and, particularly, dr. Lorenzo Bassi for providing the fiber laser source.

Prof. Federica Poli (University of Parma, Engineering Department) for the cooperation in performing the tests on ceramic samples and on the teeth.

Mr. Francisco Saia (University of Parma, Engineering Department) for the cooperation in performing the tests on teeth and on rhodamine random laser.

Prof. Elisabetta Merigo and prof. Jean-Paul Rocca (University of Cote d'Azur, Nice, Micoralis Laboratory) for the cooperation in the SEM analysis.

Prof. Nathalie Brulat-Bouchard (CEMEF, Mines ParisTech, Centre de Mise en Forme des Matériaux, CNRS-UMR 7635, Sophia Antipolis) for the cooperation in EDS analysis.

Dr. Carlo Molardi (University of Parma, Engineering Department) for the cooperation in performing the setup of random laser.

Dr. Chiara Cavatorta (University of Modena, Section of Pathologic Anatomy) for the cooperation on samples histological analysis.

Dr. Giuseppe Lagori (University of Cote d'Azur, Nice, Micoralis Laboratory) for the cooperation in the chemical aspects of Random Laser tests.